INTEGRATED
SYSTEM IDENTIFICATION/CONTROL DESIGN
WITH
FREQUENCY WEIGHTINGS

By

KA-LUN TUNG

A Thesis

submitted in partial fulfillment of the requirements

for the Degree of Master of Philosophy

Division of Systems Engineering

The Chinese University of Hong Kong

June 1995

TJ
213
T86
1995
wt

Copyright © 1995 by KA-LUN TUNG
All right reserved.

香港中文大學
大學圖書館系統
28 JUN 1996
UNIVERSITY LIBRARY SYSTEM
THE CHINESE UNIVERSITY OF HONG KONG

TO

MY MOTHER

马玉麒

Acknowledgement

I would like to like to express my gratitude to my advisor, Dr. Yeung Yam for his support and guidance throughout the course of this research. His thorough reading of this thesis and his constructive suggestions for its improvement are gratefully achnowledged. My gratitude also extended to other memebers of my thesis committe, Dr. Y. S. Hung, Dr. K. P. Lam and Dr. X. Shi for their helpful comments.

I am especially grateful to Professor Stewart L. DeVilbiss of the Air Force Institute of Technology (USA) for the stimulating discussions about his own research. His generousity for sharing his PhD thesis [1] and program codings are greatly appreciated. I have learnt from him on how a scholar should treat his own research results.

I would also like to thank Professsor S. F. Graebe of University of Newcastle (Australia) for his support and provision of the set of IFAC94 Benchmark programs; without which, chapter 8 of this thesis would not be possible.

Also, special thanks should be given to Dr. R. Y. Chiang and Professor M. G. Safonov, authors of the MATLAB Robust Control Toolbox, for their helpful discussions on the use of the package.

I thank the computing staffs of the Division of Systems Engineering and

Engineering Managment for their technical support, especially the electronic mail service, which enables me to discuss my research with the scholars from other parts of the world.

I have also benefited from many discussions with fellow classmates and colleagues, notably: Stephen Yang, Kaiser Lee, J. Y. Song.

In addition, I greatly appreciate the financial support of CUHK Postgraduate Student Grants for Overseas Academic Activities 1994/95 which grants me the chance to the *American Control Conference 1995*, Seattle, Washington, USA.

I thank Ms. Florie Tse for her wholehearted support of my decision to pursue graduate study. Finally, I would like to express my deepest gratitude to my parnets and their love and encouragement throughout my two years of study.

Abstract

In recent years, new methods have been developed to design robust controller for plant with uncertainties, the need to develop new system identification methods which incorporates robust control design arises naturally.

This thesis develops an iterative approach to integrate system identification and robust control design. The frequency weighting is important to our iterative approach. It is chosen to take into account the purpose of the control design.

A soft bound on the additive uncertainty accompanies the nominal model from the system identification procedures. The frequency information obtained from the subsequent robust controller design is used in the next system identification experiment. In such a way, it is hoped that the close-loop performance with the resulting robust controller could be improved, which exploits the advantage in the critical frequency regions. A new fractional weighting scheme is also developed.

In addition, a new frequency weighted controller model reduction scheme is developed, which the frequency weighting concept plays a central role. A comparative investigation on the design of low order controller through plant model reduction and controller model reduction in turn is carried out.

The integrated identification and control design approach is performed on a

benchmark problem. The design results are compared with that of other research groups, which illustrate the effectiveness of the integrated approach.

Publications

Research Publications

Y. Yam and K. L. Tung, "Integrated identification/control synthesis with frequency weighted balanced realization", in *Intelligent Automation and Soft Computing : Trends in Research, Development and Applications*, M. Jamshidi et al., Ed. 1994, vol. 1, TSI Press.

K. L. Tung and Y. Yam, "Integrated Identification/Control Synthesis with Approximate Fractional Frequency Weighting", in *Proceedings of the American Control Conference*, Seattle, WA, pp. 1835-1836, June 1995.

Contents

Chapter 1

Introduction

1.1 Control with Uncertainties

The issue of plant uncertainty is as old as the the invention of feedback control theory. In fact, Harold Black, the discoverer of the feedback principle in the engineering community, invented the linear feedback amplifier as an attempt to improving the adverse effects of plant uncertainty on his feedforward amplifier [2]. In designing linear controllers, it is usually necessary to assume the parameters of the system model are reasonably well known. Plant uncertainties may come into play due to slow time variation of parameters (e.g., of ambient air pressure during an aircraft flight), an abrupt change in parameters (e.g., in the inertial parameters of a robot when a new object is grasped), or unmodelled dynamics of physical system (e.g., high order or high frequency modes, nonlinearity, etc.)

With the advances of digital computer development, computers could be used to implement complicated control algorithms. High order controllers and

recursive estimation scheme for plant parameters are becoming possible. The control community has now developed two main approaches to handle plant uncertainty, namely *adaptive control* and *robust control.*

1.1.1 Adaptive Control

Current adaptive control designs apply mainly to systems with known dynamic structure, but unknown constant or slowly-varying parameters. It constitute a time-varying controller. A block diagram of an adaptive control system is shown in Figure 1.1.

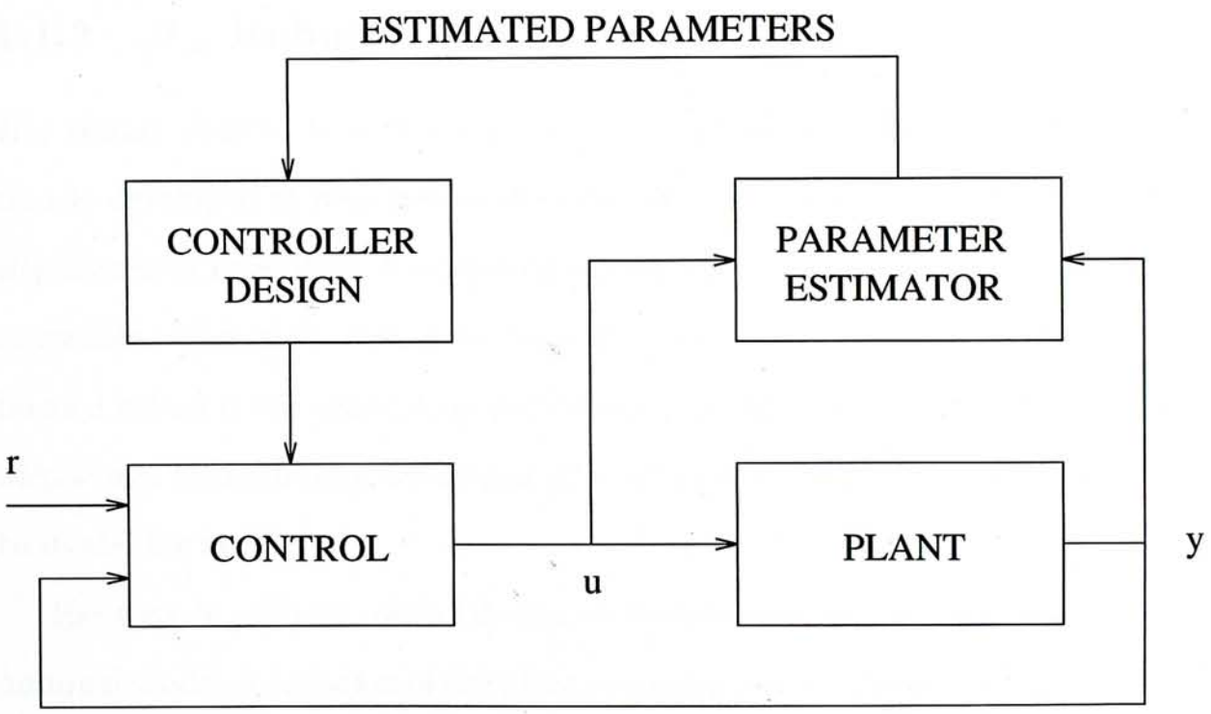

Figure 1.1: Block diagram of an adaptive control system

The system can be viewed as having two loops, an ordinary feedback loop and another loop that adjusts the parameters of the feedback loop. The parameter adjustment loop is composed of two blocks. One block performs recursive

estimation of the parameters of the process model. The other block computes the regulator gains from the estimated process parameters. A very good introduction of adaptive control is [3].

One important point should be noted: in practical implementation, adaptive control approach could only adapt to a slow-varying plant. A properly design adaptive control system will have its parameter estimate approach that of the model from the input/output data. If the plant variation is too fast, transient errors between the identified model and the true physical system can be so large as to completely disrupt the performance.

1.1.2 H_∞ Robust Control

H_∞ robust control is a frequency-domain optimization and synthesis theory that is developed in response to the need for a synthesis procedure that *explicitly* addresses questions of modelling errors. It produces a linear time-invariant controller. The basic idea is to treat the worst case scenario. A controller is termed *robust* if the closed-loop performance specification are met for all plants behaviours characterized by a nominal model subject to finite perturbations due to modelling error.

Existing H_∞ robust control design methodologies assume the availabiltiy of a nominal model description of the plant accompanied by a bounded quantification of the possible model mismatch of the model relative to the true plant.

Further details will be introduced in chapter 2.

1.2 A Unified Framework: Adaptive Robust Control

In fact, we could combine the two approaches in the last section under a unified framework.

In the traditional adaptive control system the identified model is used for on-line controller without any regard for errors between this model and the true system which generated the data. The identified model is usually selected out of a model set with unknown parameters as depicted in Figure 1.1. The controller is designed as if the parameter estimates were in fact the correct parameters for describing the plant. This is true in many cases where, there indeed exist parameters, which if known, would precisely account for the measured data. In the adverse case when the true system is not in the model set, however, both unacceptable transient or asymptotic behaviour can occur.

Figure 1.2 shows the block diagram of an adaptive *robust* control system which is similar to the one in [4]. The traditional parameter estimator is replaced with an estimator that produce a set of plants, which consists of a nominal model and accompanying uncertainty description. The traditional controller design algorithm is also replaced with a robust controller design which accepts the format of the plant set estimator output. The robust controller design algorithm produces a controller that could meet the closed-loop performance specifications for any plant in plant set with a specific confidence level. If the plant set is too large (i.e. the level of plant uncertainty is too high), or the specifications are too tight, then no robust controller will exist.

This is a grand scheme in which significance effort has been made in achieving

it [4–11]. Refer to [12] in particular. And **the scope of this thesis is to investigate the process highlighted in the block diagram of figure 1.2, i.e. integrated system identification and robust controller design** which is redrawn in figure 1.3 It is hoped that the study could contribute a small step towards the scheme. The additional *iterative reweighting* path (dashed line) in figure 1.3 is used to obtained a frequency weighted plant model and uncertainty description which would enhance performance of the closed-loop system.

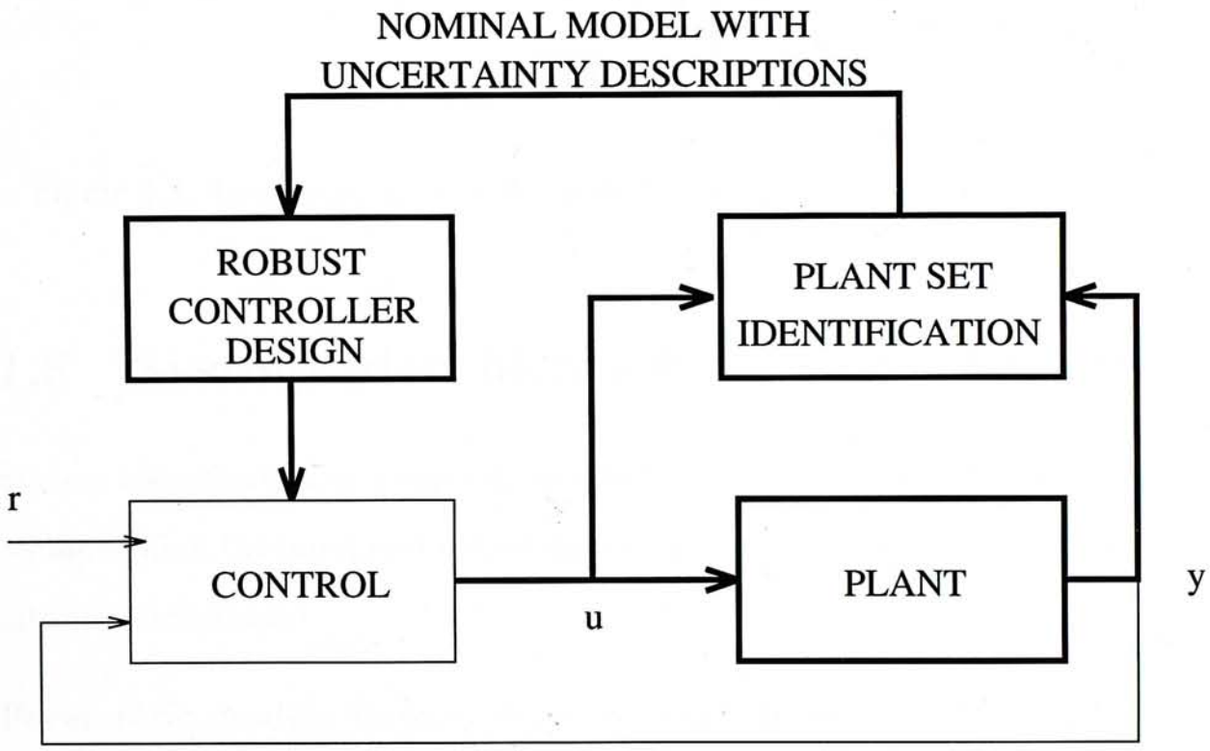

Figure 1.2: A Adaptive Robust Control System

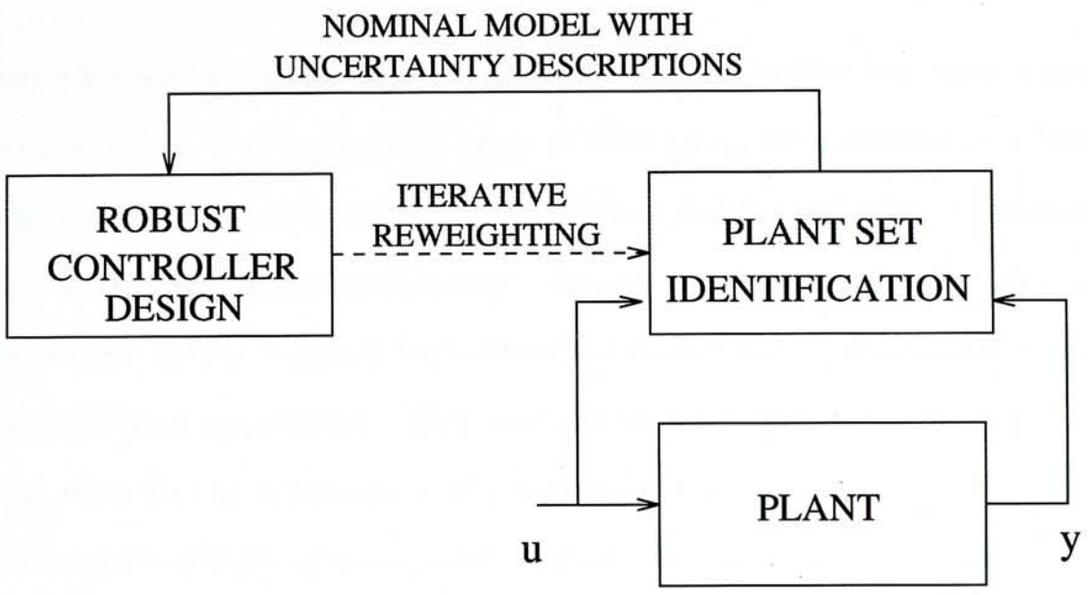

Figure 1.3: Integrated system ID/control design with iterative reweighting

1.3 System Identification for Robust Control

System identification is a experimental process, which a mathematical model is obtained from the input and output data of a plant. The model could be divided into two categories:

Parametric model: These models have been defined by a given form and are dependent on a finite number of real parameters. Examples such as systems of linear differential equations, transfer functions, partial differential equations or a model based on the known properties (e.g. physical, chemical) of the system under investigation ... etc.

Non-parametric model: These models are represented by a set of numerical value obtained from experiments. Examples include the impulse response,

spectral estimate, step response etc.

Any exercise in system identification needs to be carried out with a specific purpose in mind. For example, a piece of wire could be modelled as a lumped parametric model in low frequency application, a distributed infinite-dimensional model in high frequency application. In this thesis, system identification is performed to obtain a linear time-invariant model with statistical description of the associated uncertainty. This model with the uncertainty description will then be used for the synthesis of H_∞ robust controller.

An iterative scheme of doing identification and control in turn is investigated. The idea is to use the information from the control design of previous iteration for the next identification step in order to obtain a model (with uncertainty description) that could enhance control performance.

1.3.1 Choice of input signal

The input signal for system identification is an important and practical aspect. In [3], it has been point out that the pertubation input signal should at least be *persistently exciting.* In case of linear system this means effectively that the signal should adequately span the bandwidth of the system to be identified. Besides this requirement, we will see that the use of multi-frequency signal [13], in particular Schroeder-phased signal, possess favourable statistical properties for integrated system identification/control design.

1.4 Objectives and Contributions

The objectives of this work are:

1. To develop an integrated approach for system identification and robust control design.

2. To develop methods which incorporate frequency weightings in the integrated approach in order to improve performance.

3. To investigate the effects of frequency weightings on model reduction of controller and plant with respect to the close-loop robust performance.

4. To investigate the effectiveness of the proposed integrated approach by implementing it on a benchmark problem.

The major contributions of this work are considered to be:

1. An integrated approach for system identification and robust control design with iterative frequency re-weighting was developed. The limitations of the proposed approach was also investigated.

2. An approximate fractional frequency weighting scheme was proposed with improved performance.

3. An new integrated controller reduction scheme with iterative frequency re-weighting was proposed.

4. The effectiveness of the proposed integrated system identification and robust control design approach was demonstrated on a benchmark problem.

1.5 Thesis Outline

The remainder of this thesis is organized into eight chapters.

Chapter 2 will cover the necessary background material on H_∞ control design. It start with some basic notation and terminology; and then norms for measuring the size of signals, system gain and uncertainty will be reviewed. The uncertainty descriptions used for H_∞ control design will be introduced. The motivation for H_∞ control design will be discussed using three classical control problem. And a generalized framework for solving various control design problem will be presented.

Chapter 3 will cover the technique of non-parametric system identification with uncertainty characterization. The advantage and statistical properties of using schroeder-phased signals for identification will be discussed. A statistical formulation of additive uncertainty is then given. The non-parametric uncertainty will then be replaced by a parametric one using a linear-programming method.

Chapter 4 will review the basic algorithms of system identification and model reduction used in this research. The Eigensystem Realization Algorithm which produced a time-domain state-space model will be review, which is followed by a frequency-domain curve fitting method. The balanced model reduction algorithm and a weighted version will be presented.

Chapter 5 will cover the integrated identification/control design with iterative frequency reweighting scheme. A related model reduction/control design scheme will then follow. Model reduction will be treated as a simplified case of the system identification scheme. It will be used for investigating various aspects

of the iterative identification/control design procedures. The model reduction scheme could also be treated as a scheme for designing low order controller.

Chapter 6 will cover the controller reduction issues. The importance of frequency weighting in controller reduction will be emphasized. And a new scheme for determining the frequency weighting will be presented.

Chapter 7 will present a comparative example for the schemes proposed in chapter 5 and chapter 6. The results of the designs will be compared.

Chapter 8 will cover a example of integrated system identification/control design on a benchmark plant. The results will be compared with other groups of researchers. This serves as a convincing example of the approach used in this thesis. Various considerations for H_∞ control will also be discussed throughout the design process.

The final chapter is a summary of the results in this thesis and a discussion of future research directions.

Chapter 2

Background on Robust Control

This chapter will cover background material in the area of feedback control design including the concepts and techniques in dealing with uncertainty and the robustness issue of a closed-loop control system. We will start with mathematical notations and different kinds of norm definitions for evaluation of signals and systems.

Section 2.3 will discuss various types of uncertainty which is a very important concern for feedback control system.

Motivation for H_∞ based optimization approach for controller synthesis will then be discussed. With all the background materials introduced, we will present the problem statement of *Robust Control* in a precise mathematical way, for which we would devise solutions. Section 2.6.1 will present the augmented generalized plant which groups various control design problem under a single framework.

Finally, a brief description of the *MATLAB Robust Control Toolbox*, one of the most used tool for control design in this thesis, will be given.

2.1 Notation and Terminology

2.1.1 Notation

Suppose A is a complex-valued matrix:

- The transpose of the A will be denoted by A^T. The complex conjugate of A will be denoted by A^*. The Hermitian (complex conjugate transpose) of A will be denoted by A^H.
- Eigenvalues and singular values of A will be denoted by $\lambda[A]$ and $\sigma[A]$ respectively. The maximum and minimum singular values of A will be denote by $\overline{\sigma}[A]$ and $\underline{\sigma}[A]$, respectively.
- The trace and determinant of A will be denoted by $tr[A]$ and $\det[A]$ respectively.
- Real and imaginary parts of A will be denoted by $\mathrm{Re}[A]$ and $\mathrm{Im}[A]$ respectively.
- A positive definite A will be denoted by $A > 0$ and a positive semi-definite A by $A \geq 0$.
- A $n \times n$ Identity matrix will be denoted by I_n or I.

Definition of some often used symbols:

- The symbol $\triangleq$ is read *equal by definition.* The symbol, $\forall$ is read *for all.*
- The symbol sup is read *the supremum.*

- The symbol $\mathcal{R}$ represents the field of real scalars. The symbol $\mathcal{R}^n$ represents the space of $n \times 1$ real vectors. The symbol $\in$ is read *is an element of* (e.g. $r \in \mathcal{R}$).

2.1.2 Linear System Terminology

Continuous-time System

Consider the continuous-time linear system given by

$$\dot{\mathbf{x}} = A\mathbf{x} + B\mathbf{u} \qquad \mathbf{x} \in \mathcal{R}^n \quad \mathbf{u} \in \mathcal{R}^m \tag{2.1a}$$

$$\mathbf{y} = C\mathbf{x} + D\mathbf{u} \qquad \mathbf{y} \in \mathcal{R}^p \tag{2.1b}$$

- The order of the system is the integer n. The system has m inputs and p outputs. The transfer function, $G(s)$, of the system is given by

$$G(s) = C(sI - A)^{-1}B + D$$

- If $m = p = 1$, we called the system a single-input single-output or SISO system. If $m > 1$ and $p > 1$, we call it a multi-input multi-output or MIMO system.

- The symbols $\{A, B, C, D\}$ or $\{A, B, C\}$ (when $D = 0$) represent a realization of the transfer function of the system described by (2.1).

- The system is said to be minimal if it is completely controllable and observable.

- Transmission zeros are defined for minimal system to be the values of α such that

$$\begin{bmatrix} \alpha I - A & -B \\ -C & D \end{bmatrix} \quad \text{lose rank}$$

- The system is said to be asymptotically stable if $\mathrm{Re}[\lambda[A]] < 0$. The system is said to be minimum phase if $\mathrm{Re}[\alpha] < 0$ where α is a transmission zero of the system.

- The Laplace transform of the function, $f(t)$ will be denoted by $\mathcal{L}[f(t)](s)$, or $F(s)$ when there is no ambiguity. t will be exclusively used to denote time and s will exclusively denote the Laplace variable throughout this thesis.

Discrete-time System

Consider the discrete-time linear system given by

$$\mathbf{x}(k+1) = A\mathbf{x}(k) + B\mathbf{u}(k) \qquad \mathbf{x}(k) \in \mathcal{R}^n \quad \mathbf{u}(k) \in \mathcal{R}^m \tag{2.2a}$$

$$\mathbf{y}(k) = C\mathbf{x}(k) + D\mathbf{u}(k) \qquad \mathbf{y}(k) \in \mathcal{R}^p \tag{2.2b}$$

- The order of the system is the integer n. The system has m inputs and p outputs. The transfer function, $G(z)$, of the system is given by

$$G(z) = C(zI - A)^{-1}B + D$$

- The symbols $\{A, B, C, D\}$ or $\{A, B, C\}$ (when $D = 0$) represent a realization of the transfer function of the system describe by (2.2).

- Transmission zeros are defined for minimal system to be the values of α such that

$$\begin{bmatrix} \alpha I - A & -B \\ -C & D \end{bmatrix} \quad \text{lose rank}$$

- The system is said to be asymptotically stable if $|\lambda[A]| < 1$. The system is said to be minimum phase if $|\alpha| < 1$ where α is a transmission zero of the system.

- The $\mathcal{Z}$-transform of the function, $f(k)$ will be denoted by $\mathcal{Z}[f(t)](z)$, or $F(z)$ when there is no ambiguity. k is an integer and z will exclusively denote the $\mathcal{Z}$-transform variable throughout this thesis.

- The Tustin (or bilinear) transformation of a discrte-time model $F(z)$ in z-plane to w-plane is denoted by $F(w)$. The Tustin transformation maps a unit disc in z-plane to the left-half plane in w-plane via $z = (1+w)/(1-w)$.

For both continuous-time and discrete-time transfer functions:

- The transfer function, G, is *proper* if $G(\infty)$ is finite (degree of denominator $\geq$ degree of numerator).

- The transfer function, G, *strictly proper* if $G(\infty) = 0$ (degree of denominator $>$ degree of numerator).

2.1.3 Norms

A quantity $\|\cdot\|$ is a norm if it have the following properties:

1. $\|\mathbf{u}\| \geq 0$

2. $\|\mathbf{u}\| = 0$ if and only if $\mathbf{u} = 0$

3. $\|a\mathbf{u}\| = |a|\|\mathbf{u}\|, \qquad \forall a \in \mathcal{R}$

4. $\|\mathbf{u} + \mathbf{v}\| \leq \|\mathbf{u}\| + \|\mathbf{v}\|$

Absolute value The absolute value of a complex scalar v will be denoted by $|v|$ and is defined by $|v|^2 \triangleq vv^*$

Vector norm The norm of a complex vector $\mathbf{x}$ will be denoted by $\|\mathbf{x}\|$ and is defined by $\|\mathbf{x}\|^2 \triangleq \mathbf{x}^H\mathbf{x}$.

Maximum singular value For a matrix A, $\overline{\sigma}[A]$ is defined by $\overline{\sigma} \triangleq \lambda_{max}[A^H A]$.

L_2-norm (Frequency domain) The L_2 norm of the complex matrix valued function, $F(j\omega)$, $\omega \in \mathcal{R}$, will be denoted by

$$\|F(j\omega)\|_2^2 \triangleq \frac{1}{2\pi}\int_{-\infty}^{\infty} tr[F^H(j\omega)F(j\omega)]\,d\omega$$

H_∞-norm (Frequency domain) The H_∞ norm of a complex matrix valued function, $F(s)$ of a single complex variable, $s = \alpha + j\omega$ which is analytic in the closed right half plane will be denoted by $\|F(s)\|_\infty$ and is defined by

$$\|F(s)\|_\infty \triangleq \sup_{\alpha>0}\left\{\sup_{\omega}\bar{\sigma}[F(\alpha + j\omega)]\right\} = \sup_{\omega}\bar{\sigma}[F(j\omega)]^*$$

*The last equality is due to *maximum modulus principle*: if a function **F** (of a complex variable) is analytic inside and on the boundary of some domain $\mathcal{D}$, the the maximum modulus (magnitude) of the function **F** occurs on the boundary of the domain $\mathcal{D}$. For example, if a feedback system is closed-loop stable, the maximum magnitude of the closed-loop transfer function, $F(s)$ over the right-half of the complex plane will always occur on the imaginary axis.

2.1.4 More Terminology: A Standard Feedback Configuration

A standard feedback block diagram is shown in Figure 2.1. Referring the figure,

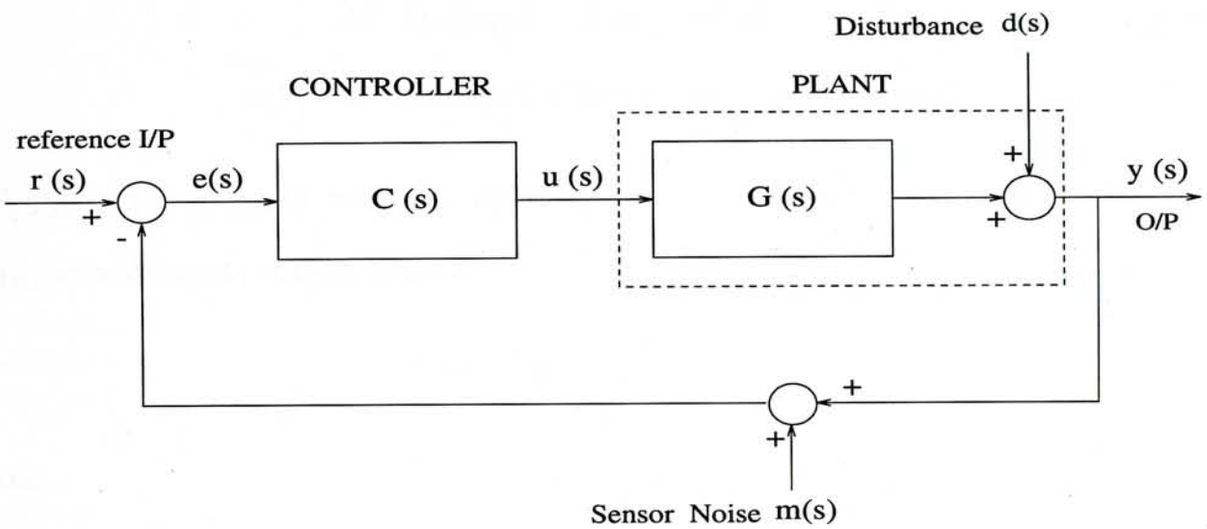

Figure 2.1: A standard feedback configuration

we define the following functions :

$$S(s) = (1 + L(s))^{-1} \tag{2.3}$$

$$L(s) = C(s)P(s) \tag{2.4}$$

$$T(s) = L(s)(1 + L(s))^{-1} \tag{2.5}$$

$$R(s) = C(s)(1 + L(s))^{-1} \tag{2.6}$$

where, $L(s)$ is *Loop Transfer Function* and $S(s)$ is called *Sensitivity Function.* Note that,

$$T(s) + S(s) = 1 \tag{2.7}$$

Thus $T(s)$ is also called *Complementary sensitivity function.*

The output $y(s)$ and error $e(s)$ is then respectively given by

$$\begin{aligned} y(s) &= r(s)T(s) + d(s)S(s) - m(s)T(s) && (2.8) \\ e(s) &= r(s) - d(s)S(s) - m(s)S(s) - y(s) \\ &= S(s)[r(s) - d(s) - m(s)] && (2.9) \\ u(s) &= e(s)C(s) = R(s)[r(s) - m(s) - d(s)] && (2.10) \end{aligned}$$

From (2.8), it could be seem that $S(s)$ is the transfer function of following important input/output pairs:

$$S(s): \quad d \to y\,; \quad r \to e\,;$$

and,

$$T(s): \quad r \to y\,; \quad m \to y\,; \qquad R(s): \quad r \to u\,; \quad d \to u$$

2.2 Norms and Power for Signals and Systems

For a scalar signal $u(t)$,

1-norm is the integral of its absolute value:

$$\|u\|_1 := \int_{-\infty}^{\infty} |u(t)|\, dt$$

2-norm

$$\|u\|_2 := \left(\int_{-\infty}^{\infty} u(t)^2\, dt\right)^{\frac{1}{2}}$$

∞-norm The least upper bound of its absolute value,

$$\|u\|_\infty := \sup_t |u(t)|$$

Points to note: Signals with finite 1-norm or 2-norm must decay as $t \rightarrow \infty$. Signals with finite ∞-norm cannot "blow up" for any t. 2-norm can represent square root of energy. For a scalar† transfer function $G(s)$,

L_2 or 2-norm

$$\|G(s)\|_2 := \left(\frac{1}{2\pi}\int_{-\infty}^{\infty} |G(j\omega)|^2\, d\omega\right)^{\frac{1}{2}}$$

H_∞ or ∞-norm

$$\|G(s)\|_\infty := \sup_\omega |G(j\omega)|$$

Points to note: Transfer functions with finite L_2-norm must roll off (tend to zero) as $\omega \rightarrow \infty$. Transfer functions with finite H_∞ norm may be nonzero at high frequencies. H_∞-norm of a transfer function is the maximum gain over frequency, i.e. the maximum gain for pure sinusoidal inputs.

Now we define the power of a signal:

Average Power The average power of a signal $u(t)$ is:

$$\lim_{T\rightarrow\infty} \frac{1}{2T}\int_{-T}^{T} u(t)^2\, dt$$

Power signal We call the signal $u(t)$ a power signal if the above limit exists, and its root mean square power, $pow(u)$ is defined as:

$$pow(u) \triangleq \left(\lim_{T\rightarrow\infty} \frac{1}{2T}\int_{-T}^{T} u(t)^2\, dt\right)^{\frac{1}{2}}$$

†From this section onwards, all the discussions will be based on single-input single-output (SISO) system for simplicity and easy understanding of concepts. For multi-input multi-output (MIMO) systems, the concept of singular values will have to be used for system gain quantification. However, for a SISO system, $G(s)$,

$$\|G\|_\infty = \sup_\omega \overline{\sigma}[G(j\omega)] = \sup_\omega G(j\omega)$$

Points to note: pow is not a norm since nonzero signal could have zero power. For example if the 2-norm of a signal is finite, its energy is limited and thus its average power is 0. On the other hand, if $pow(u(t)) \neq 0$, then $\|u(t)\|_2 \to \infty$. Unit step and sinusoidal signals are examples which have fintie power but infinite 2-norm. The relations between input, output and transfer function is given in the Table 2.1.

	$\|u\|_2$	$\|u\|_\infty$	$pow(u)$
$\|y\|_2$	$\|G\|_\infty$	∞	∞
$\|y\|_\infty$	$\|G\|_2$	$\|G\|_1$	∞
$pow(y)$	0	$\leq \|G\|_\infty$	$\|G\|_\infty$

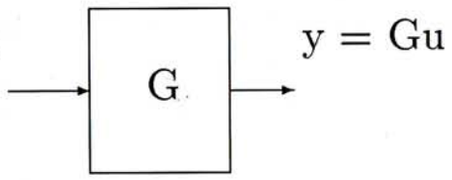

Table 2.1: Relations between Input/Output and transfer function norms

The input to the system $G(s)$ is u, having $\|u\|_2 < 1$ (the second column), $\|u\|_\infty < 1$ (the third column) or $pow(u) < 1$ (the fourth column). The the norm of the output y is shown in the respective rows. For example, if we have an input $\|u\|_2 < 1$, then the the 2-norm gain is $\frac{\|y\|_2}{\|u\|_2} = \|G\|_\infty$ in the entry (1,1) of the table. The proof of each entry could be found in [14].

2.3 Plant Uncertainty Model

No model of a physical plant is exact. One must be aware of how modelling errors will affect the performance of a control system. Modelling errors constitue a type of uncertainty. For a linear model of a plant, the source of uncertainty may come from neglected high order dynamics, neglected high frequency modes, non-linear elements of the plant, etc.

In this section, we will first differentiate between *unstructured* and *structured*

uncertainty. The we will focus on two main types of unstructured uncertainty: multiplicative and additive uncertainty. Throughout the thesis, we will concentrate on additive uncertainty. The reason will be explained in chapter 3.

2.3.1 Multiplicative Unstructured Uncertainty

Figure 2.2 shows a nominal plant, $P_n(s)$ with multiplicative unstructured uncertainty inside a feedback loop is shown in Figure 2.2. $C(s)$ is the controller. $P_n(s)$ be the nominal plant. The set of plants $\tilde{P}(s)$ which has the same unstable

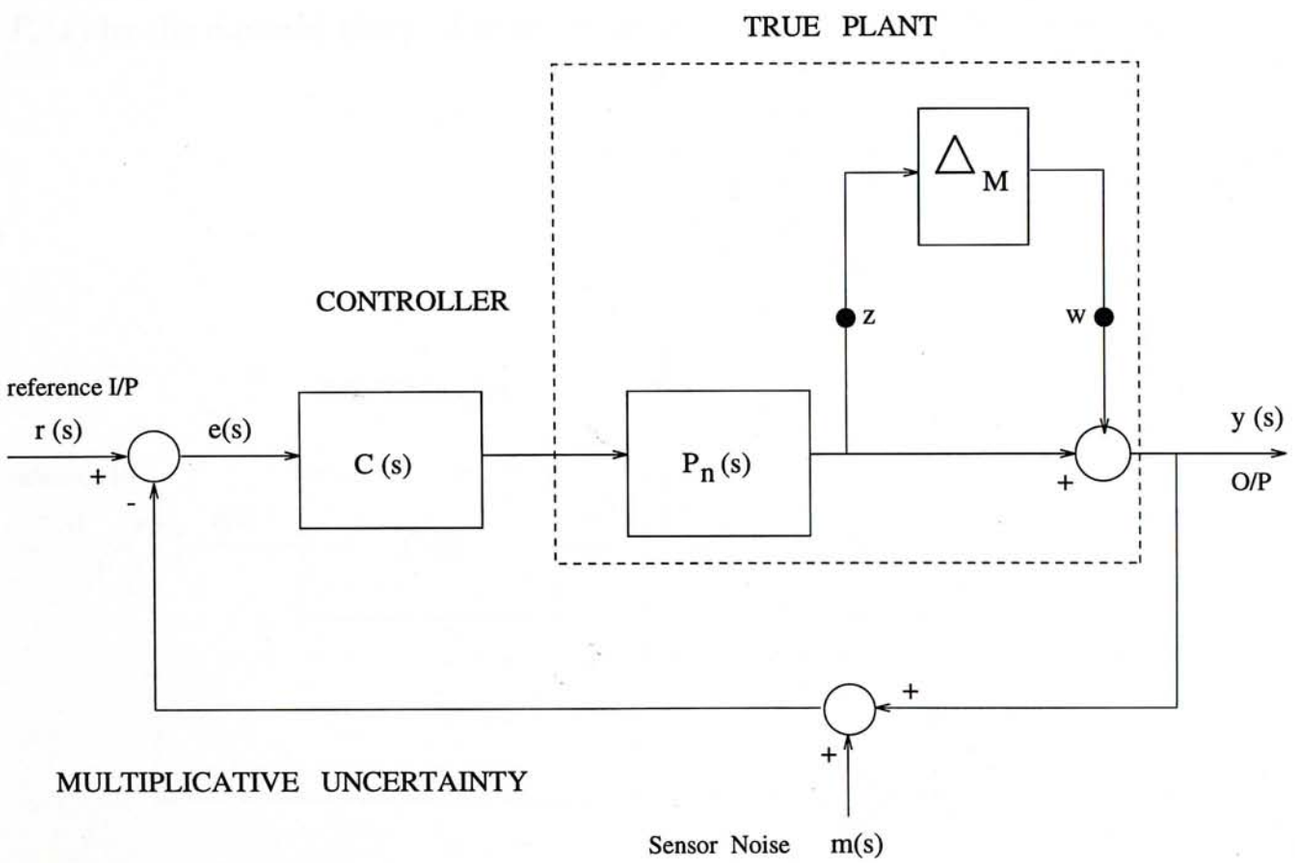

Figure 2.2: Multiplicative unstructured uncertainty

poles as $P_n(s)$ are

$$\tilde{P} = (1 + \triangle_M)P \tag{2.11}$$

where $\triangle_M$ is a linear, stable, minimum phased, time-invariant system. The idea behind the uncertainty model is that $\triangle_M$ is the normalised plant perturbation away from 1:

$$\frac{\tilde{P}}{P} - 1 = \triangle_M$$

$\tilde{P}(s)$ is assumed to contain the true plant.

2.3.2 Additive Unstructured Uncertainty

Additive unstructured uncertainty is shown in block diagrams in Figure 2.3. $P_n(s)$ be the nominal plant. The set of plants $\tilde{P}(s)$ which has the same unstable

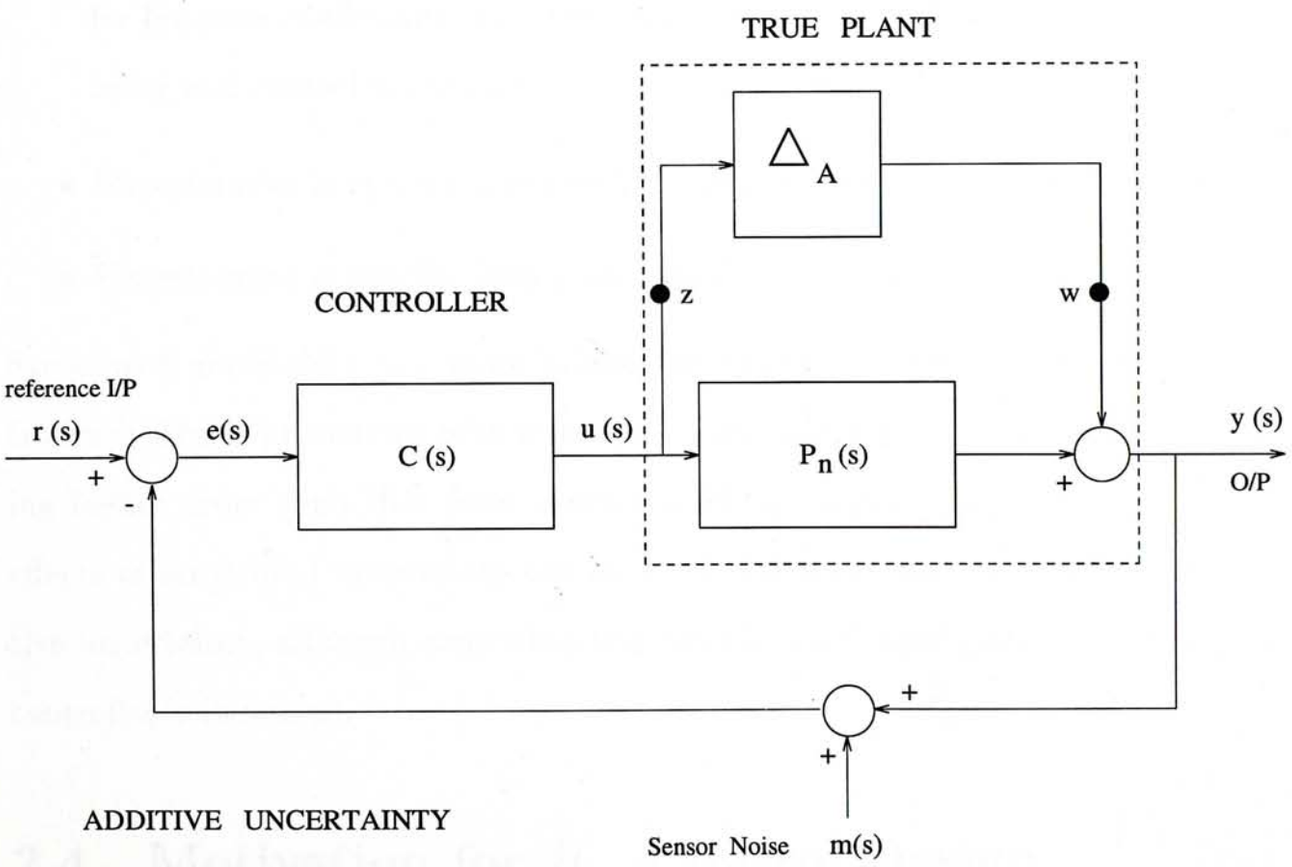

Figure 2.3: Multiplicative unstructured uncertainty

poles are

$$\tilde{P} = P_n + \triangle_A \tag{2.12}$$

where $\triangle_A$ is a linear, stable, minimum phased, time-invariant system. $\tilde{P}(s)$ is assumed to contain the true plant.

2.3.3 Structured Uncertainty

Structured uncertainty represents parametric variations in the plant dynamics, for example:

- Uncertainties in certain entries of state-space matrices $\{A, B, C\}$, or transfer function coefficients, e.g., the uncertain variations in an aircraft's stability and control derivatives.
- Uncertainties in specific poles and/or zeros of the plant transfer function.
- Uncertainties in specific loop gains/phases.

Structured uncertainty is a more tailored uncertainty. However, current controller synthesis procedures with structured uncertainty leads to controller having higher order than that from unstructured uncertainty [15]. Many of the effects of structured uncertainty can be modelled with additive or multiplicative uncertainty, although somewhat less exactly. And conservativeness of the controller is increased.

2.4 Motivation for H_∞ Control Design

In this section we will discuss the motivation behind H_∞ control design by studying three classical problems: Robust Stabilization, Tracking, and Disturbance

Rejection. In addition, to relate the H_∞-optimization theory to a practical control problem, the essential idea of "weighting functions" is introduced.

The use of "weights" or "weighting functions" is common in control system optimisation. In the case of infinity norm optimisation, the introduction of weights allows the frequency dependent characteristics of signals and systems to be captured as well as their size. For example, $\mathbf{G}$, a low-pass function may be characterized by that $\mathbf{G}(j\omega) < \mathbf{w}(j\omega)$ for all ω and some scalar low-pass weight $\mathbf{w}$. Similarly, a low-frequency disturbance is modelled by $\|\mathbf{w}^{-1}d\|_2 < 1$, rather than $\|d\|_2 < 1$, which does not contain the *a priori* knowledge about the low-frequency nature of the disturbance.

2.4.1 Robust stabilization: Multiplicative Uncertainty and Weighting function W_3

Consider the case for multiplicative uncertainty in Figure 2.2. With $r = 0$ and $m = 0$, let the transfer function from w to z is $M(s)$, then the stability properties of that system are the same as those given in Figure 2.4 with

$$M(s) = P(s)C(s)(1 + P(s)C(s))^{-1} = T(s)$$

If the perturbation $\triangle_M$ and the nominal closed-loop system, are both stable, the Nyquist criterion says that the closed-loop system is stable if and only if the Nyquist diagram of $M(s)\triangle_M$ does not encircle the -1 point. Since the condition

$$\sup_\omega M(j\omega)\triangle_M(j\omega) = \|M(s)\triangle_M(s)\|_\infty < 1 \tag{2.13}$$

ensures the Nyquist diagram of $M\triangle_M$ does not encircle the -1 point, it constitute a sufficient condition that the closed-loop system is stable provided (2.13) holds.

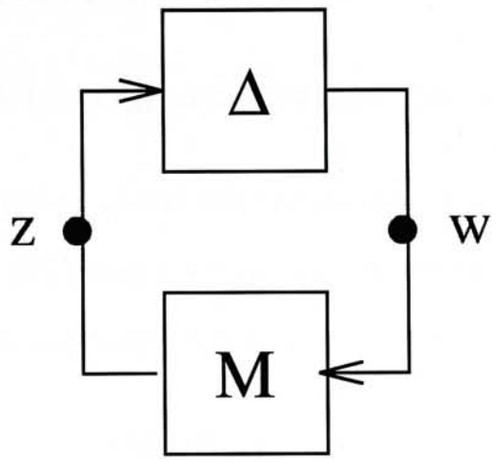

Figure 2.4: Equivalent block diagram for unstructured uncertainty

Introduction of frequency weighting $W_3(s)$

Suppose other than stability, we have additional information about the the bound of $|\triangle_M|$ in frequency domain. Then for stability evaluation purpose, the $\triangle_M$ could be replaced by $W_3(s)\triangle(s)$ with $|W_3(j\omega)| > |\triangle_M(j\omega)|$ and $\|\triangle(s)\|_\infty < 1$. Then (2.13) becomes

$$\|T(s)W_3(s)\|_\infty < 1 \tag{2.14}$$

for *robust stability* under multiplicative uncertainty.

2.4.2 Robust stabilization: Additive Uncertainty and Weighting function W_2

Similarly, consider the case for additive uncertainty in Figure 2.3, $M(s)$, the transfer function from w to z will be

$$M(s) = C(s)(1 + P(s)C(s))^{-1} = R(s)$$

and the condition for robust stability becomes:

$$\sup_{\omega} M(j\omega)\triangle_A(j\omega) = \|M(s)\triangle_A(s)\|_\infty < 1$$

And if additional information about the the bound of $|\triangle_A|$ in frequency domain could be obtained[‡], say $|W_2(j\omega)| > |\triangle_M(j\omega)|$. Then the sufficient condition for robust stability of the closed-loop system is

$$\|R(s)W_2(s)\|_\infty < 1 \tag{2.15}$$

Control Effort and $R(s)$

In addition to its relation to additive uncertainty, $R(s)$ in 2.15 is also related to the level of controller output, $u(s)$. In (2.10), we could see that $u(s)$ is related to $R(s)$. Suppose the exogenous inputs (d, m, r) span over a wide frequency range, and has a finite 2-norm or finite power, then the maximum magnitude of $u(s)$ will be $\|R(s)\|_\infty$. Here we have used the results of entry $(1,1)$ and $(3,3)$ in Table 2.1.

2.4.3 Tracking Problem

The tracking problem is to design the system in Figure 2.1 in such a way that the output $y(t)$ tracks the command or reference signal $r(t)$. Suppose, for the time being, the disturbance d and sensor noise m in (2.9) are zero, then the tracking error $e(s) = S(s)r(s)$. Usually, r is not known in advance - few control systems are designed for one and only one input. We consider several classes of common input to illustrate the role of the ∞-norm plays.

[‡]The method to obtain a "soft" bound for $\triangle_A$ will be discussed in detail in chapter 3.

1. Suppose the reference input, r is composed of sum of N filtered sinusoids of the form $r = W_1 r_{pf}$, where r_{pf}, the pre-filtered input, is sum of pure sinusoids each with amplitude ≤ 1. Then the maximum amplitude of e is bounded by

$$N(\sup_{\omega}[W_1 S]) = N\|W_1 S\|_\infty$$

2. Suppose r is finite 2-norm signal with specific energy spectrum shaped by $W_1(s)$, i.e.

$$\{r : r = W_1 r_{pf}, \quad \|r_{pf}\|_2 \leq 1\}$$

For example, if W_1 were a bandpass filter, the energy spectrum of r would be confined to the passband. More generally, W_1 could be used to shape the energy spectrum of the expected class of reference inputs[§]. Now suppose the tracking error measure is the 2-norm of e. Then from Table 2.1 entry $(1,1)$,

$$\sup_r \|e\|_2 = \sup\{\|SW_1 r_{pf}\|_2 : \|r_{pf}\|_2 \leq 1\} = \|W_1 S\|_\infty$$

3. Suppose r is of finite power. Similar to above, from Table 2.1, entry $(3,3)$, the supremum of $pow(e)$ over all r_{pf} with $pow(r_{pf}) \leq 1$ is $\|W_1 S\|_\infty$. So W_1 could also be used to shape the power spectrum of the expected class of r's.

2.4.4 Disturbance Rejection (or Sensitivity Minimization)

The signal d in Figure 2.1, represents an exogenous disturbance such as load variation or wind gust that affects the output y. The disturbance rejection

[§]More detail discussion of the selection of W_1 will be given in section 8.2.2

problem is to find some means of reducing or eliminating the influence of d on y. If we consider d alone in (2.8), $y = Sd$. Using similar reasoning as in section 2.4.3, disturbance rejection of a certain class of frequency weighted d (by W_1) would boiled down to the minimization of ∞-norm of the weighted *sensitivity function*, i.e. $\|W_1 S\|_\infty$.

2.5 The Robust Control Problem Statement

In section 2.4.1 and 2.4.2, we have discussed the problem of robust stability. And the performance aspect of a feedback control system has been covered in section 2.4.3 and 2.4.4. In this section, we put the two together, the performance of a plant with uncertainty: *robust performance*. For a SISO system, the necessary and sufficient condition for robust performance under multiplicative uncertainty is

$$\| \, |W_1 S| + |W_3 T| \, \|_\infty < 1 \tag{2.16}$$

and for additive uncertainty is

$$\| \, |W_1 S| + |W_2 R| \, \|_\infty < 1 \tag{2.17}$$

The proofs could be found in [14]. If the condition of (2.16) or (2.17) could not be met, a performance index factor, $0 < \gamma < 1$, could be inserted in the conditions, then (2.16) and (2.17) becomes (2.18) and (2.19) respectively.

$$\| \, |\gamma W_1 S| + |W_3 T| \, \|_\infty < 1 \tag{2.18}$$

$$\| \, |\gamma W_1 S| + |W_2 R| \, \|_\infty < 1 \tag{2.19}$$

However, synthesis of controllers meeting the above stated condition remains unsolved. Existing methods for an approximate solution require the use of complicated μ-synthesis techniques and will generate very high order controllers. Interested reader could refer to [15] for detail procedures.

An alternative approach is to solve a more conservative problem which admits much simplified and nearly equivalent problem: the *the mixed sensitivity* problem.

2.5.1 The Mixed-Sensitivity Approach

The mixed-sensitivity problem is based on the following observation:

For two scalars x and y,

$$x^2 + y^2 < \frac{1}{2} \quad \Rightarrow \quad x + y < 1 \tag{2.20}$$

Using the ∞-norm, notation, the mixed-sensitivity synthesis problem could be stated as follows.

1. For plant under multiplicative uncertainty perturbation, a feedback controller that satisfies the following conditions can achieve robust performance with performance index γ, $(0 < \gamma < 1)$:

$$\sup_{\omega} \left\| \begin{bmatrix} \gamma W_1 S \\ W_3 T \end{bmatrix} \right\|_{\infty} = \sup_{\omega} \overline{\sigma} \begin{bmatrix} \gamma W_1 S \\ W_3 T \end{bmatrix} = \sqrt{|\gamma W_1 S|^2 + |W_3 T|^2} < \sqrt{\frac{1}{2}} \tag{2.21}$$

2. For plant under additive uncertainty perturbation, a feedback controller that satisfies the following conditions can achieve robust performance with

performance index γ:

$$\sup_{\omega} \left\| \begin{bmatrix} \gamma W_1 S \\ W_2 R \end{bmatrix} \right\|_{\infty} = \sup_{\omega} \overline{\sigma} \begin{bmatrix} \gamma W_1 S \\ W_2 R \end{bmatrix} = \sup_{\omega} \sqrt{|\gamma W_1 S|^2 + |W_2 R|^2} < \sqrt{\frac{1}{2}} \tag{2.22}$$

For general MIMO case, refer to [16].

2.6 An Augmented Generalized Plant

Rather than solving the individual problems presented in section 2.4 and section 2.5.1 one by one, we will try to group all the problems under a single generalized framework: an *Augmented Plant.* The augmented plant could capture many H_∞ optimization problems of general interest as special cases.

Then we will use this augmented plant to formulate the *sensitivity minimization* problem and the *mixed-sensitivity* problem. These serve to illustrate the power of the generalized approach.

2.6.1 The Augmented Plant

The augmented plant is shown in Figure 2.5. The augmented plant $G(s)$ is

$$\left[\begin{array}{c} y_{1a} \\ y_{1b} \\ y_{1c} \\ \hline y_2 \end{array}\right] = \left[\begin{array}{c|c} W_1 & -W_1 P \\ 0 & W_2 \\ 0 & W_3 P \\ \hline I & -P \end{array}\right] \left[\begin{array}{c} u_1 \\ \hline u_2 \end{array}\right] \tag{2.23}$$

or in a more simplified form,

$$\begin{bmatrix} y_1 \\ y_2 \end{bmatrix} = \begin{bmatrix} G_{11}(s) & G_{12}(s) \\ G_{21}(s) & G_{22}(s) \end{bmatrix} \begin{bmatrix} u_1 \\ u_2 \end{bmatrix} \tag{2.24}$$

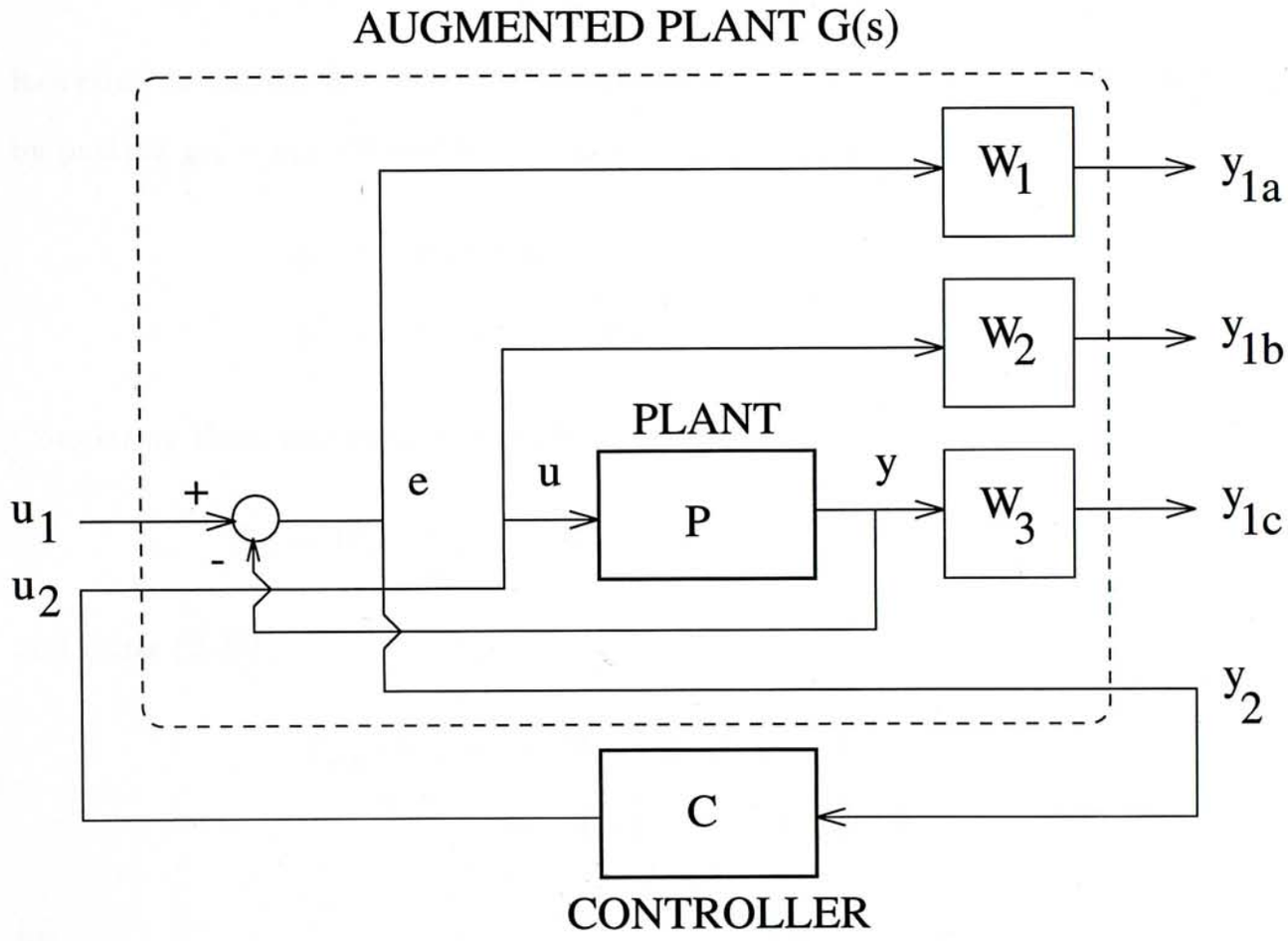

Figure 2.5: The Augmented Plant

With $u_2 = Cy_2$, we obtain $y_1 = T_{y_1u_1}(G, C)u_1$, where

$$T_{y_1u_1}(G, C) = G_{11}(s) + G_{12}(s)C(s)[I - G_{22}(s)C(s)]^{-1}G_{21}(s) \qquad (2.25)$$

2.6.2 Adaptation of Augmented Plant to Sensitivity Minimization Problem

Referring to (2.23), the sensitivity Minimization Problem could be formulated by putting $y_{1b} = y_{1c} = 0$ and $u_1 = r(s)$

$$\begin{aligned} y_1 &= W_1e = W_1(r - y) = W_1r - W_1Pu_2 \\ y_2 &= r - y = r - Pu_2 \end{aligned}$$

Comparing these two equations with (2.24):

$$G_{11} = W_1, \quad G_{12} = -W_1P, \quad G_{21} = I, \quad G_{22} = -P$$

and using (2.25)

$$\begin{aligned} T_{y_1u_1}(G, C) &= W_1 - W_1PC(I + PC)^{-1} \\ &= W_1(I + PC)^{-1} = W_1S \end{aligned}$$

i.e.

$$\|T_{y_1u_1}\|_\infty < 1 \Rightarrow \|W_1S\|_\infty < 1$$

2.6.3 Adaptation of Augmented Plant to Mixed-Sensitivity Problem

The mixed sensitivity problem for additive uncertainty could be formulated by putting

$$u_1 = r \qquad y_1 = \begin{bmatrix} y_{1a} \\ y_{1b} \end{bmatrix} \qquad y_{1c} = 0$$

$$y_1 = \begin{bmatrix} y_{1a} \\ y_{1b} \end{bmatrix} = \begin{bmatrix} \gamma W_1 e \\ W_2 u_2 \end{bmatrix} = \begin{bmatrix} \gamma W_1 (u_1 - P u_2) \\ W_2 u_2 \end{bmatrix} = \begin{bmatrix} \gamma W_1 \\ 0 \end{bmatrix} u_1 + \begin{bmatrix} -\gamma W_1 P \\ W_2 \end{bmatrix} u_2$$

and

$$y_2 = e = u_1 - P u_2 = \begin{bmatrix} I & -P \end{bmatrix} \begin{bmatrix} u1 \\ u2 \end{bmatrix}$$

Rewriting the above two equations,

$$\left[\begin{array}{c} y_1 \\ \hline y_2 \end{array}\right] = \left[\begin{array}{c|c} \gamma W_1 & -\gamma W_1 P \\ 0 & W_2 \\ \hline 1 & -P \end{array}\right] \left[\begin{array}{c} u_1 \\ \hline u_2 \end{array}\right]$$

Thus by (2.25),

$$\begin{aligned} T_{y_1 u_1} &= \begin{bmatrix} \gamma W_1 \\ 0 \end{bmatrix} + \begin{bmatrix} -\gamma W_1 P \\ W_2 \end{bmatrix} C(I + PC)^{-1} = \begin{bmatrix} \gamma W_1 - \gamma W_1 P C (I + PC)^{-1} \\ W_2 C (I + PC)^{-1} \end{bmatrix} \\ &= \begin{bmatrix} \gamma W_1 (1 - T) \\ W_2 R \end{bmatrix} = \begin{bmatrix} \gamma W_1 S \\ W_2 R \end{bmatrix} \end{aligned}$$

And the mixed-sensitivity problem is transformed to

$$\|T_{y_1 u_1}\|_\infty < 1 \Rightarrow \left\| \begin{bmatrix} \gamma W_1 S \\ W_2 R \end{bmatrix} \right\|_\infty < 1 \tag{2.26}$$

2.7 Using MATLAB Robust Control Toolbox

The main tool used for H_∞ optimal controller synthesis is the *Robust Control Toolbox* for use with MATLAB. Two important routines have been used repeatedly and worth a brief description :

augss.m function form the augmented plant discussed in section 2.6 for the mixed-sensitivity approach.

hinf.m function perform H_∞ optimal controller synthesis in s-plane or w-plane which gives a controller that enable the closed-loop transfer function satisfies the ∞-norm inequality

$$\|T_{y_1 u_1}\|_\infty < 1$$

For implementation of the robust controller on digital computer, a discrete-time controller in z-plane, $C(z)$, is required. However, the design algorithm (namely "hinf.m") carries out the design in continuous-time s-plane (or w-plane). To obtain $C(z)$, [15] has suggested the Tustin (or bilinear) transformation approach. This approach use the Tustin transform which can guarantee that any given function that is analytic in a half-plane can be mapped to a disc without changing its H_∞ norm. [17] and [18] have shown that for the time invariant case, this bilinear approach exactly equivalent to the continuous H_∞ case with the same existence conditions and equivalent two Riccati Hamiltonians. The following outlines the procedures:

Step 1: Transform the discrete plant, $P(z)$ obtained from system identification to a continuous plant $\breve{P}(w)$ via the transformation $z = (1 + w)/(1 - w)$.

Step 2: Design the controller $\breve{C}(w)$ for $\breve{P}(w)$ as a regular continuous H_∞ optimization problem.

Step 3: Apply the inverse transformation $w = (1-z)/(1+z)$ to the controller $\breve{C}(w)$ to obtain $C(z)$

A remark should be given here: the "hinf.m" function gives controller with $\|T_{y_1u_1}\|_\infty < 1$ rather than $\|T_{y_1u_1}\|_\infty < 1/\sqrt{2}$. To enable the controller to achieve real robust performance, the element in $T_{y_1u_1}$ should have been multiplied with a factor $\sqrt{2}$. However, this was not done in the MATLAB Robust Control Toolbox or in any of the examples in the manual. This point was discussed with one of the author of the toolbox, Dr. R. Y. Chiang of Jet Propulsion Laboratory. The conclusion was that since the results of "hinf" would be within $3db$ ($\sqrt{2}$) from the "real" robust control problem; and[¶]

```
'' cost #1: || [W1 S; W3 T] ||_inf < 1
   ...
   in achieving Exact mixed-sensitivity loop shaping (cost # 1)
the unstability situation is rarely seen in practice.''
```

Thus the factor $\sqrt{2}$ was not pre-multiplied to the elements of $T_{y_1u_1}$ during the controller synthesis process.

[¶]Content of electronic mail reply by Dr. Chiang

Chapter 3

Statistical Plant Set Estimation for Robust Control

This chapter mainly summarizes the results in [9, 10, 19–21]. These papers together describes a rigorous method for combining classical system identification with modern control design, in order to determine H_∞ controllers from raw input/output data. The methods discussed in this chapter form the foundation of of our design approach in the subsequent chapters.

A key issue in control design from raw input/output data is the question of whether the controller will work when applied to the true system. The main feature of this approach is that the resulting controller is guaranteed to work as designed (when applied to the true system) to a prescribed statistical confidence.

3.1 An Overview

An overview of the identification and robust control design approach is given in Figure 3.1, which is composed of the following steps:

1. The input/output time-domain data are gathered. The input is a Schroeder-phased multisinusoidal signal (section 3.2), which is applied to the plant until the output reaches steady-state.

2. A parametric plant model $\hat{P}$ is then calculated using system identification method such as Eigensystem Realization Algorithm (section 4.1) or Frequency-domain curve-fitting (section 4.2).

3. An averaged plant spectral estimate P^* is also calculated together with an non-parametric additive uncertainty ball $l_A^{1-\alpha} \geq (\hat{P} - P^*)$ having a statistical confidence $(1-\alpha) \times 100\%$ (section 3.3). The confidence level is specified by the designer.

4. The profile $l_A^{1-\alpha}(\omega_i)$ is overbounded (tightly) using a linear programming spectral overbounding and factorization algorithm (section 3.4) to give a parametric minimum-phased transfer function W_2 of specified order*.

5. Using $\hat{P}$ and W_2, available robust control design methods† can be used to design a controller which will ensure some specified stability/performance for all plants within the uncertainty set.

---

*Refer to section 2.4.2

†MATLAB Robust Control Toolbox in particular.

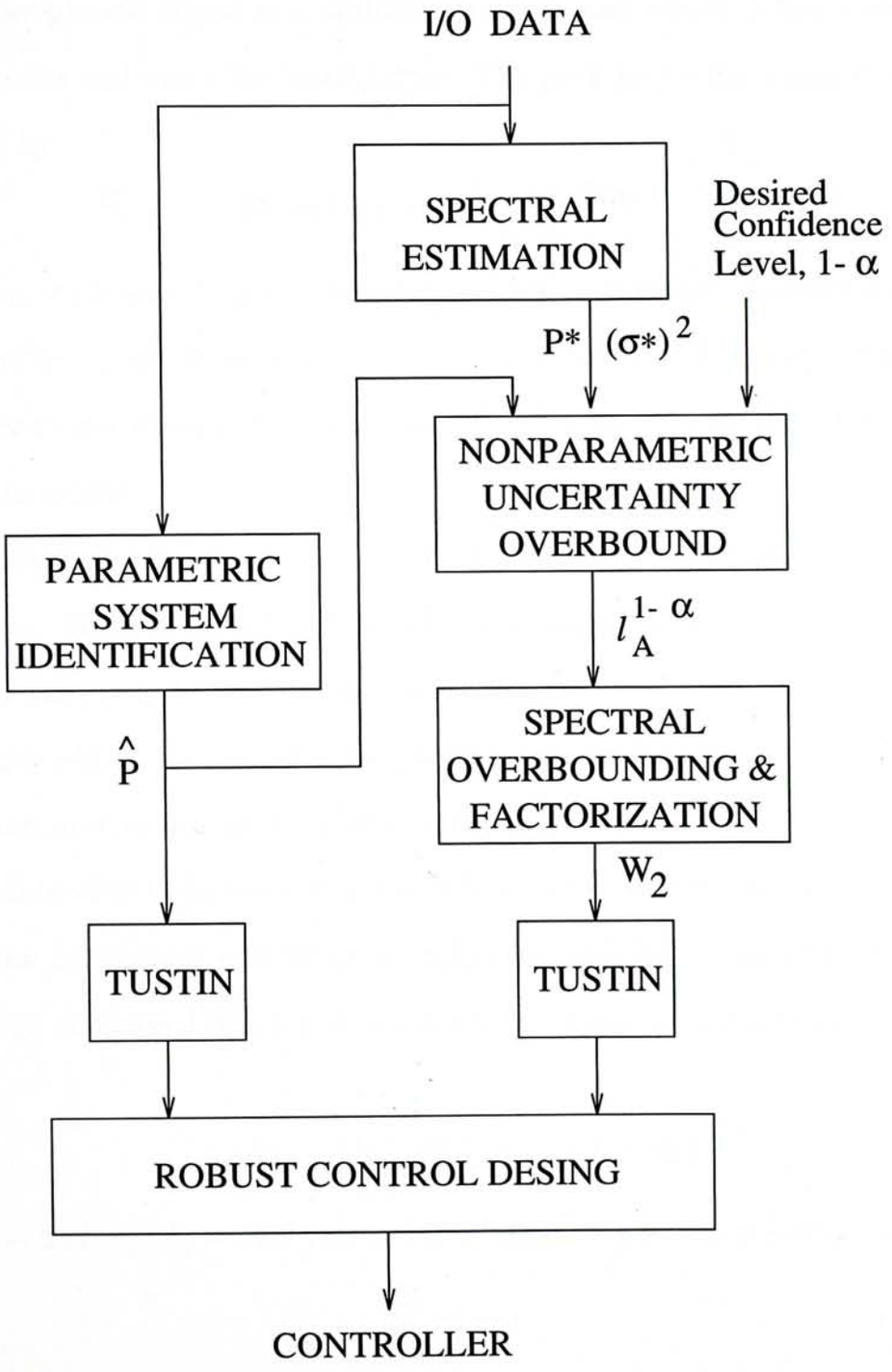

Figure 3.1: System identification and robust control design

3.2 The Schroeder-phased Input Design

A Schroeder-phased signal is a multisinusoidal signal which is the sum of specified harmonics and has a low *peak factor*. The *peak factor* for a signal $u(t)$ could be defined by

$$Peak factor = \frac{x_{max} - x_{min}}{2\sqrt{2}x_{rms}} \tag{3.1}$$

where x_{max}, x_{min} and x_{rms} are, respectively the maximum, minimum and RMS values of $u(t)$. A signal with a low peak factor will has few large peaks occurring at some time during the signal period, with only a small signal amplitude between the peaks.

For system identification, the input signal should be designed to have a low peak factor. Since a signal having a large peak factor will cause system non-linearities, particularly saturation non-linearities, be easily reached; while the small amplitude of the signal throughout most of the rest of the period could lead to inaccuracies due to amplitude quantization if the signal is digitized.

A considerable reduction in peak factor can be achieved in most cases by phasing the harmonics according to Schroeder [13, 22]. Consider the periodic input design composed of a harmonically related sum of sinusoids with sampling period T,

$$u_s(k) = \beta \sum_{i=1}^{n_s} \sqrt{2\alpha_i} cos(\omega_i kT + \Phi_i) \tag{3.2}$$

where $\omega_i = 2\pi i/T_p$, $T_p = N_s T$, $n_s = N_s/2$. The power is normalized as,

$$\sum_{i=1}^{n_s} \alpha_i = 1 \tag{3.3}$$

In order to achieve a low peak factor, the sinusoids are phased as,

$$\Phi_i = 2\pi \sum_{j=1}^{i} j\alpha_j \tag{3.4}$$

In this thesis, we have also set $\alpha_i = 1/n_s$ for all i, resulting $\Phi_i = \frac{\pi}{n_s}(i^2 + i)$.

3.3 The Statistical Additive Uncertainty Bounds

In this section we will present the statistical analysis results of the spectral estimate using multisinusoidal signal as input signal (Schroeder-phased signal is a multisinusoidal signal).

Assuming the true plant to be identified is an unknown exponentially stable linear time-invariant system assumed to have a sampled-data representation $P_{true}(z^{-1})$ and has a parametric nominal estimate $\hat{P}$, we have the following definitions.

Definition 3.3.1 *A set of plants $\Omega_A(\hat{P}, l_A(\omega))$ associated with a specified overbound $l_A(\omega)$ on the additive error, i.e.,*

$$\Omega_A(\hat{P}, l_A(\omega)) = \{P : (P - \hat{P}) \leq l_A(\omega), \quad \forall\, \omega \in [0, \pi/T]\}$$

T is the sampling period.

Definition 3.3.2 *$l_A^{1-\alpha}(\omega)$ is said to be an* overbound on the additive uncertainty with statistical confidence $(1 - \alpha) \times 100\%$ *if,*

$$Prob\,\{P_{true} \in \Omega_A(\hat{P}, l_A^{1-\alpha}(\omega))\} \geq 1 - \alpha$$

Definition 3.3.3 DFT Frequency Domain Estimator (Spectral Estimate) *with m windows*

$$P^*(\omega_i) = \frac{\frac{1}{m}\sum_{l=1}^{m} Y_s^l(\omega_i)}{U_s(\omega_i)} \tag{3.5}$$

†It is emphasized that the DFT is evaluated precisely on the points of support of the Schroeder-phased input

where,

$$Y_s^l(\omega_i) = \frac{1}{N_s}\sum_{k=0}^{N_s-1} y_s^l(k)e^{-j\omega_i kT}; \quad U_s(\omega_i) = \frac{1}{N_s}\sum_{k=0}^{N_s-1} u_s(k)e^{-j\omega_i kT} \tag{3.6}$$

Definition 3.3.4 Noise Variance Estimator

$$(\sigma^*)^2 = \frac{\sum_{l=1}^{m}\sum_{i=1}^{N_s}|Y_s^l(\omega_i) - \bar{Y}(\omega_i)|^2}{N_s(mN_s - 2n_s)} \tag{3.7}$$

where,

$$\bar{Y}(\omega_i) = \frac{1}{m}\sum_{l=1}^{m} Y_s^l(\omega_i) \tag{3.8}$$

We now summarized the main results in the following theorem.

Theorem 3.3.1 ([9]) *Assume the Schroeder-phased sinusoidal input u_s, defined in (3.2) is applied to P_{true}, giving rise to the steady-state output y_s. Assuming white measurement noise. Let the spectral estimate defined in (3.5), be computed based on $m > 1$ periods of u_s and y_s. Then,*

1. *If σ, measurement noise variance, is known, the exact error probability distributions are given as,*

$$\frac{|P_{true}(e^{-j\omega_i T}) - P^*(\omega_i)|^2}{\sigma^2 c_{ii}} \sim \chi^2(2) \tag{3.9}$$

$$c_{ii} = 1/(\alpha_i m N_s) \tag{3.10}$$

where $\chi^2(\nu)$ denotes a Chi-Squared distribution with ν degrees of freedom.

2. *If σ is unknown, and estimated using (3.7), the exact error probability distributions are given as,*

$$\frac{|P_{true}(e^{-j\omega_i T}) - P^*(\omega_i)|^2}{2(\sigma^*)^2 c_{ii}} \sim F(2, mN_s - 2n_s) \tag{3.11}$$

where $F(\nu_1, \nu_2)$ denotes a Fisher distribution with ν_1 over ν_2 degrees of freedom.

For proof, refer to [9]. The following corollary to Theorem 3.3.1 could be used if statistical confidence regions are desired.

Collary 3.3.1 ([9]) *Under the conditions of Theorem 3.3.1, the* $(1-\alpha)\times 100\%$ *confidence bounds associated with the DFT estimates are summarized below,*

$$|P_{true}(e^{-j\omega_i T})-P^*(\omega_i)|^2 \leq \begin{cases} c_{ii}\sigma^2\chi^2_{1-\alpha}(2) & \text{for } \sigma^2 \text{ known} \\ c_{ii}(\sigma^*)^2 F_{1-\alpha}(2, mN_s - 2n_s) & \text{for } \sigma^2 \text{ estimated by } (\sigma^*)^2 \end{cases} \tag{3.12}$$

Several important properties of the spectral estimates are summarized below [9]:

1. $P^*(\omega_i)$ is unbiased and consistent estimator of $P_{true}(e^{-j\omega_i T})$.

2. $P^*(\omega_i)$ is statistically independent of $P^*(\omega_j)$ for $i \neq j$. Thus, suppose the spectral estimate has n_s number of points, and the overbound $l_A^{1-\alpha}(\omega)$ has a overall specified confidence $(1-\alpha)$; then for each grid point at ω_i, $i = 1, \ldots, n_s$, a quantity $1-\kappa$ could be determined such that $1-\alpha = (1-\kappa)^{n_s}$. This is the confidence factor for the uncertainty overbound for each grid point.

3. $(\sigma^*)^2$ is an unbiased and consistent estimator of σ^2.

Figure 3.2 shows a Nyquist plot of the spectral estimate and the corresponding disc of uncertainty. The confidence region for the case of σ^2 estimated by $(\sigma^*)^2$ is seen as a circular disc centered at $P^*(\omega_i)$ of radius ϵ_i (from 3.11),

$$\epsilon_i^2 = 2(\sigma^*)^2 c_{ii} F_{1-\alpha}(2, mN_s - 2ns) \tag{3.13}$$

where $F_{1-\alpha}(\nu_1, \nu_2)$ denote the $(1-\alpha)\times 100$ percentiles for the Fisher distribution with ν_1 over ν_2 degrees of freedom. The case is similar when σ is known.

The discussions in this section could be summarized in Figure 3.3.

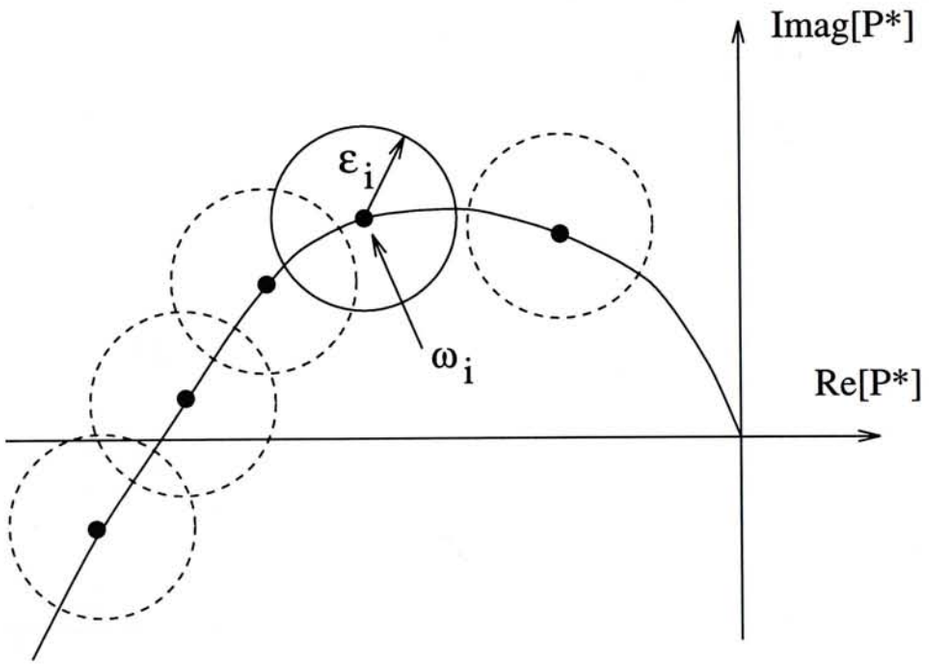

Figure 3.2: Nyquist plot showing spectral estimate $P^*(\omega_i)$ with $(1-\alpha) \times 100\%$ confidence radius ϵ_i [23]

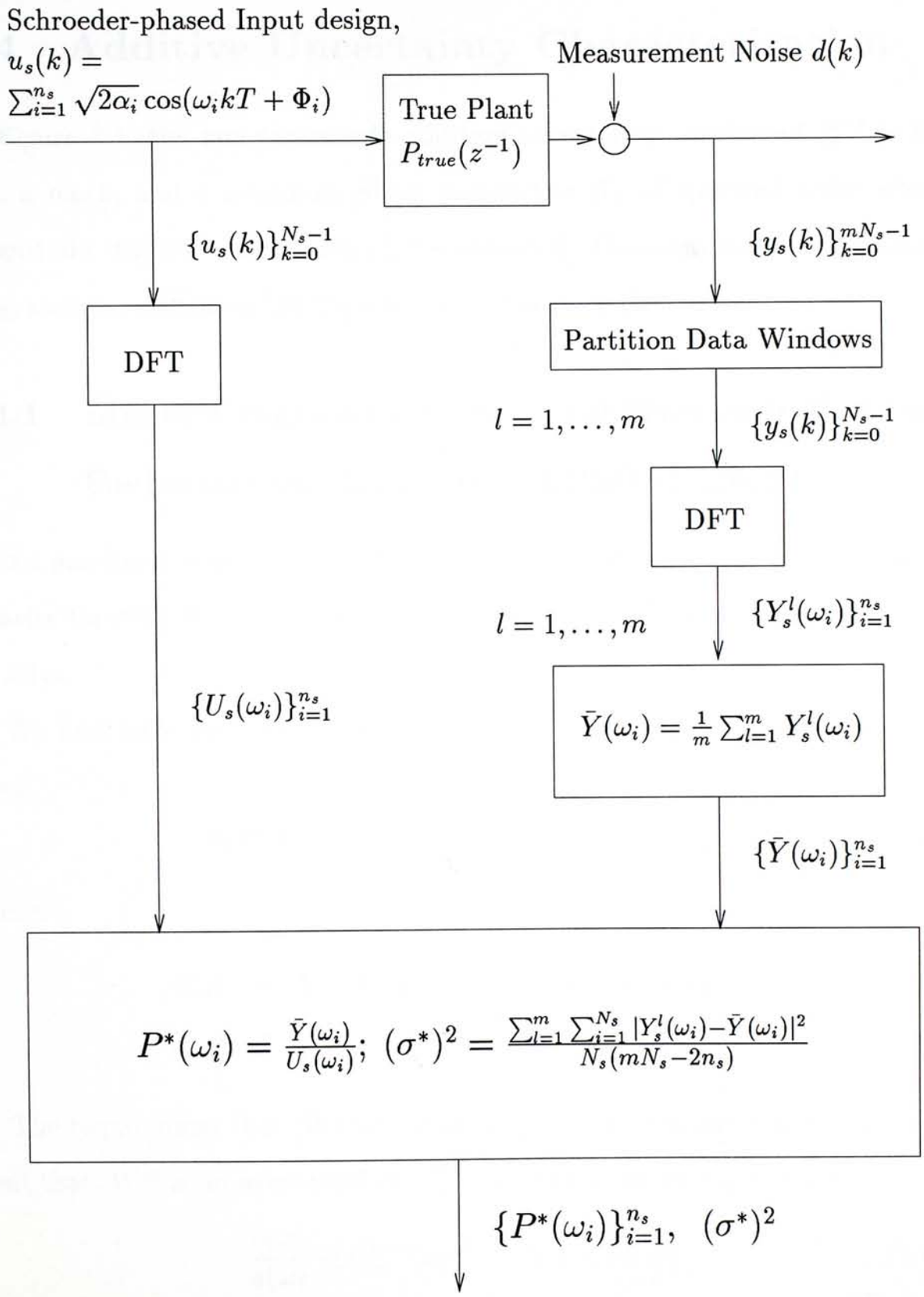

Figure 3.3: Frequency domain estimation using Schroeder-phased sinusoid input design [9]

3.4 Additive Uncertainty Characterization

In Figure 3.1, the non-parametric additive uncertainty overbound $l_A^{1-\alpha}$ is fed into a block, and a minimum phase parametric W_2 of specified order whose magnitude "tightly" overbounds $l_A^{1-\alpha}$ is obtained. This section describe a linear programming algorithm [20,21] which could achieve this aim.

3.4.1 Linear Programming Spectral Overbounding and Factorization Algorithm (LPSOF) [20,21]

First a non-linear constrained optimization is posed to compute a minimal-phase transfer function W of order m such that $|W|$ is a tight overbound on $l_A^{1-\alpha}(\omega)$ for all ω.

We first form the quantity $W(z)W(z^{-1})$ and evaluating on the unit circle gives,

$$W(z)W(z^{-1}) = W^*(z^{-1})W(z^{-1}) = \frac{b(\omega)}{a(\omega)} \tag{3.14}$$

where,

$$b(\omega) = b_0 + b_1\cos(\omega T) + \cdots + b_m\cos(m\omega T) \tag{3.15a}$$

$$a(\omega) = 1 + a_1\cos(\omega T) + \cdots + a_m\cos(m\omega T) \tag{3.15b}$$

The requirement that $|W|$ overbounds $l_A^{1-\alpha}(\omega)$ is equivalent to the requirement that $|W|^2$ is an overbound on $(l_A^{1-\alpha}(\omega))^2$ and can be expressed as,

$$\frac{b(\omega)}{a(\omega)} \geq (l_A^{1-\alpha}(\omega))^2 \qquad \forall\, \omega \in [0, \frac{\pi}{T}] \tag{3.16}$$

The requirement that $|W|^2$ be a "tight" overbound can be expressed as,

$$\min_{a(\omega),b(\omega)} \delta \quad \text{where} \quad \delta = \max_{\omega}\{(\frac{b(\omega)}{a(\omega)} - (l_A^{1-\alpha}(\omega))^2)q^{-1}(\omega)\} \tag{3.17}$$

This criterion minimizes a worst-case error δ, which is frequency weighted by the quantity $q^{-1}(\omega)$.

The requirement that the overbound b/a has spectral factorization W^*W can be satisfied by the following constraints:

$$b(\omega)/a(\omega) > 0 \qquad \forall\, \omega \in [0, \pi/T] \tag{3.18a}$$

$$a(\omega) > 0 \qquad \forall\, \omega \in [0, \pi/T] \tag{3.18b}$$

(3.18) could be enforced by the following constraints,

$$a(\omega) \geq \underline{a}(\omega) > 0 \tag{3.19a}$$

$$b(\omega) \geq \underline{b}(\omega) > 0 \tag{3.19b}$$

for some small $\underline{a}$ and $\underline{b}$.

The linear programming algorithm could solve the constrained nonlinear optimization problem described by (3.16), (3.17) and (3.19) on grid of points $\Lambda = \{\omega_1, \ldots, \omega_{n_s}\}$. The constrained optimization problem restricted to points of the set Λ can be written as,

$$\min_{\delta,\, a_j,\, b_j} \tag{3.20a}$$

subject to

$$b(\omega_i) - (l_A^{1-\alpha}(\omega_i))^2 a(\omega_i) \geq 0 \tag{3.20b}$$

$$b(\omega_i) - (l_A^{1-\alpha}(\omega_i))^2 a(\omega_i) \leq \delta q(\omega_i) a(\omega_i) \tag{3.20c}$$

$$b(\omega_i) > \underline{b}\,; \quad a(\omega_i) > \underline{a} \tag{3.20d}$$

$$\forall\, \omega_i,\ i = 1, \ldots, n_s$$

For a fixed δ, (3.20) is simply a linear programming problem to find a *feasible* solution for the coefficients a_j and b_j. Hence, the joint optimization problem

can be solved by a nested search procedure where an outer-loop systematically decreases δ while an inner loop finds feasible solutions in the variables a and b for fixed δ. The procedures terminates when the smallest δ is found which admits a feasible solution. In this thesis, the method of bisection is used to find the minimum δ.

By choosing the the grid points set Λ dense enough, the inequalities in (3.20) will not be violated *in-between* grid points. Further modifications of the algorithm to ensure the non-violation of the inequalities in-between grid points could be found in [21].

Chapter 4

Basic System Identification and Model Reduction Algorithms

In this chapter, we will briefly cover the basic system identification algorithms and model reduction algorithms employed in this research. Section 4.1 will present the *Eigensystem Realization Algorithm* (ERA) which use time-domain input/output data to obtain a discrete-time state space model of the plant. Section 4.2 will introduce a frequency-domain identification method which use frequency-domain input/output data (spectral estimate) to obtain a transfer function model of the plant.

A brief discussion of the *balanced model reduction* algorithm will follow (sections 4.3 and 4.4). This technique will be used to generate results in chapter 5 to chapter 8.

4.1 The Eigensystem Realization Algorithm

We will describe the basic algorithm first, which requires system Markov parameters to realize a discrete-time state space model [24, 25]. Then the method to obtain system Markov parameters from time-domain input/output data will be covered.

4.1.1 Basic Algorithm

Given a nth order discrete-time state equation with m inputs and p outputs:

$$\mathbf{x}(k+1) = A\mathbf{x}(k) + B\mathbf{u}(k) \qquad \mathbf{x}(k) \in \mathcal{R}^n \quad \mathbf{u}(k) \in \mathcal{R}^m \tag{4.1a}$$

$$\mathbf{y}(k) = C\mathbf{x}(k) + D\mathbf{u}(k) \qquad \mathbf{y}(k) \in \mathcal{R}^p \tag{4.1b}$$

Solving for $y(k)$:

$$y(k) = CA^k x_0 + \sum_{i=0}^{k-1} \left(CA^{k-i-1} Bu(i) \right) + Du(k) \tag{4.2}$$

Define the *system Markov parameters*:

$$\begin{aligned} Y(0) &= D \\ Y(1) &= CB \\ Y(2) &= CAB \\ &\vdots \\ Y(k) &= CA^{k-1}B \end{aligned}$$

equation (4.2) becomes:

$$y(k) = CA^k x_0 + \sum_{i=0}^{k} (Y(k-i)u(i)) + Y(0)u(k) \tag{4.3}$$

To obtain estimate $\{\hat{A}, \hat{B}, \hat{C}, \hat{D}\}$ of $\{A, B, C, D\}$, we form two Hankel matrix with $Y(i)$:

$$
\begin{aligned}
H_{rs}(0) &= \begin{bmatrix} Y(1) & Y(2) & \cdots & Y(s) \\ Y(2) & Y(3) & \cdots & Y(s+1) \\ \vdots & & \vdots & \\ Y(r) & Y(r+1) & \cdots & Y(r+s-1) \end{bmatrix} \\
&= \begin{bmatrix} C \\ CA \\ \vdots \\ CA^{r-1} \end{bmatrix} \begin{bmatrix} B & AB & \cdots & A^{s-1}B \end{bmatrix} = \mathcal{P}_r \mathcal{Q}_s \\
H_{rs}(1) &= \begin{bmatrix} Y(2) & Y(3) & \cdots & Y(s+1) \\ Y(3) & Y(4) & \cdots & Y(s+2) \\ \vdots & & \vdots & \\ Y(r+1) & Y(r+2) & \cdots & Y(r+s) \end{bmatrix} \\
&= \begin{bmatrix} C \\ CA \\ \vdots \\ CA^{r-1} \end{bmatrix} A \begin{bmatrix} B & AB & \cdots & A^{s-1}B \end{bmatrix} = \mathcal{P}_r A \mathcal{Q}_s
\end{aligned}
$$

where $\mathcal{P}_r = [CA^T C^T \cdots (A^{r-1})^T C^T]^T$ and $\mathcal{Q}_s = [BAB \cdots A^{s-1}B]$ are the observability matrix and controllability matrix respectively. Performing *Singular Value Decomposition* (SVD) on $H_{rs}(0)$ and $H_{rs}(1)$:

$$H_{rs}(0) = \mathcal{P}_r \mathcal{Q}_s = R_n \Sigma_n^{\frac{1}{2}} \Sigma_n^{\frac{1}{2}} S_n^T \tag{4.4a}$$

$$H_{rs}(1) = \mathcal{P}_r \mathcal{Q}_s = R_n \Sigma_n^{\frac{1}{2}} A \Sigma_n^{\frac{1}{2}} S_n^T \tag{4.4b}$$

Define O_i as a null matrix of order i, $E_m^T = [I_m\, O_p\, \cdots\, O_p\, O_p]$ where p is the number of outputs, and $E_m^T = [I_m\, O_m\, \cdots\, O_m]$ where m is the number of inputs. Then

$$\begin{aligned} Y(k) &= CA^{k-1}B \\ &= E_p^T R_n \Sigma_n^{\frac{1}{2}} \left[\Sigma_n^{-\frac{1}{2}} R_n^T H(1) S_n \Sigma_n^{-\frac{1}{2}}\right]^{k-1} \Sigma_n^{\frac{1}{2}} S_n^T E_m \end{aligned} \tag{4.5}$$

For proof of (4.5), see [26].

The following could be then be taken as an estimate of $\{A, B, C, D\}$:

$$\hat{A} = \Sigma_n^{-\frac{1}{2}} R_n^T H(1) S_n \Sigma_n^{-\frac{1}{2}} \tag{4.6a}$$

$$\hat{B} = \Sigma_n^{\frac{1}{2}} S_n^T E_m \tag{4.6b}$$

$$\hat{C} = E_p^T R_n \Sigma_n^{\frac{1}{2}} \tag{4.6c}$$

$$\hat{D} = Y(0) \tag{4.6d}$$

Note that the resultant estimate in (4.6) produces a *balanced state-space realization* i.e. the controllability grammian and observability grammian will be equal (see section 4.3).

4.1.2 Estimating Markov Parameters from Input/Output data: Observer/Kalman Filter Identification (OKID)

The Markov parameters have to be estimated from the I/O data, and one of the method is the Observer/Kalman filter Identification (OKID) algorithm [26–28]. The basic idea of OKID algorithm is to use an asymptotically stable observer to form a stable discrete state-space model for the system to be identified. The observer could be a deadbeat one. Then the fast decaying observer Markov parameters are identified rather than the slow decaying Markov parameters.

Here, we only outlined the OKID method briefly, the detail concepts and procedures could be found in [26–28]. The system in (4.1) with a observer is

$$\mathbf{x}(k+1) = \bar{A}\mathbf{x}(k) + \bar{B}\mathbf{u}(k) \tag{4.7a}$$

$$\mathbf{y}(k) = C\mathbf{x}(k) + D\mathbf{u}(k) \tag{4.7b}$$

where

$$A = A + MC \qquad B = [\ B + MD \quad -M\ ] \qquad v(i) = \begin{bmatrix} u(i) \\ y(i) \end{bmatrix}$$

M is the observer gain, which could be chosen such that the a deadbeat observer is obtain. Fast decay of observer Markov parameters will result. We have done so in our implementation. For such a dead beat observer and assuming zero initial conditions:

$$\underline{y} = \bar{\mathcal{Y}}\mathbf{V} \tag{4.8}$$

where

$$\begin{aligned}
\underline{y} &= [\ y(0) \quad y(1) \quad y(2) \quad \cdots \quad y(q) \quad \cdots \quad y(l-1)\ ] \\
\bar{\mathcal{Y}} &= [\ D \quad C\bar{B} \quad C\bar{A}\bar{B} \quad \cdots \quad C\bar{A}^{q-1}\bar{B} \quad \cdots \quad C\bar{A}^{q-1}\bar{B}\ ] \\
&= [\ \bar{Y}_{-1} \quad \bar{Y}_0 \quad \bar{Y}_1 \quad \cdots \quad \bar{Y}_{q-1} \quad \cdots \quad \bar{Y}_{q-1}\ ]
\end{aligned}$$

$$\mathbf{V} = \begin{bmatrix}
u(0) & u(1) & u(2) & \cdots & u(q) & \cdots & u(l-1) \\
 & v(0) & v(1) & \cdots & v(q-1) & \cdots & v(l-2) \\
 & & v(0) & \cdots & v(q-1) & \cdots & v(l-2) \\
 & & & \ddots & \vdots & \cdots & \vdots \\
 & & & & v(0) & \cdots & v(l-q-1)
\end{bmatrix}$$

l is the number of data points. Note that

$$\bar{Y}_k = C\bar{A}^k\bar{B}$$

$$
\begin{aligned}
&= [\ C(A+MC)^k(B+MD) \quad -C(A+MC)^kM\ ] \\
&= [\ \bar{Y}_k^{(1)} \quad \bar{Y}_k^{(2)}\ ], \qquad k=0,1,2,\cdots
\end{aligned}
$$

If zeros initial conditions could not be assumed, we change $\mathbf{V}$ to $\bar{\mathbf{V}}$ and $\underline{y}$ to $\underline{\bar{y}}$

$$
\bar{\mathbf{V}} = \begin{bmatrix}
u(q) & u(q+1)\cdots & & u(l-1) \\
v(q-1) & v(q) & \cdots & v(l-2) \\
v(q-2) & v(q-1) & \cdots & v(l-3) \\
\vdots & \vdots & \vdots & \ddots \\
v(0) & v(1) & \cdots & v(l-q-1)
\end{bmatrix}
$$

$$
\underline{\bar{y}} = [\ y(q+1) \quad y(q+2) \quad \cdots \quad y(l-1)\ ]
$$

We select q to be the number of observer Markov parameters. q must be chosen such that $pq > n$. And the least squares solution for (4.8) would be

$$
\begin{aligned}
\bar{\mathcal{Y}} &= \underline{y}\mathbf{V}^T[\mathbf{V}\mathbf{V}^T]^{-1} \qquad \text{for zero initial conditions} \\
\bar{\mathcal{Y}} &= \underline{\bar{y}}\bar{\mathbf{V}}^T[\bar{\mathbf{V}}\bar{\mathbf{V}}^T]^{-1} \qquad \text{for non-zero initial conditions}
\end{aligned}
$$

The actual system Markov parameters ($[Y_0 \cdots Y_k]^T$) and the observer Markov parameters are connected by the following matrix:

$$
\begin{bmatrix}
I_q & & & \\
-\bar{Y}_0^{(2)} & I & & \\
\vdots & \cdots & \ddots & \\
-\bar{Y}_{k-1}^{(2)} & -\bar{Y}_{k-2}^{(2)} & \cdots & I
\end{bmatrix}
\begin{bmatrix} Y_0 \\ Y_1 \\ \vdots \\ Y_k \end{bmatrix}
=
\begin{bmatrix}
\bar{Y}_0^{(1)} + \bar{Y}_0^{(2)}D \\
\bar{Y}_1^{(1)} + \bar{Y}_1^{(2)}D \\
\vdots \\
\bar{Y}_k^{(1)} + \bar{Y}_k^{(2)}D
\end{bmatrix} \tag{4.9}
$$

The Markov parameters could be unique determined by solving the above equations. Then the ERA algorithm could be applied the these estimated Markov parameters to obtain $\{\hat{A}, \hat{B}, \hat{C}, \hat{D}\}$

4.2 The Frequency-Domain Identification via 2-norm Minimization

This section will briefly discuss the frequency-domain MIMO identification via 2-norm minimization develop in [29,30]. A Gauss-Newton iteration is developed to minimize the 2-norm of the error between frequency domain data and a matrix fraction transfer function estimate.

Let $\hat{P}(\zeta)$ be a m-input/p-output transfer function matrix in the complex variable ζ, where ζ can be chosen as any complex variable of interest (in frequency domain), for example,

- the Laplace operator: $\zeta = j\omega$, or
- the shift z operator: $\zeta = e^{j\omega T}$, or
- the delta operator [31]: $\zeta = (e^{j\omega T} - 1)/T$

The method tries to fit $\hat{P}$ to noisy frequency response data (spectral estimate) $\mathcal{P}$ obtained over a grid of N frequency points:

$$\mathcal{P}(\omega_i) \approx \hat{P}(\zeta(\omega_i)) \qquad \text{i=1, } \cdots, N$$

The goal is to find a transfer function estimate $\hat{P}$ which minimizes the 2-norm of the error between the estimate and the data,

i.e.,

$$\mathcal{F} = \sum_{i=1}^{N} W_f^2(\omega_i) \| \mathcal{P}(\omega_i) - \hat{P}(\zeta(\omega_i)) \|_f^2 \tag{4.10}$$

where $W_f(\omega_i)$ is a specified non-parametric frequency weighting, and the $\| \cdot \|_f$ denote the Frobenious norm:

$$\| X \|_f^2 = tr(X^H X)$$

4.3 Balanced Realization and Truncation

The balance realization and balance truncation (model reduction) has been covered in many advanced text books [32–35]. Thus we only give a brief review of the algorithm. Here, only the continuous-time case is discussed; the discrete-time case is exactly the same except a change in the Lyapunov equations.

Definition 4.3.1 *Given an nth order, m-input, p-output, linear time-invariant, asymtotically stable system with transfer function matrix $G(s)$, a minimal realization of $G(s) = C(sI - A)^{-1}B + D$ is internally balanced if $\{A, B, C\}$ satisfy the following Lyapunov equations*

$$\mathcal{Q}A^T + A\mathcal{Q} + BB^T = 0 \tag{4.11a}$$

$$\mathcal{P}A + A^T\mathcal{P} + CC^T = 0 \tag{4.11b}$$

$$\mathcal{Q} = \mathcal{P} = \Lambda \tag{4.11c}$$

and

$$\Lambda = \begin{bmatrix} \lambda_1 & & & \\ & \lambda_2 & & \\ & & \ddots & \\ & & & \lambda_n \end{bmatrix} \tag{4.12a}$$

where $\lambda_i \geq \lambda_{i+1} \geq 0, \quad i = 1, 2, \ldots, n-1.$

In (4.11a), $\mathcal{Q}$ is the controllability grammian, and in (4.11b), $\mathcal{P}$ is the observability grammian. Thus, a system is *balanced* when its controllability and observability grammians are equal and have a diagonal form. Partitioning the system

$\{A, B, C\}$ and Λ as

$$A = \begin{bmatrix} A_r & A_{12} \\ A_{21} & A_{22} \end{bmatrix}, \quad B = \begin{bmatrix} B_r \\ B_2 \end{bmatrix}, \quad C = \begin{bmatrix} C_r & C_2 \end{bmatrix}, \quad \Lambda = \begin{bmatrix} \Lambda_r & 0 \\ 0 & \Lambda_2 \end{bmatrix} \tag{4.13}$$

where A_r, $\Lambda_r \in \mathcal{R}_{r\times r}$, $B_r \in \mathcal{R}_{r\times m}$, $C_r \in \mathcal{R}_{p\times r}$ and $r < n$. Then the reduced-order system $\{A_r, B_r, C_r\}$ is a good approximation of the system $\{A, B, C\}$ if $\lambda_r \geq \lambda_{r+1}$. And the following two properties are true:

Theorem 4.3.1 ([36]) *For a balanced asymptotically stable system $\{A, B, C\}$ with minimal state space realization, and with $\mathcal{P}$, $\mathcal{Q}$ in the form of (4.12a) satisfying (4.11c) and partitioned as in (4.13), if $\lambda > \lambda_{r+1}$, then both subsystem $\{A_r, B_r, C_r\}$ and $\{A_2, B_2, C_2\}$ are asymtotically stable.*

Theorem 4.3.2 ([37]) *With the same assumptions as in Theorem 4.3.1, there holds a frequency error bound*

$$\| C(j\omega I - A)^{-1}B - C_r(j\omega I - A_r)^{-1}B_r \|_\infty \leq 2(\lambda_{r+1} + \cdots + \lambda_n) = 2tr(\Lambda_2). \tag{4.14}$$

According to (4.14), if for a particular r, $\lambda_r \gg \lambda_{r+1}$, then the subsystem $\{A_r, B_r, C_r\}$ could be a good reduced-order model of $\{A, B, C\}$ since the maximum of the error in the frequency domain will be bounded by a small value $(2tr[\Lambda_2])$.

4.4 Frequency Weighted Balanced Truncation

Now consider a frequency weighted balanced truncation. The aim is to approximate $\{A, B, C\}$ more accurately in some frequency regions at the expense of larger error at other frequency regions. Stating mathematically, consider a stable

input weight $W_i(s)$ and a stable output weight $W_o(s)$, realized in their minimal state space form as

$$\begin{aligned} W_i(s) &= C_i(sI - A_i)^{-1}B_i + D_i \\ W_o(s) &= C_o(sI - A_o)^{-1}B_o + D_o \end{aligned}$$

Then the weighted reduction problem is to find a stable lower-order transfer function G_r (of order $r < n$), such that the norm $\| W_i(s)[G(s) - G_r(s)] \|_\infty$ is minimal or at least is approximate minimal. The algorithm achieving approximate minimal is describe below [37].

The frequency-weighted transfer function $W_o(s)G(s)W_i(s)$ has a representation with the following state space matrices:

$$\bar{A} = \begin{bmatrix} A_o & B_oC & B_oDC_i \\ 0 & A & BC_i \\ 0 & 0 & A_i \end{bmatrix}, \quad \bar{B} = \begin{bmatrix} B_oDD_i \\ BD_i \\ B_i \end{bmatrix},$$

$$\bar{C} = [\, C_o \quad D_oC \quad D_oDC_i \,], \quad \bar{D} = D_oDD_i.$$

Let

$$\bar{\mathcal{Q}} = \begin{bmatrix} Q_o & Q_{12} & Q_{13} \\ Q_{12}^T & Q & Q_{23} \\ Q_{13}^T & Q_{23}^T & Q_i \end{bmatrix}, \qquad \bar{\mathcal{P}} = \begin{bmatrix} P_o & P_{12} & P_{13} \\ P_{12}^T & P & P_{23} \\ P_{13}^T & P_{23}^T & P_i \end{bmatrix}$$

be the solutions of the following Lyapunov equations:

$$\bar{Q}\bar{A}^T + \bar{A}\bar{Q} + \bar{B}\bar{B}^T = 0 \tag{4.15a}$$

$$\bar{P}\bar{A} + \bar{A}^T\bar{P} + \bar{C}^T\bar{C} = 0 \tag{4.15b}$$

$\mathcal{Q}$ and $\mathcal{P}$ can be regarded as the frequency-weight controllability and observability grammians for the original transfer function $G(s)$. Consider a linear transformation $\{A, B, C\}$ which makes $\mathcal{Q}_{new} = \mathcal{P}_{new} = \Sigma = diag(\sigma_1, \sigma_2, \ldots, \sigma_n)$,

$\sigma_i \geq \sigma_{i+1}$. The new realization $\{A, B, C\}$ is called a frequency-weighted balanced realization.

Partition $\{A, B, C\}$ as in (4.13) and Σ as

$$\Sigma = \begin{bmatrix} \Sigma_r & 0 \\ 0 & \Sigma_2 \end{bmatrix}, \qquad \text{where} \quad \Sigma_r \in \mathcal{R}_{r\times r} \quad \text{and} \quad r < n$$

As in section 4.3, the reduction is achieved by eliminating the rows and columns of A, B and C corresponding to Σ_2 in Σ.

Chapter 5

Plant Model Reduction and Robust Control Design

The main purpose of the research done in this chapter is to investigate the feasibility of a new Iterative Reweighting Scheme for Integrated System Identification/Robust Control Design. To start with, a simplified case is first investigated: Integrated Plant Model Reduction/ Robust Control Design with iterative reweighting. And then we move to the system identification case.

Section 5.2 will introduce the iterative model reduction scheme and the detail procedures. Then a design example will followed. A improved version of the scheme will be presented in section 5.5. Finally, the integration of system identification with the iterative reweighting scheme will be investigated.

5.1 Problem Formulation

The integrated ID/Robust Control synthesis problem can be posed as follows :

Given experimental data χ and performance weighting W_1,

$$\max_{\hat{P}C} \gamma \tag{5.1a}$$

subject to

$$J(\gamma, \chi, \hat{P}, C) < 1 \tag{5.1b}$$

with,

$$J = \| \gamma |W_1(j\omega) S(\hat{P}, C)| + |\ell_A(\omega) R(\hat{P}, C)| \|_\infty \tag{5.1c}$$

where, $\hat{P}$ is the identified model, C the robust controller, $S(\hat{P}, C) = (I + \hat{P}C)^{-1}$ the sensitivity function, and $\ell_A(\omega)$ the nonparametric overbound of the additive uncertainty. ℓ_A could be the statistical overbound described in section 3.3. $R(\hat{P}, C) = C(I + \hat{P}C)^{-1}$ is termed the R-parameter.

The problem as formulated in (5.1) is intractable. A pseudo-relaxation (PR) approach [10] [38] is adopted to obtain an approximate solution. As depicted in Figure 5.1, the PR algorithm conducts control design and frequency weighted system identification steps iteratively.

5.2 Iterative Reweighting Scheme

The Iterative Reweighting Scheme [38] [39] could be summarized in figure 5.1.

Expressing the PR scheme in words :

1. A non-parametric plant estimate, P^* is obtained from the experimental data using spectral estimation method over a grid of frequency points. The input to the plant is chosen to be Schroeder phased signals, which has a favourable statistical description and low peak factor (Chapter 3).

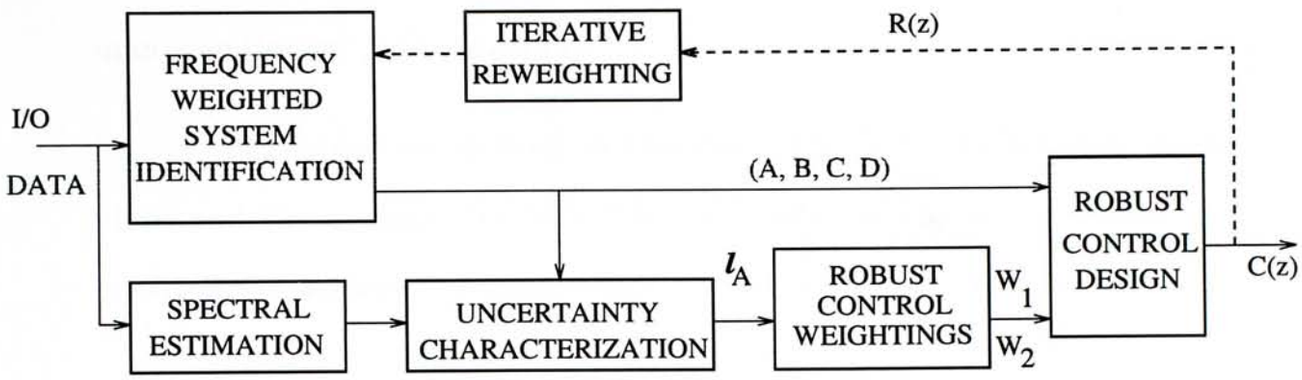

Figure 5.1: An Integrated System ID/Robust Control Design with Iterated Reweighting Scheme

2. A parametric system model, $\hat{P}(z)$ is also obtained using either system identification algorithm with time-domain (e.g. ERA) or frequency-domain input/output data (e.g. frequency weighted curve fitting).

3. A non-parametric statistical bound (ℓ_A) on the additive error, $\delta = P^* - \hat{P}(e^{j\omega T})$ is obtained using the results in section 3.3. T is the sampling time.

4. A parametric overbound is then obtained manually or by spectral overbounding and factorization technique (section 3.4). This is the $W_2(s)$ in section 2.4.

5. The plant model, $\hat{P}$, and the parametric overbound, W_2 are then incorporated into a robust control design using MATLAB Robust Control Toolbox.

6. Performance is then enhanced by conducting iterative frequency weighted system identification with weighting function $R(z)$ to yield an update parametric plant model.

7. The iteration is continued until no further improvement in control performance indicator*, γ, is possible.

8. Tustin transformation is used to transform the function between the z-plane and the w-plane (for MATLAB controller synthesis procedures). A controller in z-plane is required for implementation on digital computer.

5.2.1 Rationale Behind the Scheme

The rationale behind the PR algorithm is that the control design step would minimize the first term in J dominantly while the weighted identification step would minimize the second term dominantly. In practice, upon determination of a parametric model $\hat{P}$ and the function W_2 which overbounds $\ell_A(\omega)$, the control design step is performed using MATLAB Robust Control Tool Box [15] which solved a weighted mixed-sensitivity H_∞ problem with modified cost function:

$$J = \| \quad \gamma |W_1(j\omega) S(\hat{P}, C)|^2 + |W_2(\omega) R(\hat{P}, C)|^2 \quad \|_\infty \tag{5.2}$$

A few remarks concerning the minimization of the cost in (5.2) (cf. [10]):

1. The norms are frequency weighted by expressions which involve the performance W_1 and the controller from the previous iteration. This property is consistent with the philosophy that the best model for control design requires advanced knowledge of the inputs "seen" by the model, and hence the process of determining model and controller are inevitably "iterative" in nature.

*See section 2.5

2. The expression is complicated by dependence on W_2 which is itself a function of the raw I/O data and the plant estimate $\hat{P}$. However, the additional complexity ensures that the additive uncertainty is "frequency shaped" by the identification step to best support the robust performance objective.

3. The additive uncertainty bound W_2 is weighted by R in the second term of (5.2). Hence the criteria forces the fitted model to be most accurate in the vicinity of the critical point of the Nyquist plant (i.e., where $\hat{P}C$ approach -1) since this is where the denominator of R approaches 0. This agrees well with engineering intuition which states that for control application, accurate plant knowledge is most crucial in the vicinity of the critical point.

5.3 Integrated Model Reduction/ Robust Control Design with Iterated Reweighting

In this section we consider a noiseless case of the PR scheme outline in the previous section. The purpose is two fold:

1. To investigate the feasibility and problems encountered in the scheme under a simplified framework. It is hope that the process and the limitation of the scheme could be better understood.

2. To develop an integrated model Reduction/robust control design with iterated reweighting scheme.

When the system identification part in is replace by model reduction, the block diagram is redrawn in Figure 5.2

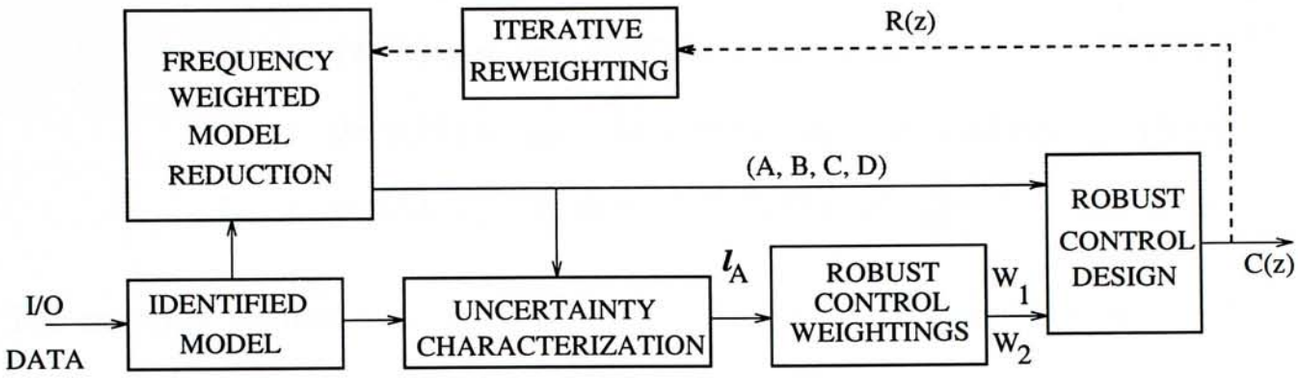

Figure 5.2: An Integrated Model Reduction/Robust Control Design with Iterated Reweighting Scheme

We denote this scheme as FWBR (Frequency Weighted Balanced Realization). The frequency weight R (w-plane) generated by the MATLAB program is transformed to z-plane by Tustin transformation for discrete-time frequency weighted model reduction.

5.4 A Design Example

The following simulation case study results are taken directly from [39].

5.4.1 The Plant and Specification

The true plant (simulation model), P^* is a 7th order, consisting of 3 resonant modes and a 1st order pole from sensor dynamics. Specifically,

$$P^* = \mathcal{F}(s)\grave{P}(s) \tag{5.3}$$

where,

$$\grave{P}(s) = \sum_{i=1}^{3} \frac{n_i}{s^2 + 2 * \zeta_i \omega_i s + \omega^2} \tag{5.3a}$$

$$\mathcal{F}(s) = \alpha/(s+\alpha) \tag{5.3b}$$

$$n_1 = 14.7331,\ n_2 = -25.4740,\ n_3 = -46.4318 \tag{5.3c}$$

$$\omega_1 = 2\pi(0.2749),\ \omega_2 = 2\pi(1.4924),\ \omega_3 = 2\pi(4.8354); \tag{5.3d}$$

$$\zeta_1 = 0.1654,\ \zeta_2 = 0.0300,\ \zeta_3 = 0.0084;\ \alpha = 2\pi \tag{5.3e}$$

The model is nonminimum phase. The performance weighting W_1 is specified by,

$$W_1(s) = \frac{(s+40)^2}{20(S+4)^2} \tag{5.4}$$

This plant has been used in [10], which is a model identified experimentally on the JPL Large Structure Control Laboratory. The input/output data for system identification by ERA method is simulated by adding white noise to the output data. The magnitude of the noise is 1 percent of the maximum output.

5.4.2 First Iteration

Figure 5.3 shows the identified plant (7th order) and the initial reduced model of 6th order generated with balanced reduction [37] of uniform weighting (section 4.3. Figure 5.4 shows the additive error and overbound W_2. The 6th order parametric model and the weightings W_1, W_2 are used for *Robust Control Design* as shown in the block diagram in Figure 5.2. Figure 5.5 illustrates that the performance are met and the system is robustly stable This figure also shows the frequency range where the controller design has reached its limits. The maximum performance index γ defined in equation (2.22) is equal to 0.4961.

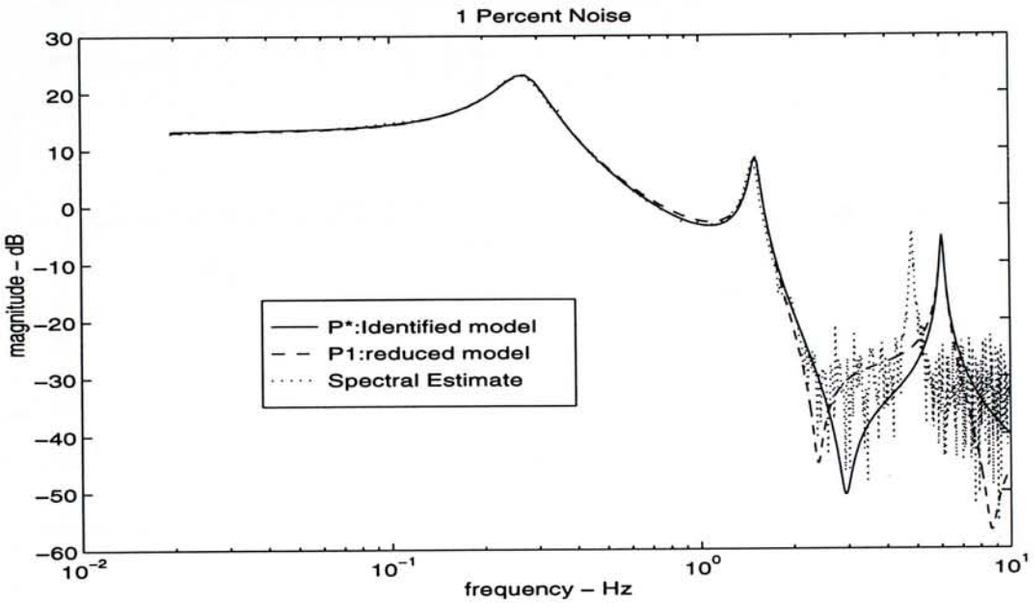

Figure 5.3: Identified and the reduced plant : First Iteration

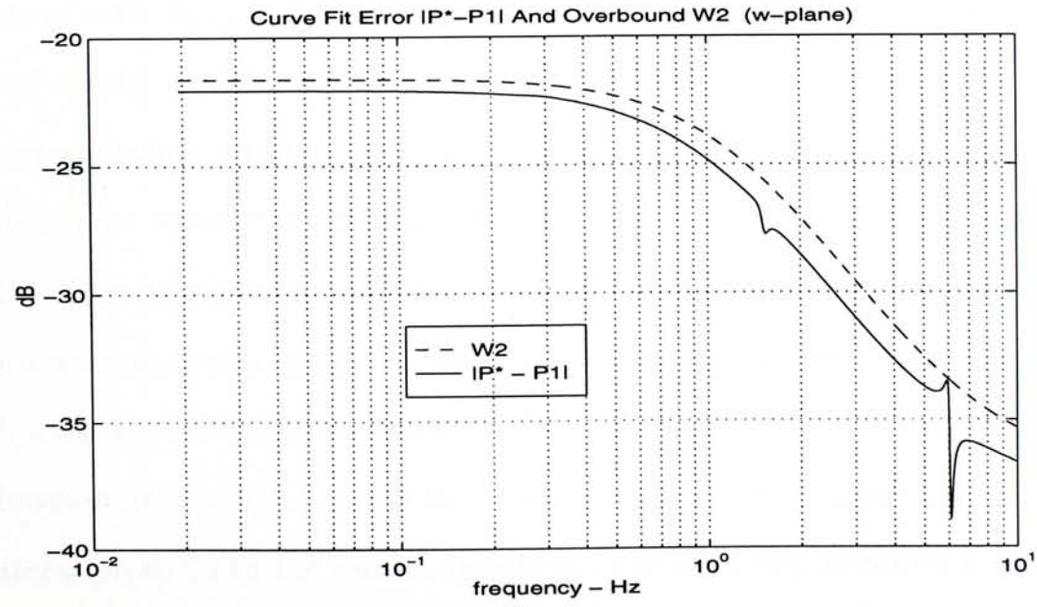

Figure 5.4: The additive error and the overbound : First Iteration

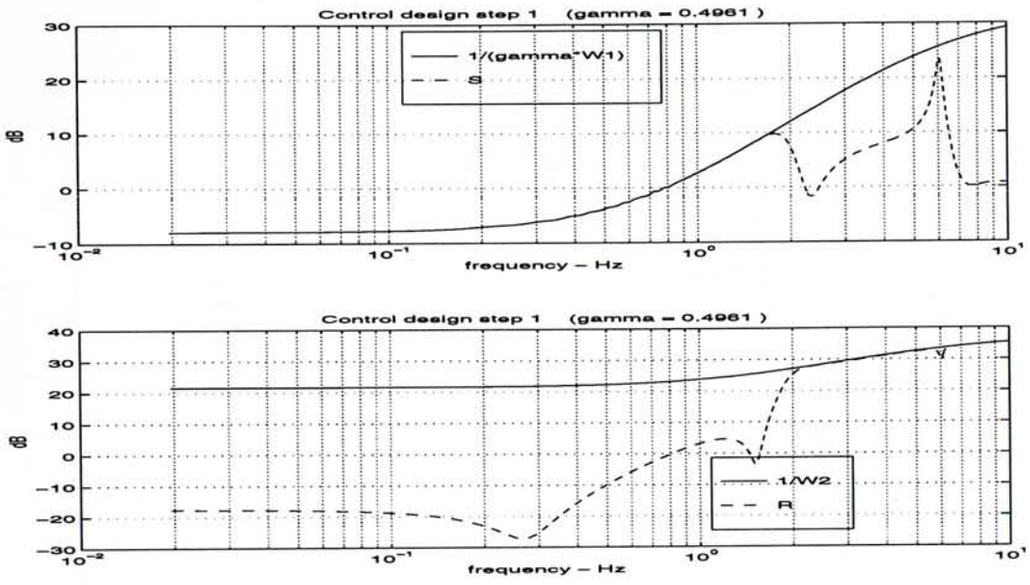

Figure 5.5: Performance of the controller design : First Iteration

5.4.3 Second Iteration

In the second iteration, the 6th order model is obtained by balanced model reduction with $R(z)$ as frequency weighting. It could be seen in Figure 5.6 the reduced model is different from that in the first iteration. Figure 5.7 shows the corresponding additive error and overbound. It should be noted that the additive error where the controller begins to be limited in the first iteration is smaller. This may give some more room for the controller design to improve its performance as shown in Figure 5.8. The performance index now reached 0.5391 which means a 8.6 % improvement.

However, it should be noted that the controller order increases from 9 in the first iteration to 14 in the second iteration. The situation becomes a decision of compromising the controller order and performance.

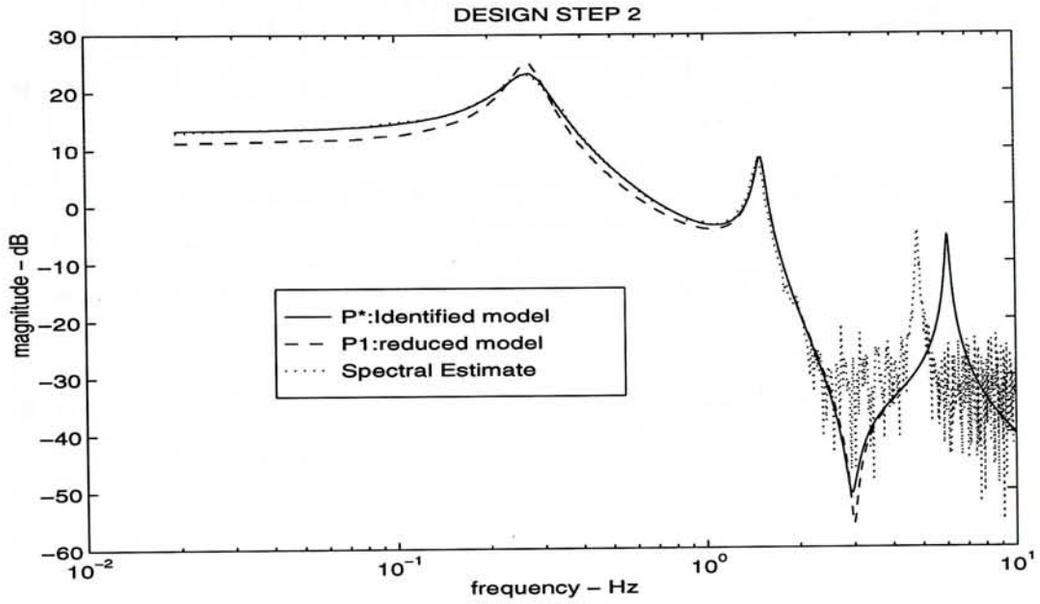

Figure 5.6: Identified and the reduced plant : Second Iteration

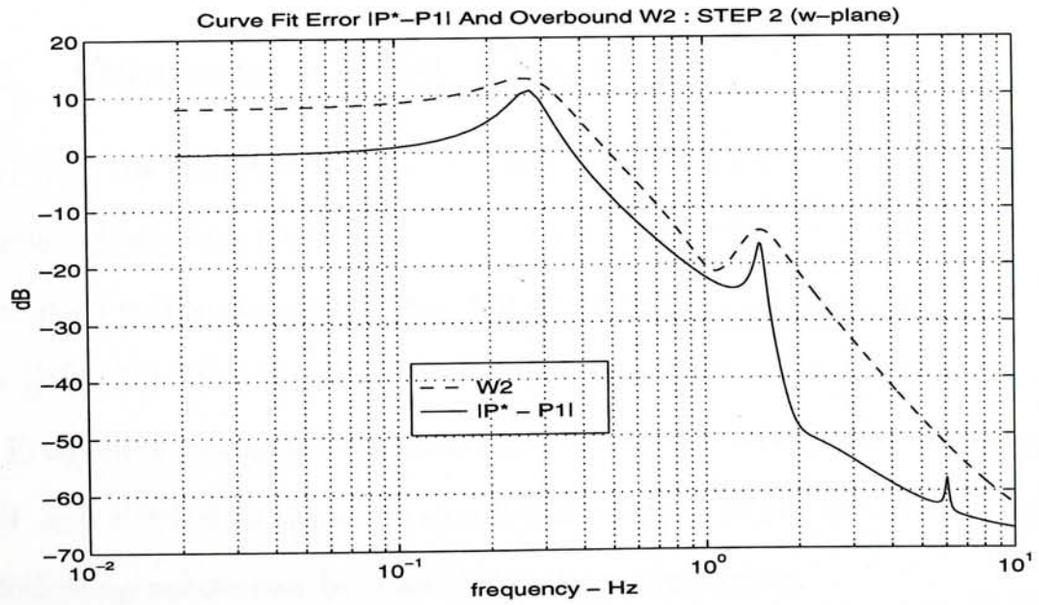

Figure 5.7: The additive error and the overbound : Second Iteration

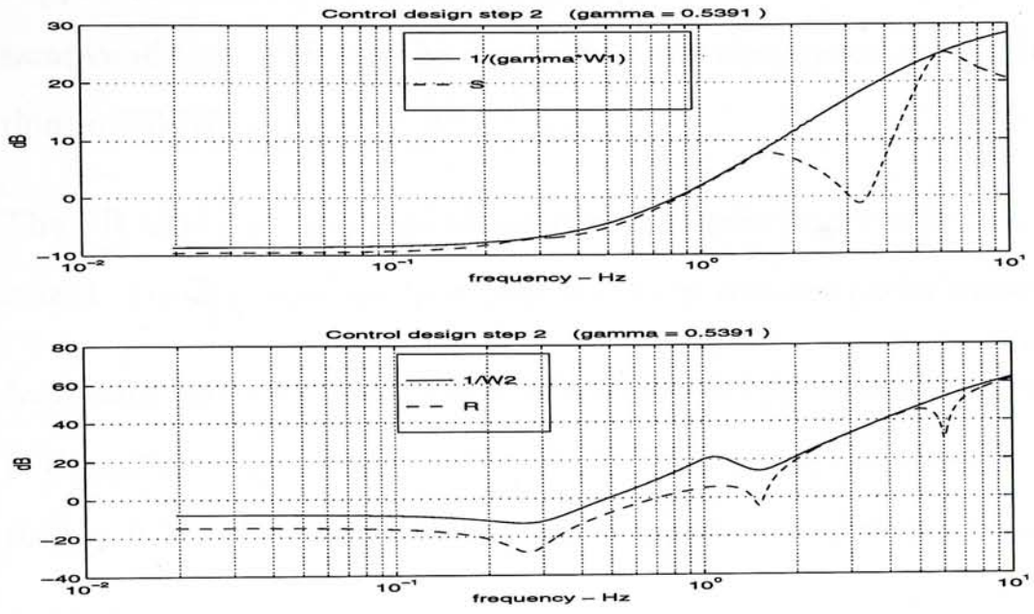

Figure 5.8: Performance of the controller design : Second Iteration

5.5 Approximate Fractional Frequency Weighting

5.5.1 Summary of Past Results

In [38] [10], the frequency weighted identification block in Figure 5.2 utilized a Frequency Weighted Curve Fitting (FWCF) algorithm to conduct 4-norm approximation to the ∞-norm minimization of the second term $|W_2(\omega)R(\hat{P}, C)|^2$.

In [39]†, the system identification block utilized high order ERA followed by a Frequency Weighted Balanced Realization (FWBR). Results of applying FWCF and FWBR to the same simulation case study are included in Table 5.1. The following points can be made from their comparison :

1. As indicated by the case where *wo* (order of W_2) = 2, FWBR achieves

†Results are shown in section 5.4

roughly the same performance with less iteration than FWCF under the same condition. This may be due to the more rigorous ∞-norm minimization in FWBR.

2. The PR algorithm manages to improve the performance only to a certain extent. Further iteration from that results in reduced performance.

3. Increasing the order of W_2 achieves a tighter bound on the complex shape of the additive error and hence, improves performance ($wo : 2 \rightarrow 6$, led to $\gamma : 0.49 \rightarrow 0.54$). The order of the controller, however, increases accordingly.

Number of iterations	FREQUENCY WEIGHTED CURVE FIT (FWCF)	ERA with FREQ. WEIGHTED BALANCED REALIZATION		
		FULL WEIGHTING (FWBR)		APPROX. FRACTIONAL WEIGHTING (FWBR-FW)
	$wo = 2$ $co = 10$	$wo = 2$ $co = 10$	$wo = 6$ $co = 14$	$wo = 2$ $co = 10$
0	$\gamma = 0.45$	$\gamma = 0.49$	$\gamma = 0.49$	$\gamma = 0.49$
1	$\gamma = 0.5$	-	$\gamma = 0.54$	$\gamma = 0.59$
2	-	-	-	$\gamma = 0.62$

wo : order of error overbound function co : controller order

Table 5.1: Simulation case study results using FWCF, FWBR, FWBR-FW

5.5.2 Approximate Fractional Frequency Weighting Approach [40]

In view of the past results, an approximate fractional frequency weighting approach is proposed [40]. Instead of using $R(z)$ as generated from the control system design step, the iterative reweighting block now utilizes a modified weighting $R_M(z)$ which approximates the square root of $R(z)$. The present approach

is termed FWBR-FW (fractional weighting) and constitutes identification at "half" step as compared to previous works.

Rationale for this approach is the following : in light of the various numerical approximations in the PR algorithm, it is prudent to take on the next iteration more conservatively than using full step size. The "half" step approach would enable a more gradual evolvement of the various functions and their adjustment and manipulate for enhanced final performance.

At present, the modified weighting $R_M(z)$ can be obtained manually by cascading first or second order transfer functions together to approximate the magnitude of the square root of $R(z)$.

5.5.3 Simulation Results

The idea discussed above is illustrated using the same simulation case study in section 5.4. In this study, all the $R_M(z)$ are generated in this way with second order polynomials in both numerator and denominator. Figure 5.13 shows the $R(z)$ as generated and the corresponding R_M-weighting function actually adopted for the first iteration. The R_M-function adopted for the second iteration is also shown. It can be observed in successive iterations that the magnitude of the adopted R_M increases in the high frequency range. This indicates the need to have a more accurate model at high frequencies at the expense low frequency accuracy for improved performance. Figure 5.10 presents the additive errors for the first and second iteration of system identification step using the adopted $R_M(z)$ weighting function. For comparison, the resulting additive error if $R(z)$ were to be used as weighting function for the first iteration is also included. Note that the second peak of the additive error, if R-weighting function were to be

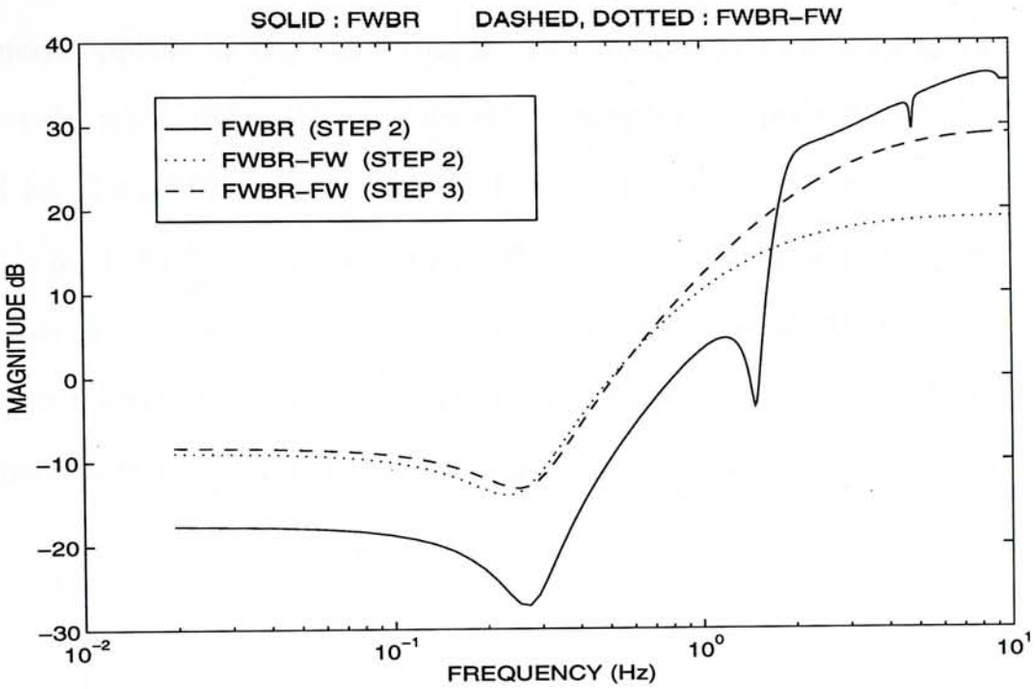

Figure 5.9: The weighting functions for model reduction

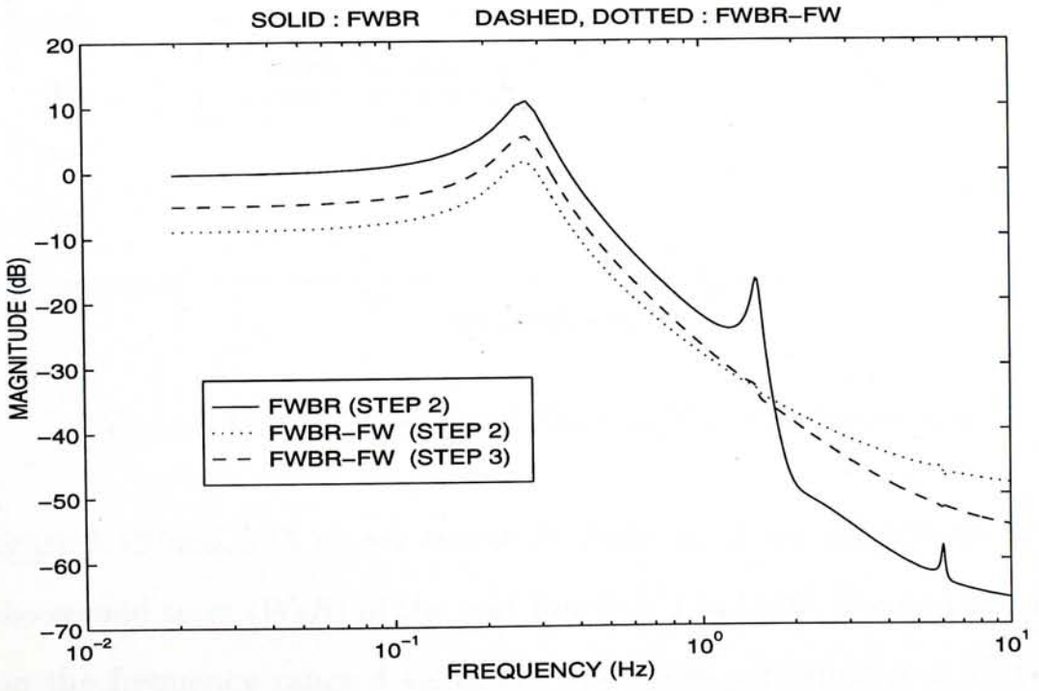

Figure 5.10: Additive error of weighted model reduction

utilized, disappears in FWBR-FW when R_M-weighting is used. This is due to the smooth profile of R_M-weighting as compared to R-weighting in Figure 5.10. As a result, a low order W_2 (= 2 for this example) is sufficient to provide a tight bound for the additive error of FWBR-FW. This contrasts to the situations in FWCF and FWBR, where high order W_2 is needed for tight bounding the error.

Figure 5.11 shows the correspond second order overbound W_2 for the first and second iteration. The sixth order W_2 required to overbound if R-weighting were used is also shown for comparison.

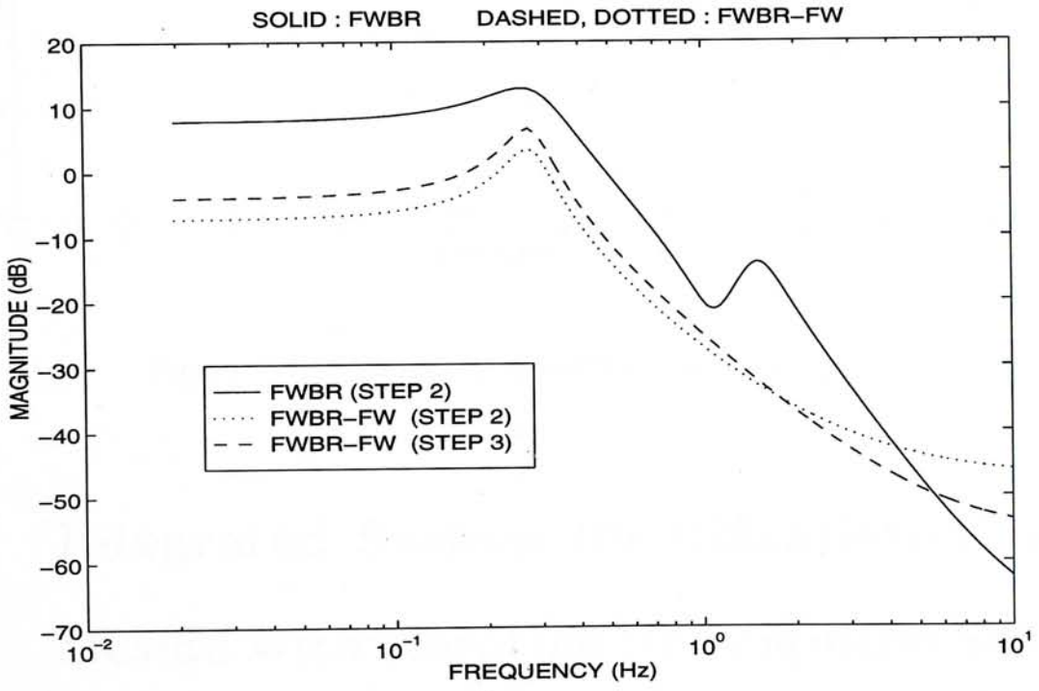

Figure 5.11: The overbound function W_2 of additive error

Figure 5.12 and 5.13 shows the evolvement of of the magnitude of (W_1S) and the second term (W_2R) of the cost function J in (5.2). It could be observed that in the frequency range 4 to 10 Hz where the performance is dictated by the tradeoff of W_2R and W_1S, the present approach manages to decrease W_2R

while keeping $W_1 S$ more or less the same in successive iteration. This results in an increased γ.

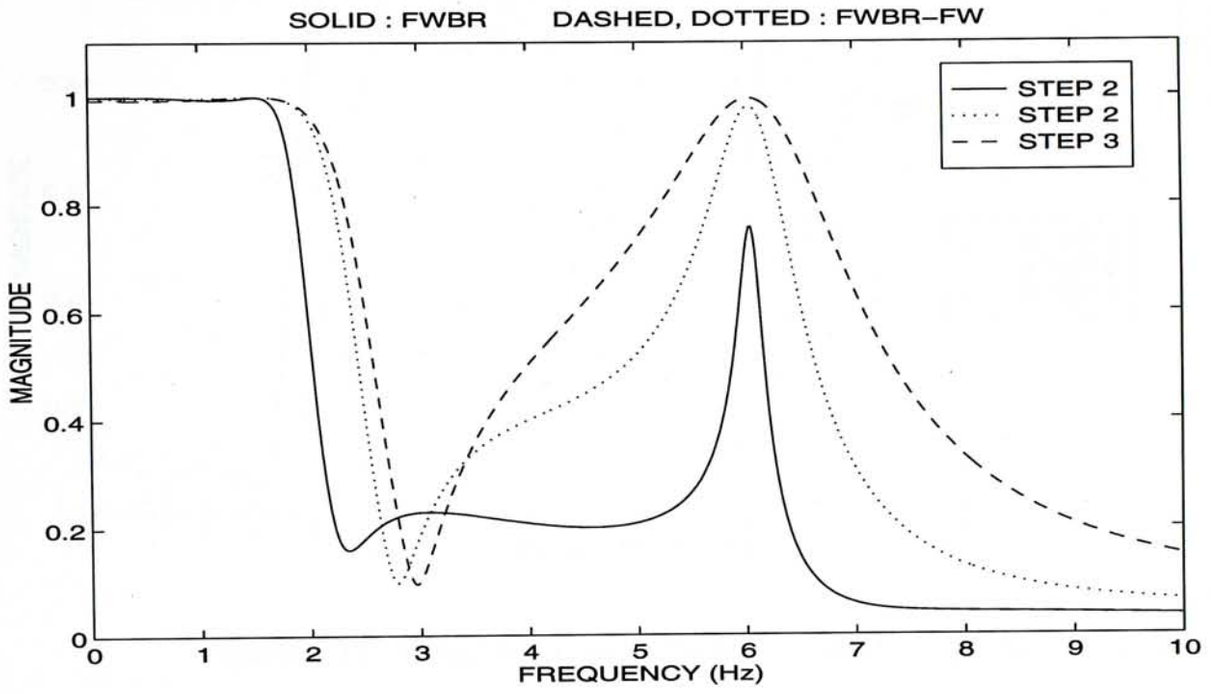

Figure 5.12: Weighted sensitivity function $\gamma_o W_1 S$

5.6 Integrated System Identification/Control Design with Iterative Reweighting Scheme

In this section we will try to implement the complete procedures of Integrated System Identification/Control Design with Iterative Reweighting Scheme (Figure 5.1). The experience gained in the simplified noiseless model reduction case study will also considered.

In this case study, we used the scheme in Figure 5.1 without approximate fractional weighting. The procedures was gone through two iterations. And the

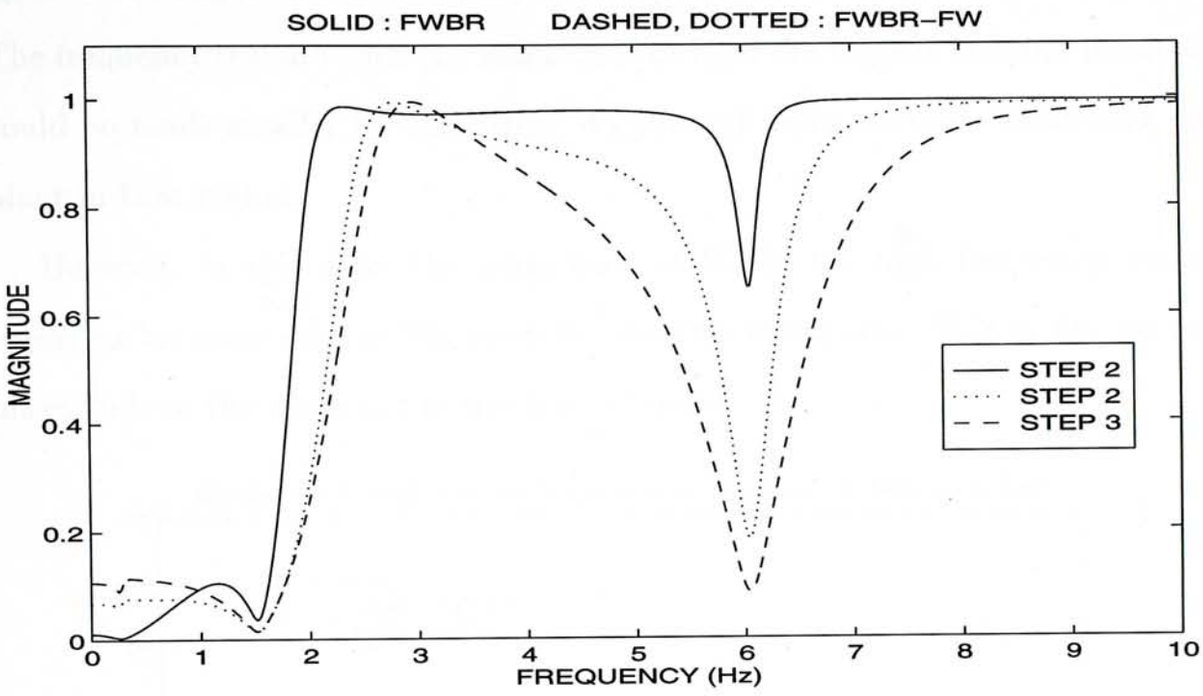

Figure 5.13: Weighted error sensitivity function W_2R

design results is summarized in table 5.2. The weighted system identification block is carried out by the frequency domain curve fitting algorithm (section ref-fid:cf). A frequency weighted ERA is not available yet.

Iteration	curve fit 2-norm error	Weighted 2-norm error	Order of W_2	Max. γ, γ_o achieved	Order of controller
1	0.88	6.23	2	0.418	11
2	3.89	5.06	2	0.410	11

Table 5.2: Summary of design results of Integrated System Identification/Control Design with Iterated Reweighting

It could be seen that no improvement could be made in the second iteration. Figures 5.14 to 5.17 show the resulting functions $S(s)$ and $R(s)$ together with the corresponding W_1 and W_2. In the model reduction case in section 5.4,

γ_o could be improved by exploring the advantage in the high frequency region. The frequency region which the magnitude of W_2R are large in the first iteration could be made smaller by decreasing W_2 through more accurate modelling the plant in that region.

However, in this case, the magnitude of W_2 in the high frequency region seems to be more or less the same for the two iterations. This is due to the magnitude of the noise in the spectral estimate.

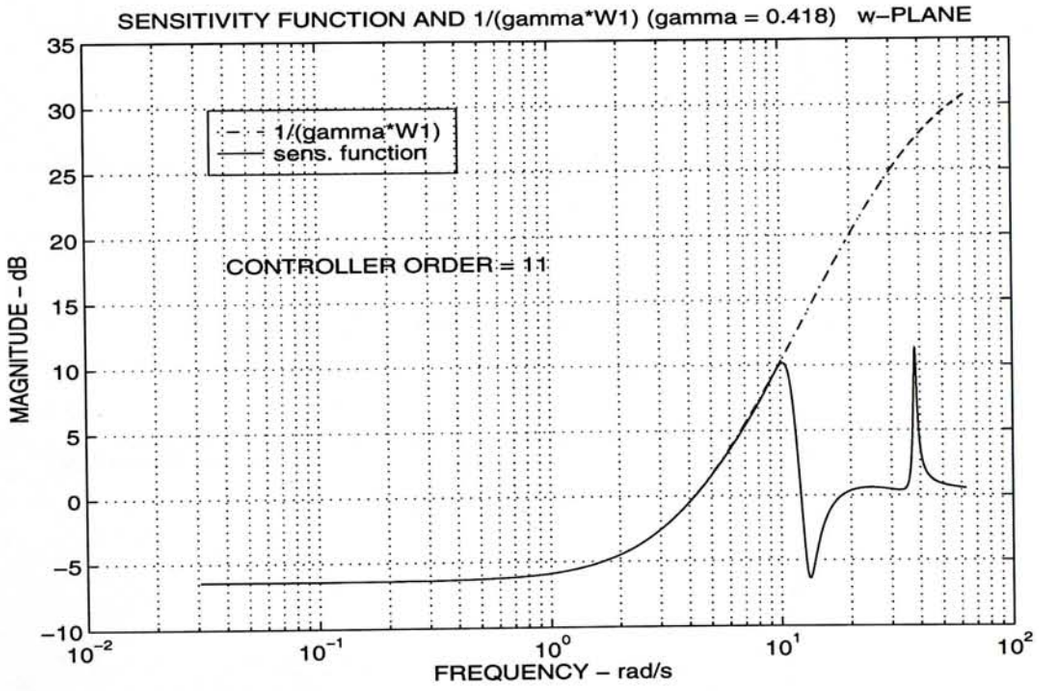

Figure 5.14: First Iteration : S and $\gamma_o W_1$

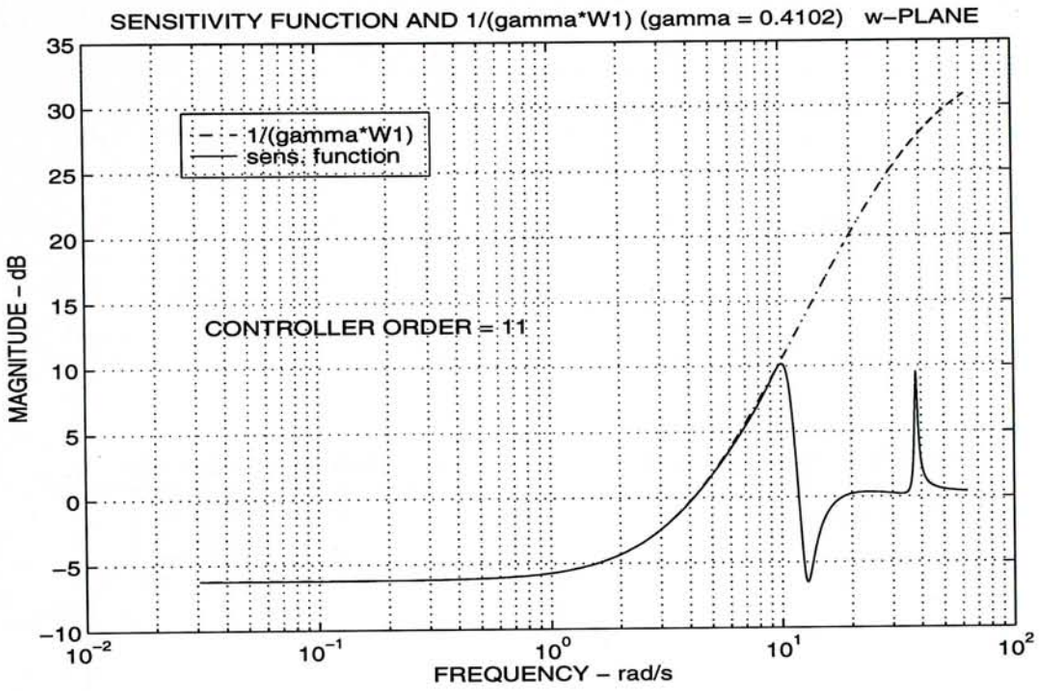

Figure 5.15: Second Iteration : S and $\gamma_o W_1$

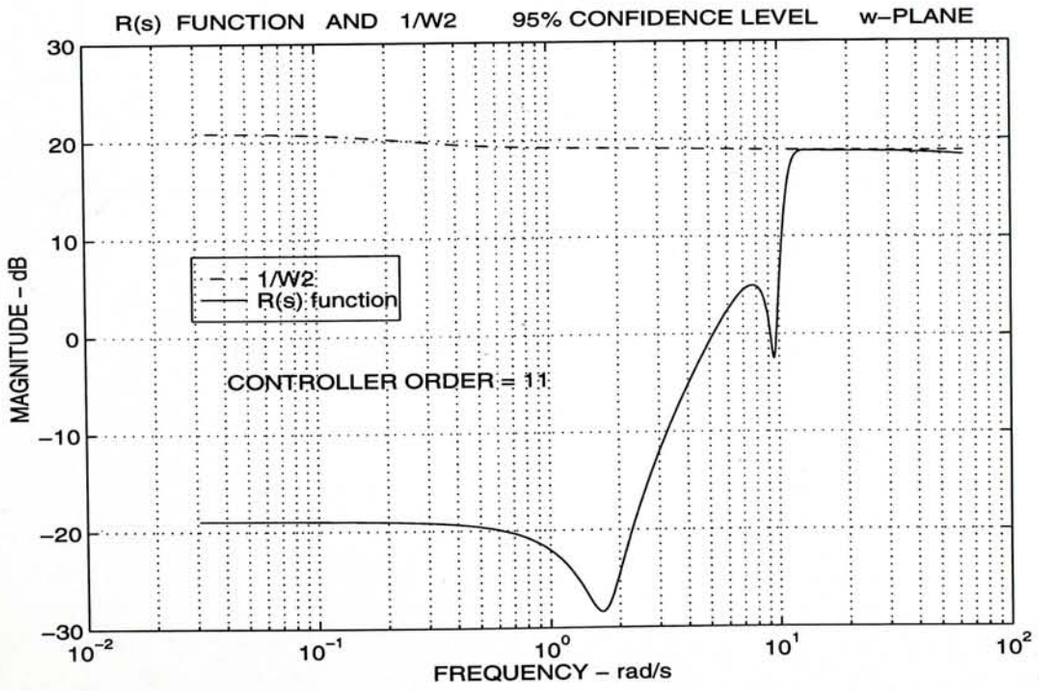

Figure 5.16: First Iteration : R and W_2

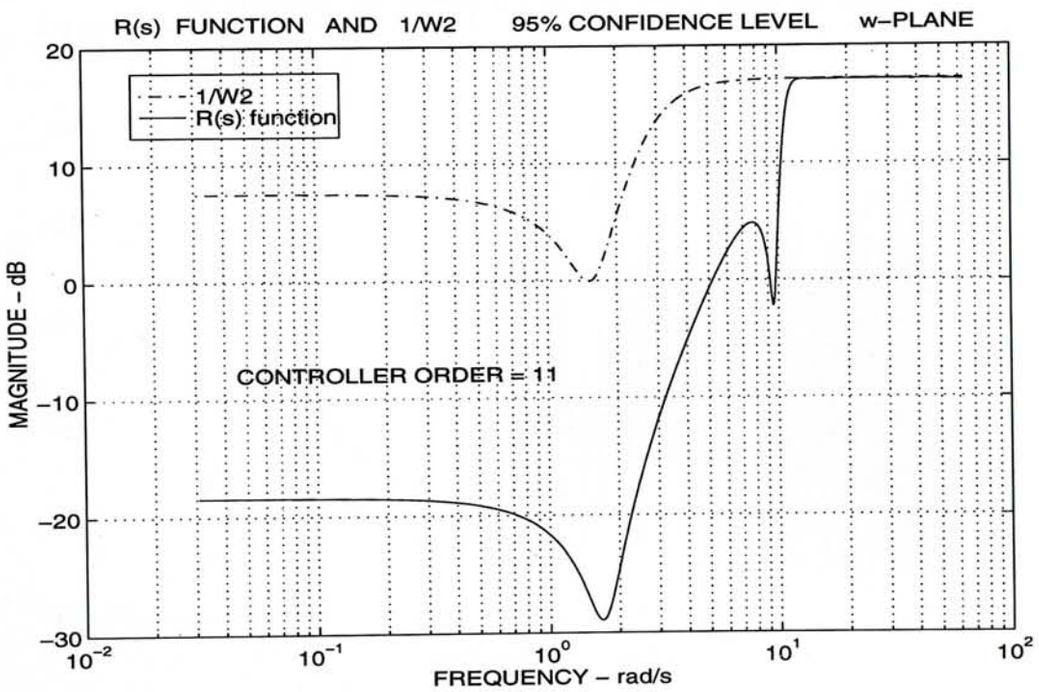

Figure 5.17: Second Iteration : R and W_2

The Effect of Consideration of Noise

Figures 5.18 and 5.19 shows the nonparametric statistical bounds, ℓ_A with 95% confidence level and the corresponding second order parametric overbound in the first and second iteration. The W_2 overbound is obtained by the LPSOF algorithm described in section 3.4. We could see that the frequency weighting, $R(s)$ is in effect in the curve fitting step.

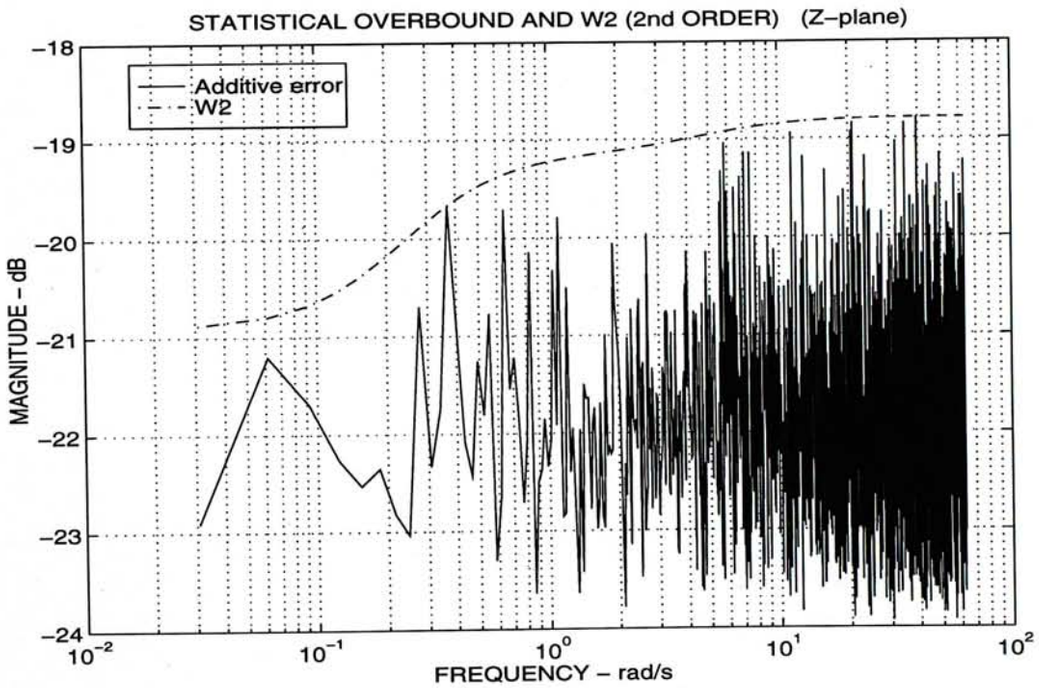

Figure 5.18: First Iteration : parametric and non-parametric uncertainty bounds

In Figure 5.20, we "zoom in" the high frequency region of the non-parametric overbound , the magnitude of the envelop is about the same for the two iterations. This limits the magnitude of W_2 from getting lower in the second iteration for improved performance. Due to the magnitude of the noise itself, the spectral estimate in the low magnitude region is relatively noisy and could not accurately represent the frequency domain information of the true plant. In short,

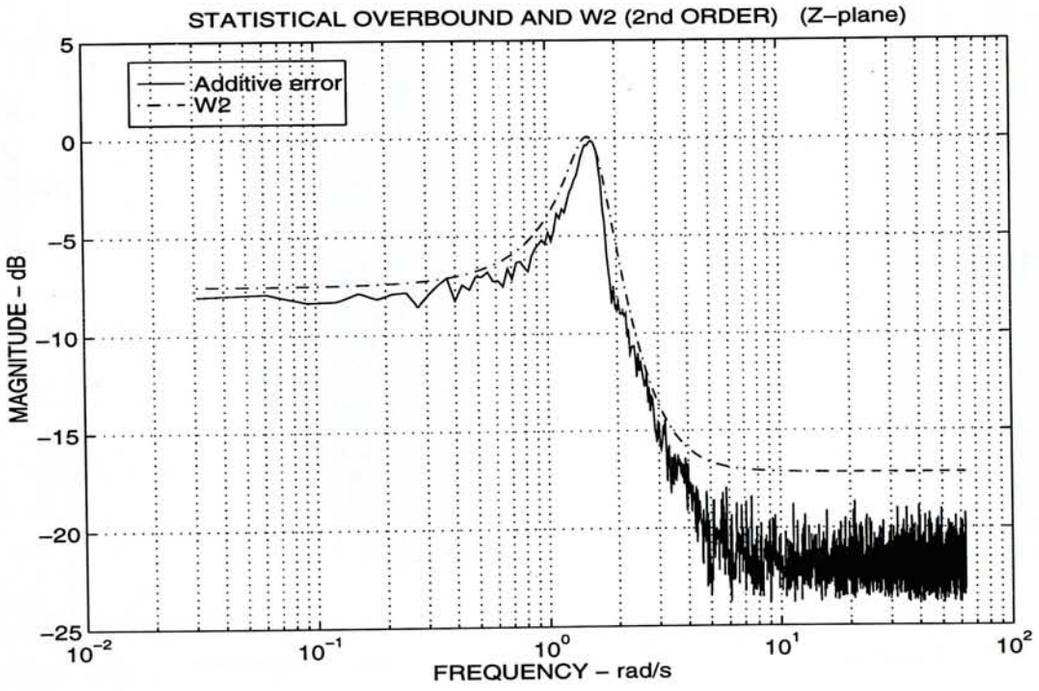

Figure 5.19: Second Iteration : parametric and non-parametric uncertainty bounds

the true plant is immersed in the "sea" of noise when the plant roll off in the high frequency region.

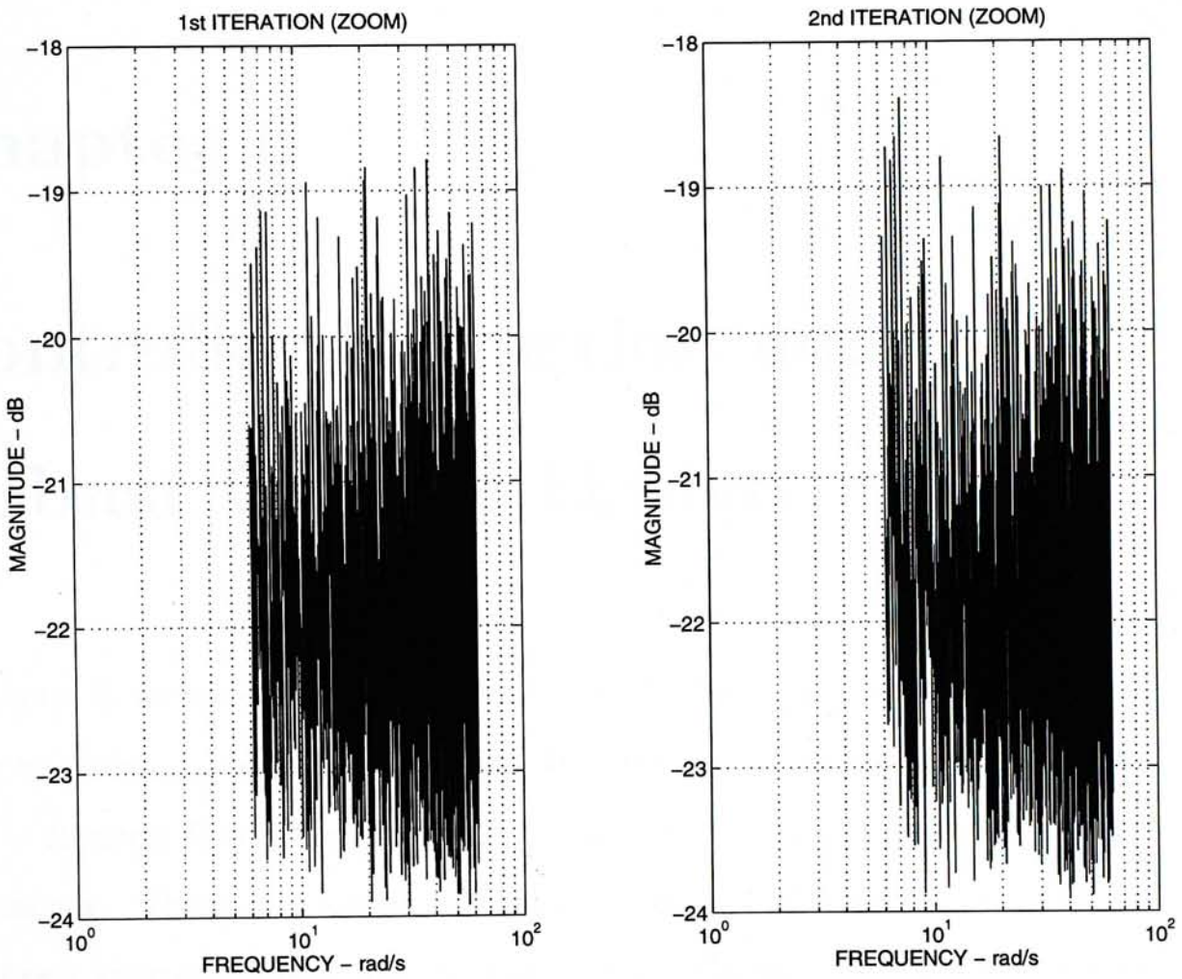

Figure 5.20: Comparison of the nonparametric statistical overbound in the high frequency region for iteration 1 and 2

Chapter 6

Controller Reduction and Robust Control Design

In chapter 5, we have develop an iterative method for plant model reduction in order to design a low order controller. In this chapter, we work on a different path : *Iterative* Controller Reduction. Figure 6.1 illustrates the two different approaches. These two approached have been termed *indirect**, compare to the *direct* approach which has the parameters defining a low-order controller computed by some optimization or other procedure. We will not discuss the direct approach in this thesis. Interested reader are referred to [42,43] for further discussions.

In section 6.2, we will discuss the importance of frequency weighting in controller reduction for robust performance. And a iterative controller reduction scheme is proposed in section 6.3.

*cf. [41]

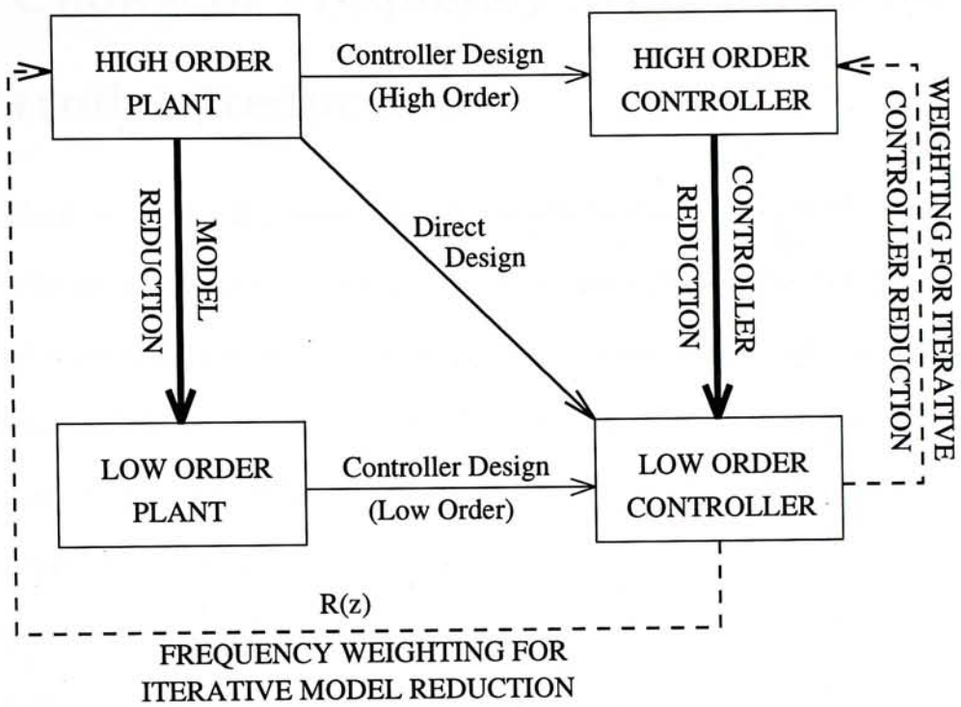

Figure 6.1: Iterative Low order controller design methods

6.1 Motivation for Controller Reduction

We quote from [44] about the motivation for controller reduction:

> "What do practising engineers need? They need controllers which
>
> - are low complexity,
> - operate in discrete-time, i.e., are computer-implementable, and
> - when implemented are free of numerical problems."

The low complexity issue mentioned above is related to the order of the controller. Low order controller has fewer things to go wrong in the hardware or bugs to fix in the software; they are easier to understand; and the computational requirements are less.

6.2 Choice of Frequency Weightings for Controller Reduction

The problem of controller reduction is different from the problem of open-loop model reduction because of the presence of the plant. As the plant and controller are obviously determining factor to the closed-loop performance (such as bandwidth, stability, robustness and performance index, γ) which is to be well approximated, any controller reduction procedures ought to take into account the existence of the plant.

Such considerations lead to frequency-weighted controller reduction problem as we shall show in the following sections. The choice of frequency weight is influenced by the choice of criterion considered most important in the reduction process.

6.2.1 Stability Margin Considerations

Let $P(s)$ be the linear time-invariant plant transfer function, and $C(s)$ be a stabilizing high-order controller. Let $C_r(s)$ be the sought after reduced-order controller. Then the closed-loop system with $C_r(s)$ replacing $C(s)$ could be as depicted in Figure 6.2. Based on the discussion in section 2.3 and exchanging the symbols for plant and controller in (2.15), we have if:

1. $C(s)$ and $C_r(s)$ have the same number of pole in $Re\,(s) > 0$ and no poles on the imaginary axis; and

2.
$$\| [C(s) - C_r(s)]P(s)[I + C(s)P(s)]^{-1} \|_\infty < 1, \tag{6.1}$$

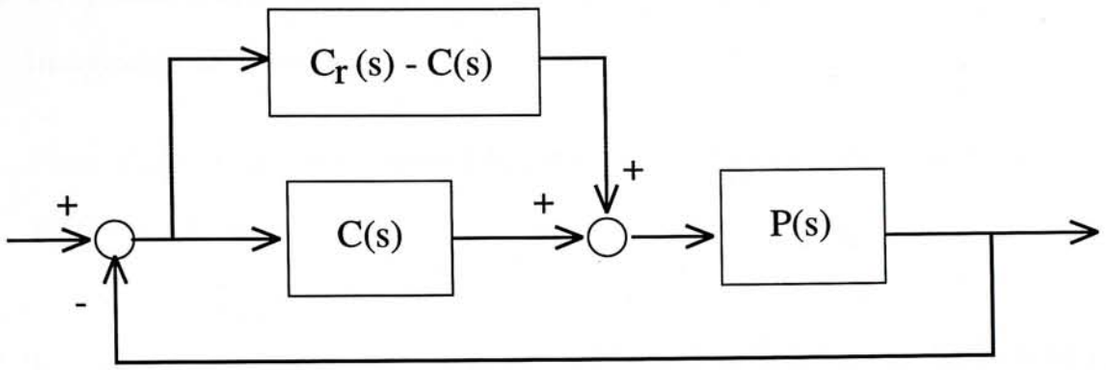

Figure 6.2: Equivalent close-loop block diagram with $C_r(s)$ replacing $C(s)$

then $C_r(s)$ is a stabilizing controller.

In [41], the authors have suggested a minimization solution to the problem: find a $C_r(s)$ having the same number of unstable pole as $C(s)$ (condition 1), which at the same time minimizes the left side of 6.1 and acquires a reduced order. The function $P(s)(I+CG)^{-1}$ acts as a *frequency weighting* for controller reduction optimization.

6.2.2 Closed-Loop Transfer Function Considerations

The closed-loop transfer function with $C(s)$, $C_r(s)$ are

$$\begin{aligned} T(s) &= P(s)C(s)[I+P(s)C(s)]^{-1} = I-[I+P(s)C(s)]^{-1} \\ T_r(s) &= P(s)C_r(s)[I+P(s)C_r(s)]^{-1} = I-[I+P(s)C_r(s)]^{-1} \end{aligned}$$

Neglecting terms of second order in $C_r - C$,

$$T_r(s)-T(s) = P(s)C_r(s)[I+P(s)K(s)]^{-1}P(s)[C_r(s)-C(s)][I+P(s)C(s)]^{-1}$$

and [41] hence suggested another reduction problem: find $C_r(s)$ of a reduced degree such that:

1. $C(s)$ and $C_r(s)$ have the same number of poles in $Re(s) > 0$ and no imaginary axis poles;

2. Find $C_r(s)$ that minimizes $\| V_1(s)[C_r(s) - C(s)]V_2(s) \|_\infty$ with $V_1 = (I + PC)^{-1}P$, $V_2 = (I + PC)^{-1}$.

6.2.3 A New Way to Determine Frequency Weighting

A reduce order controller could only has a optimal performance index, γ_o^{red}, less than or equal to a full order controller, γ_o^{full}. The objective of frequency weighted controller reduction is to approximate the full order controller at suitable frequency range so as the improve the achievable performance, i.e. to make γ_o^{red} as close to γ_o^{full} as possible.

The achievable performance is limited by two factors.

1. The performance requirement imposed by $W_1(s)$, especially in the low frequency region.

2. Uncertainty and controller effort imposed by $W_2(s)$, especially in the high frequency region.

Usually, the two factors limit the performance improvement in two distinct frequency regions. Our new scheme is to explore such a difference and introduce a frequency weighting to improve performance, by observing the region of limitation, mainly for the limitation imposed by W_1.

6.3 A Scheme for Iterative Frequency Weighted Controller Reduction (IFWCR)

We outline the IFWCR scheme as follows:

1. At $k = 1$, we start with a full-order stabilizing controller $C(s)$ and denote the optimal performance index as $\gamma = \gamma_o^0 = \gamma_o^{full}$, and obtained a reduced order controller, $C_r^1(s)$ by balanced truncation† with uniform weighting.

2. If $C_r^1(s)$ is stabilizing controller, we calculate the new *reduced* optimal performance index as $\gamma = \gamma_o^1$ using binary search for the satisfaction of

$$\| \, |\gamma W_1 S|^2 + |W_2 R|^2 \, \|_\infty < 1 \tag{6.2}$$

3. If $\gamma_o^1 < \gamma_o^0$, then set $k = 1$ and the weighting function $W_f^0(s)$ to be 0.

   Step 1 By comparing $\gamma_o^0 W_1$ and the new sensitivity function S_r^k formed by the C_r^k, we parallel a band-pass weighting function $W_f^k(s)$ to $W_f^{k-1}(s)$at region which S_r^k exceeds or extremely close to $\gamma_o^{full} W_1$.

   Step 2 Use $W_f^k(s)$ as weighting in *frequency weighted balanced truncation* (4.4) to reduce $C(s)$ to C_r^k which has the same order as C_r^{k-1}.

   Step 3 Calculate the new γ_o^k using binary search for the satisfaction of (6.2)

   Step 3 Set $k := k + 1$

   Step 4 If $|\gamma_o^k - \gamma_o^{k-1}| < \epsilon$ or $\gamma_o^k < \gamma_o^{k-1}$, then STOP; otherwise, go to **Step 1.**

†The unstable part of the controller could not be reduced, further details in section 6.3

4. Otherwise, STOP.

The basic idea is to applied frequency weightings in regions which the $S_r(s)$ of the reduced controller violate the inequality,

$$\|\gamma_0^{full} W_1 S_r(k)\|_\infty < 1$$

most severely. The weightings introduced is directed towards shaping the reduced controller for close approximation of the full order optimal controller in critical frequency regions.

In chapter 7, we will illustrate the scheme by an example.

Unstable controller and Discrete-time implementation issues

A unstable controller could be a stabilizing controller itself. Since the number of unstable poles for $C(s)$ and $C_r(s)$ must be the same, the unstable poles of the controller could not be truncated. Using the "stabproj" function in MATLAB[‡] , the unstable controller $C(s)$ could be divided into stable and unstable projections such that

$$C(s) = [C(s)]_- + [C(s)]_+$$

where $[C(s)]_-$ denotes the stable part of $C(s)$, and $[C(s)]_-$ denotes the unstable part. Then $[C(s)]_-$ is approximated by a lower order $[C_r(s)]_-$ using balanced truncation (frequency weighted). The final $C_r(s)$ is:

$$C_r(s) = [C_r(s)]_- + [C(s)]_+$$

The unstable part of $C(s)$ are copied into $C_r(s)$.

[‡]cf. [15]

In order to implement the controller on computer, the final $C_r(s)$ obtained in ω-plane is transformed to discrete-time z-plane $C_r(z)$ by Tustin transformation. This procedure is used to obtain z-plane controllers in this thesis. Presently, the IFWCR scheme is carried out in ω-plane.

Chapter 7

A Comparative Design Example

In this chapter, we will compare the design results for a low order controller following the two different approaches in Figure 6.1. For one approach, we use the scheme in section 5.3:

Higher Order Plant $\rightarrow$ Low Order Plant $\rightarrow$ Low Order Controller

For the other approach, we use the schemes in section 6.2.1 and section 6.3:

Higher Order Plant $\rightarrow$ High Order Controller $\rightarrow$ Low Order Controller

We use the same example represented by (5.3) and the specification (5.4) in section 5.4 for this comparison. Throughout this chapter the controller to be design is specified to be of 7th order.

7.1 Plant Model Reduction Approach

In this section, we use the scheme in section 5.3. Since the order of the controller will be the sum of three terms: order of the plant, order of $W_1(s)$ and order of

$W_2(s)$. The minimum order for W_2 other than a constant is order 1; W_1 is a second order function. Thus, for a 7th order controller, the 7th order plant must be reduced to a 4 order plant. Only results of the first iteration in Figure 5.2 will be compared, since the second iteration could not achieve an improved result.

Figure 7.1 shows the additive error between the the 7th order plant and the reduce 4th order model and the 1st order overbound W_2. Note that in the lower plotting, the performance limitation due to uncertainty starts at around 12 dB, which is lower compared with Figure 5.5. This is due to a larger additive error and a low order($= 1$) W_2. The performance index, $\gamma_o = 0.369$. Figure 7.2 shows the cost function, the close-loop sensitivity function and its limits $(\gamma_o W_1)^{-1}$.

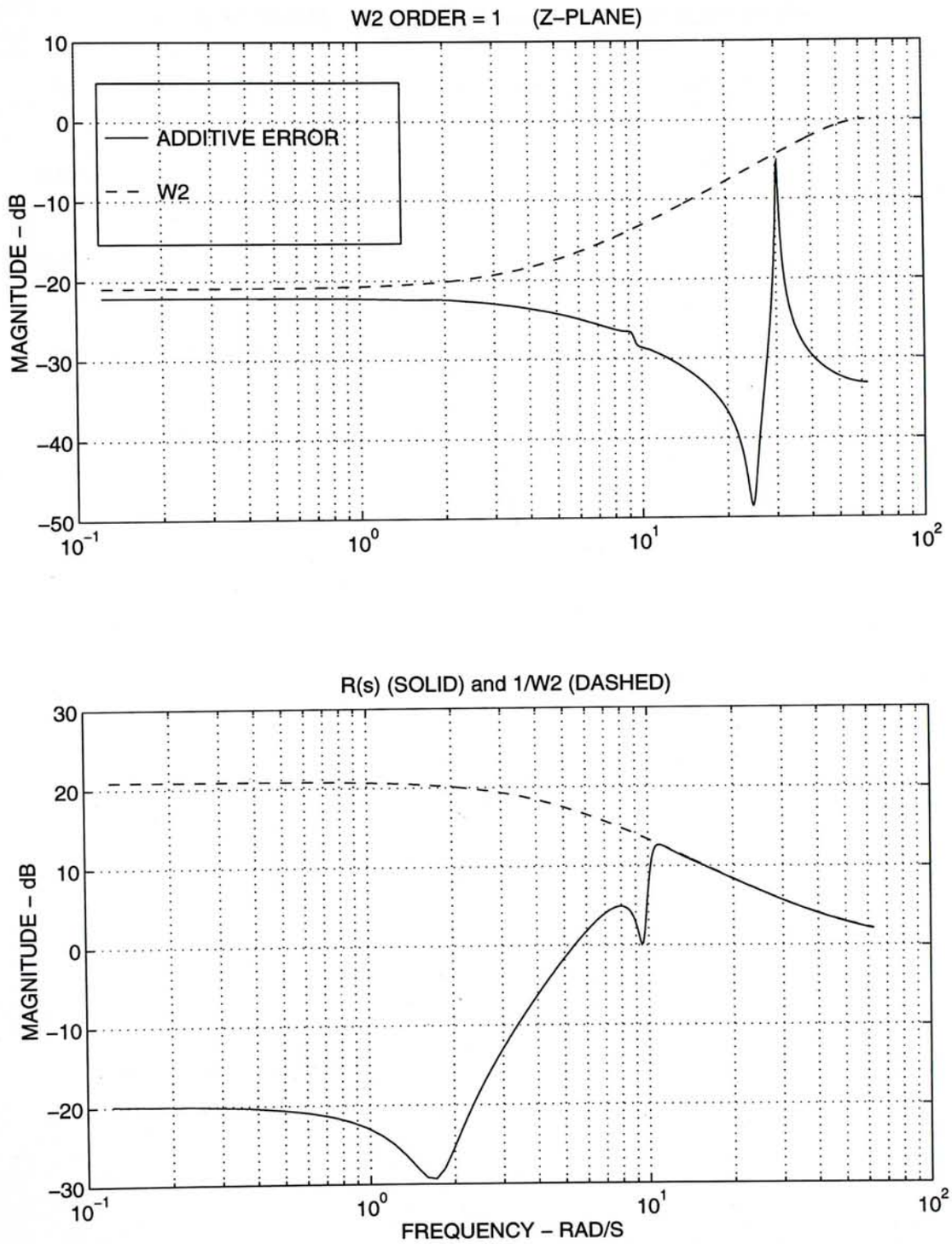

Figure 7.1: Plant model reduction approach (1st iteration): W_2, additive error [Above], and R , W_2^{-1} [Below]

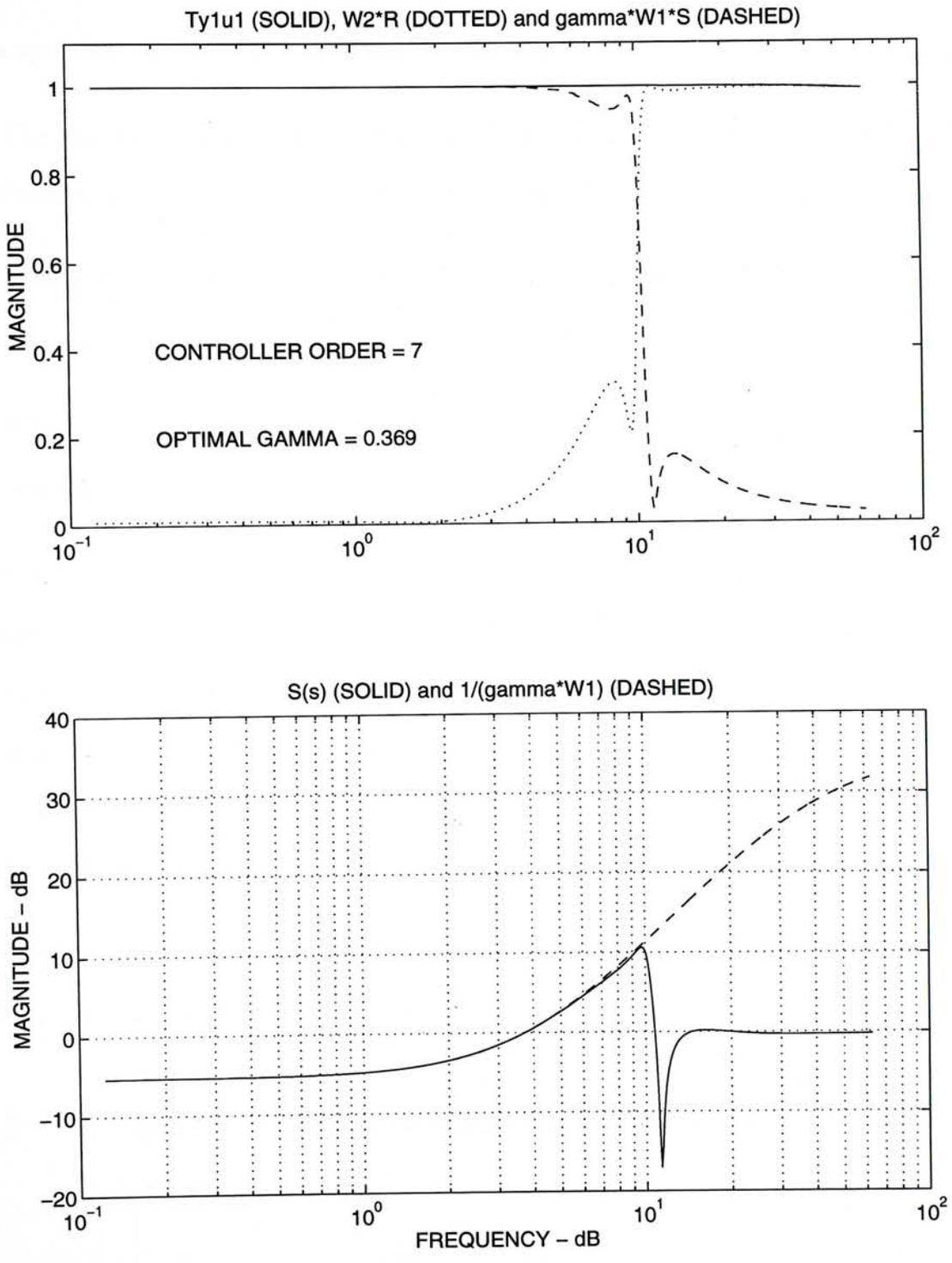

Figure 7.2: Plant model reduction approach (1st iteration): Cost function ($T_{y_1 u_1}$) [Above] and $(\gamma_o W_1)^{-1}$, S [Below]

7.2 Weighted Controller Reduction Approach

In this section, we had the following assumptions:

1. The model is an accurate representation of the plant with very little uncertainty (both structured and unstructured).

2. The plant and actuator saturation level is high enough for the controllers designed in this section.

3. Based on assumptions 1 and 2, we arbitrarily assigned the $W_2(s)$ to be a constant and equals to 0.002.

In practice, the above assumptions must be checked. Here, we made these assumption for keeping the simplicity of this design example. A 9th order controller was then designed in the following subsection. Two controller reduction approachs were used to reduce the full order controller to 7th order.

7.2.1 A Full Order Controller

Figure 7.3 shows the results of the full order(= 9) controller design. The optimal gamma, γ_o, is equal to 0.6806.

7.2.2 Weighted Controller Reduction with Stability Considerations

Using the frequency weighting, $W_f(s)$

$$W_f(s) = P(s)(1 + P(s)C(s))^{-1}$$

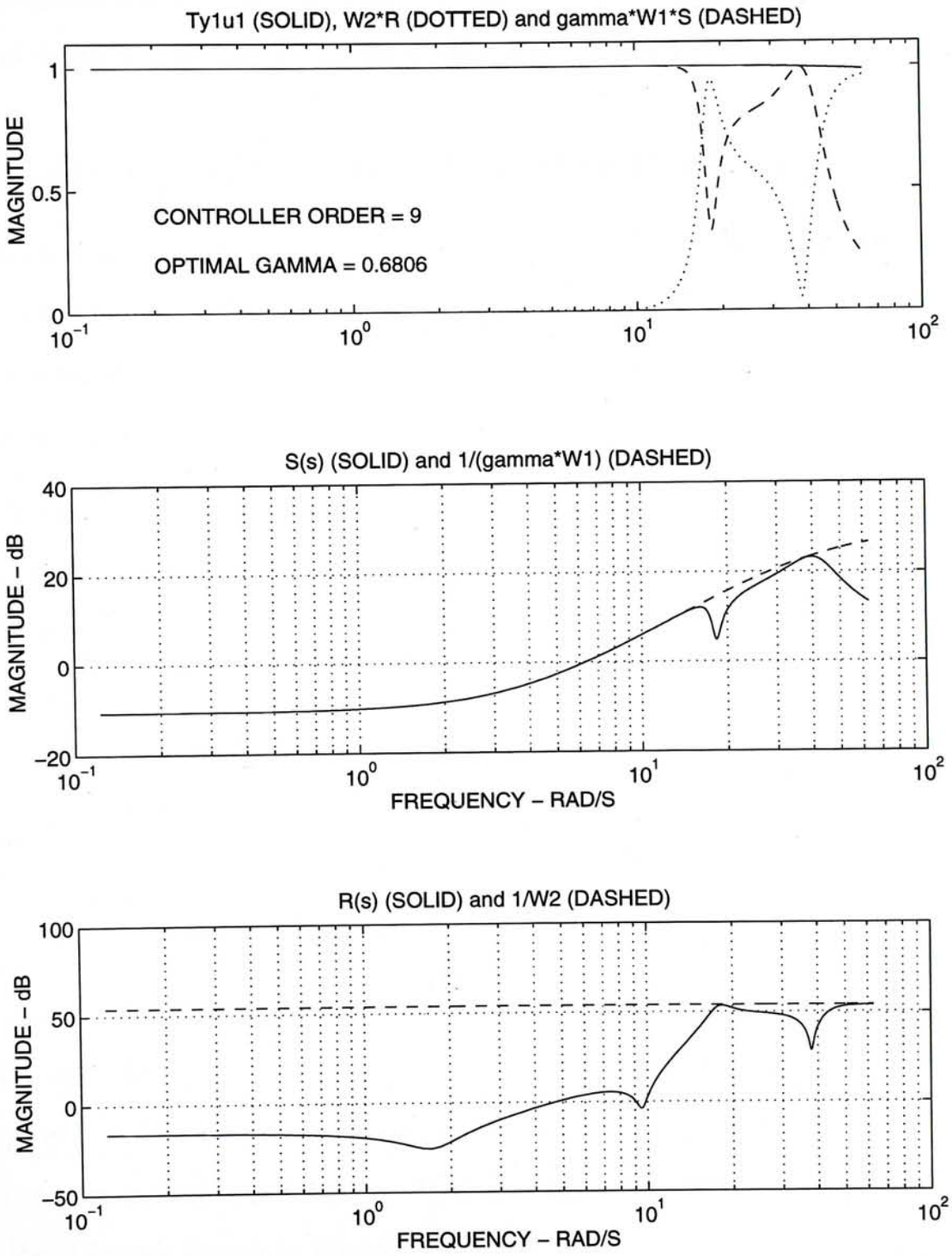

Figure 7.3: Full order(= 9) controller design results

as suggested in section 6.2.1* to reduce the full order controller to 7th order, the optimal gamma is $\gamma_o = 0.4945$, which is higher than that of controller reduction without frequency weighting (as we shall see in Table 7.1).

7.2.3 Iterative Weighted Controller Reduction

In this section we, reduce the controller to 7th order using the IFWCR scheme in section 6.3. We iterate the reduction process for 5 times starting with a 7th order controller by balanced truncation with uniform weighting ($k = 0$). The results is summerized in the following table:

Iteration No., k	γ_o achieved	$W_f(s)$ used
0	0.3350	1
1	0.5052	$W_L(s)$
2	0.5583	$W_L(s) + W_H(s)$
3	0.5769	$3W_L(s) + W_H(s)$
4	0.5902	$6W_L(s) + W_H(s)$
5	0.5769	$7W_L(s) + W_H(s)$

$W_L(s) = \frac{0.9s}{s^2+0.9s+1.2}$, and $W_H(s) = \frac{3}{s^2+3s+1558}$ are first order band-pass filters with passband $0.7 < \omega_p < 1.6$ rad/s and $38 < \omega_p < 41$ rad/s respectively.

Figures 7.4 and 7.5 show the process of iteration. At each iteration k, the $\gamma_o^{full} W_1$ and the S_r^k are compared and a new W_f^{k+1} is determined as described in section 6.3. The maximum γ_o obtained through the iteration trials is 0.5902.

The corresponding cost functions $T_{y_1 u_1}$ and its components ($\gamma_o W_1 S$, $W_2 R$) at each iteration are shown in Figures 7.6 and 7.7.

*The results of using $W_f(s)$ suggested in section 6.2.2 with closed-loop consideration is not shown because it does not give a stabilizing controller.

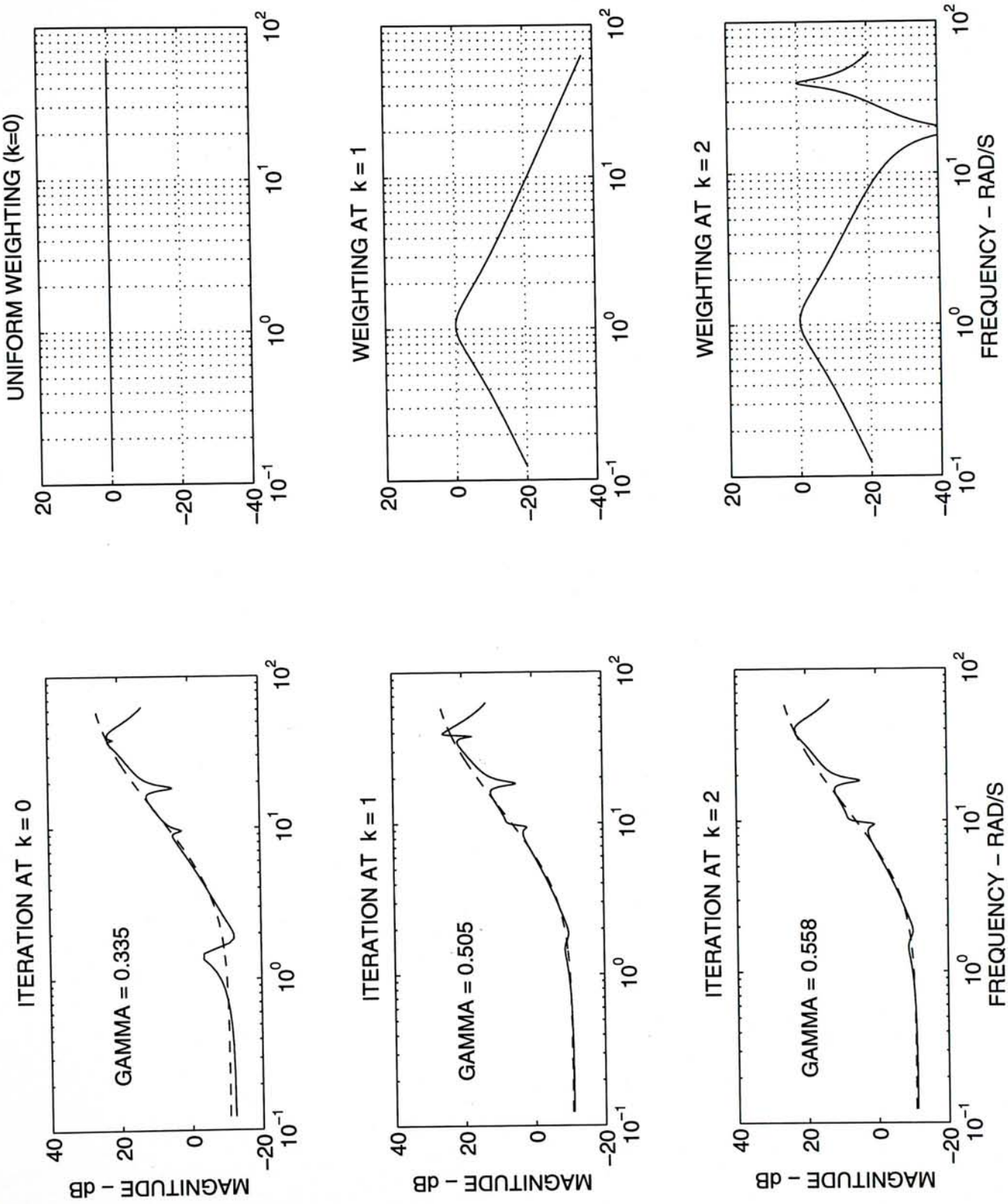

Figure 7.4: IFWCR iterations: $\gamma_o^{full} W_1$ (dashed) and S_r^k (solid) [Left] and corresponding weighting W_f [Right]

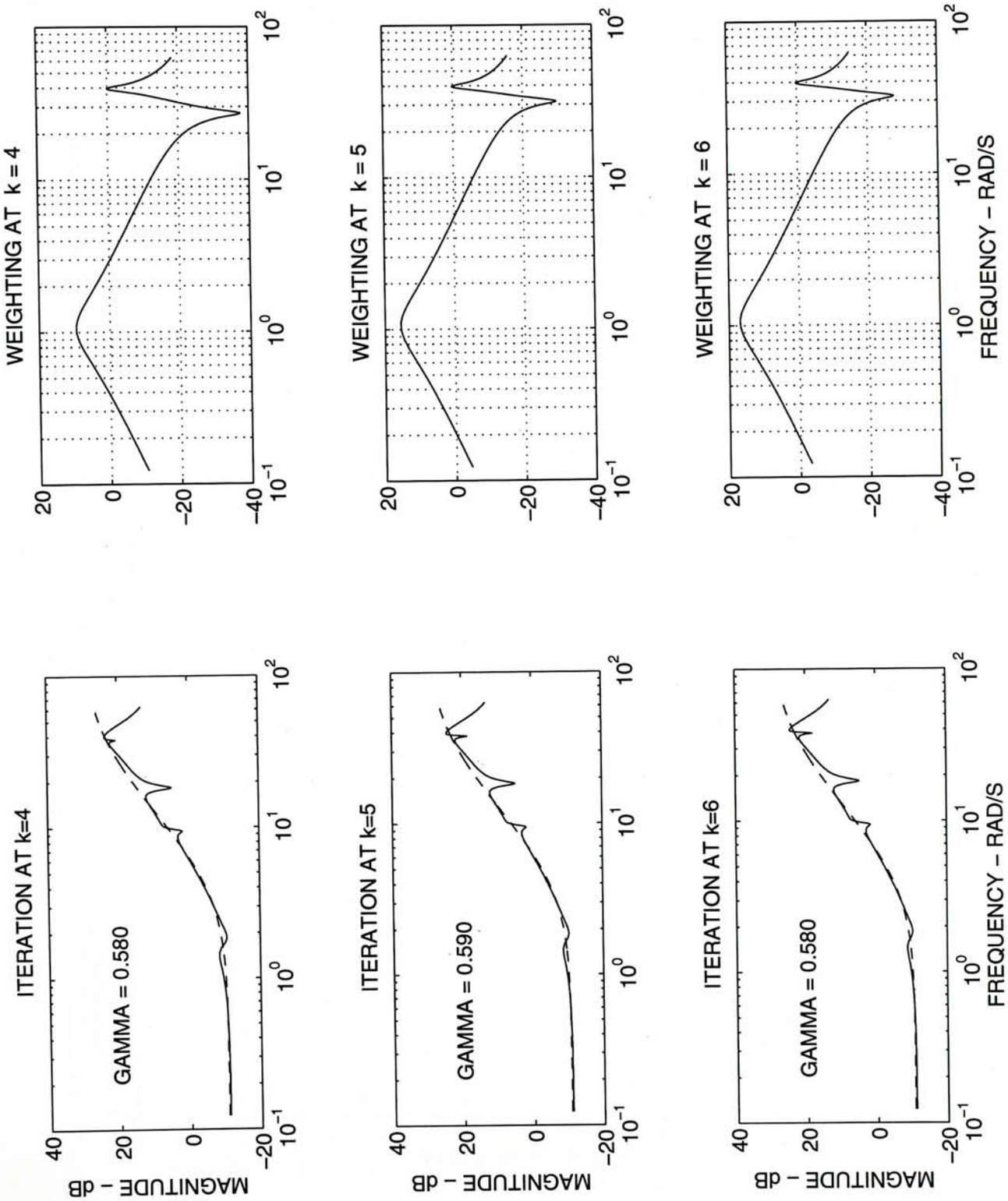

Figure 7.5: IFWCR iterations: $\gamma_o^{full} W_1$ (dashed) and S_r^k [Left] and corresponding weighting W_f [Right]

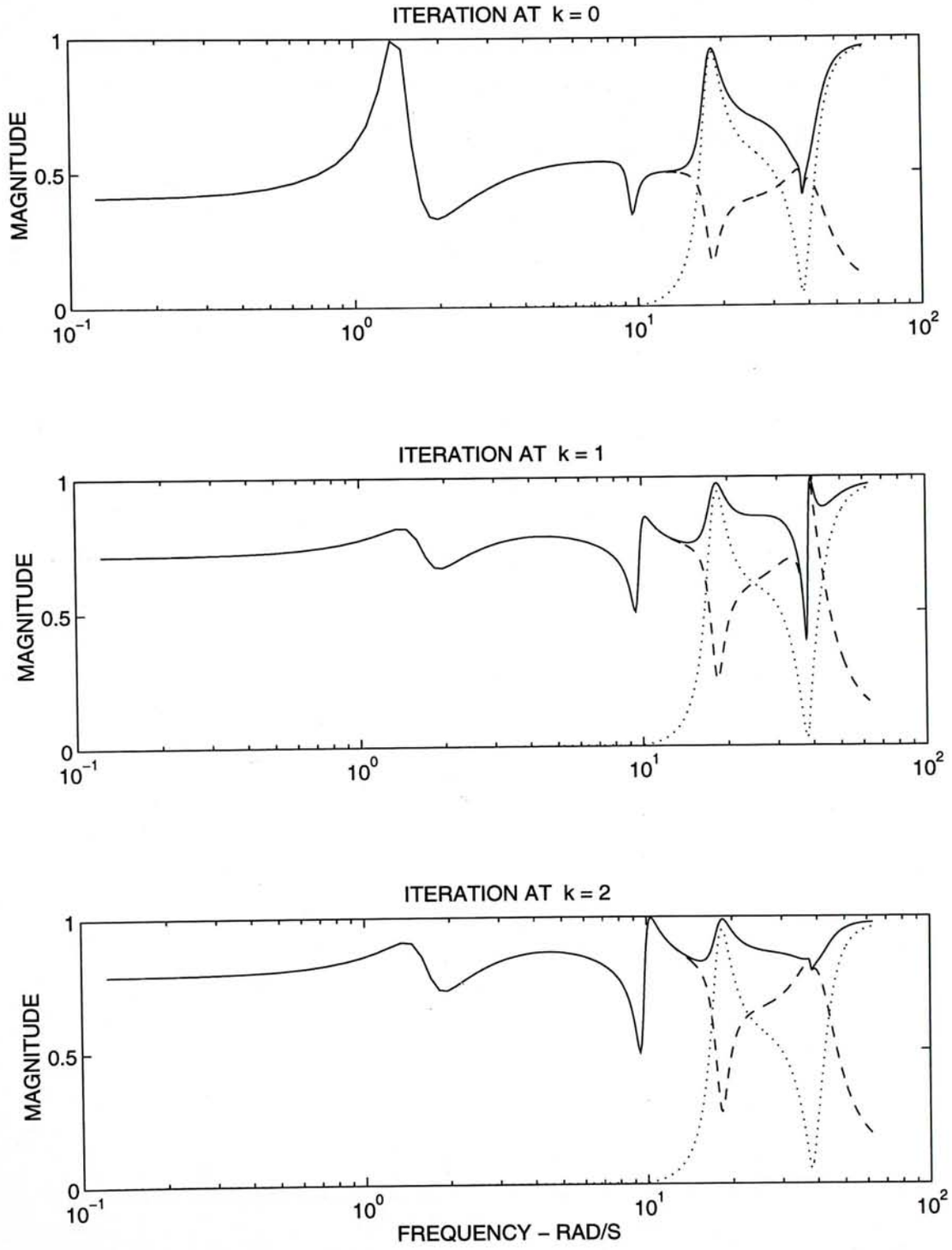

Figure 7.6: IFWCR iterations: $T_{y_1 u-1}$ (solid), $\gamma_o W_1 S$ (dashed) and $W_2 R$ (dotted)

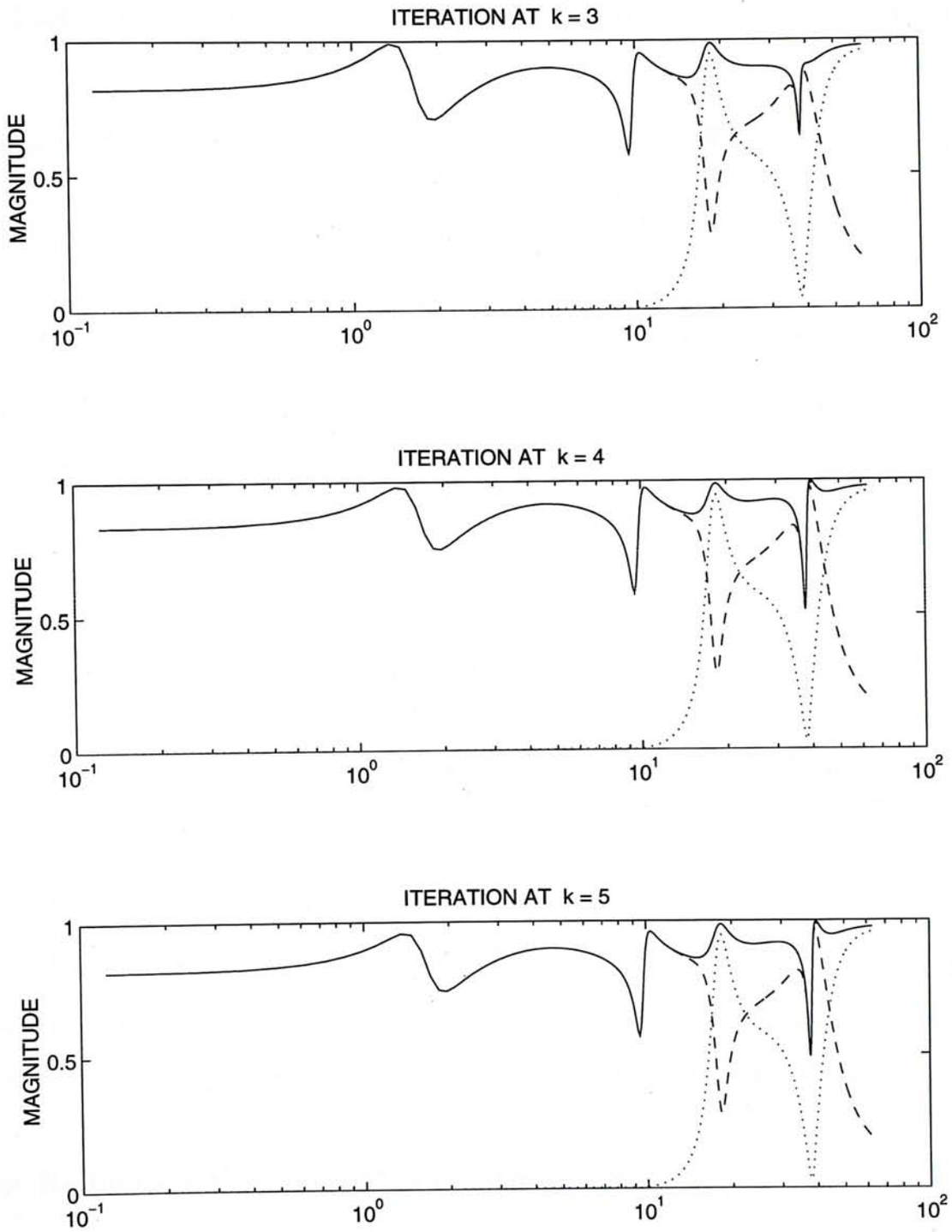

Figure 7.7: IFWCR iterations: $T_{y_1 u-1}$ (solid), $\gamma_o W_1 S$ (dashed) and $W_2 R$ (dotted)

7.3 Summary of Results

To facilitate discussions, table 7.1 summarizes all the design results in this chapter.

Method/ Section	maximum γ_o achieved	Controller Order	Plant order for design	Order of $W_1(s)$	Order of $W_2(s)$
Balanced Truncation†	0.335	7	7	2	0
7.1	0.3690	7	4	2	1
7.2.2	0.4945	7	7	2	0
7.2.3 i.e. (IFWCR)	0.5902	7	7	2	0

Table 7.1: Summary of design results in this chapter

7.4 Discussions of Results

Controller Reduction: Frequency Weighting Versus Uniform Weighting

In this example, the IFWCR scheme is able to iterate into a reduce order controller which achieve better performance than balanced truncation with uniform weighting (0.5902 Versus 0.335). Plain controller reduction without frequency weighting gives the worse performance amongst the three methods in this case.

Plant Reduction Versus Controller Reduction

When the plant reduction approach is compared with the IFWCR, the latter achieve 60% increase in performance (0.369 $\rightarrow$ 0.5902). This is mainly due to

†Uniform weight balanced truncation of the 9th order controller in section 7.2.1

the limitation imposed by the $W_2(s)$. The smaller the magnitude of W_2, the better the performance could be achieved (in the sense of increasing γ_o). The magnitude of W_2 is determined by two factors as pointed out in section 2.4:

1. The level of additive uncertainty of the nominal plant.

2. The available controller/actuator output level and the plant input saturation level.

The plant reduction process in section 7.1 introduces a large magnitude of additive uncertainty (in the ∞-norm sense). Thus W_2 which must overbound the additive uncertainty, has to attain a larger magnitude. Even if a large control effort is available and the plant itself could endure a large input, the W_2 could not explore these advantages.

Whereas in the IFWCR case, W_2 could be set to the limit of the control effort and plant input level. This aspect is being illustrated in Figure 7.8 which shows the step response and the corresponding controller output. The IFWCR controller use a much greater effort to achieve better performance.

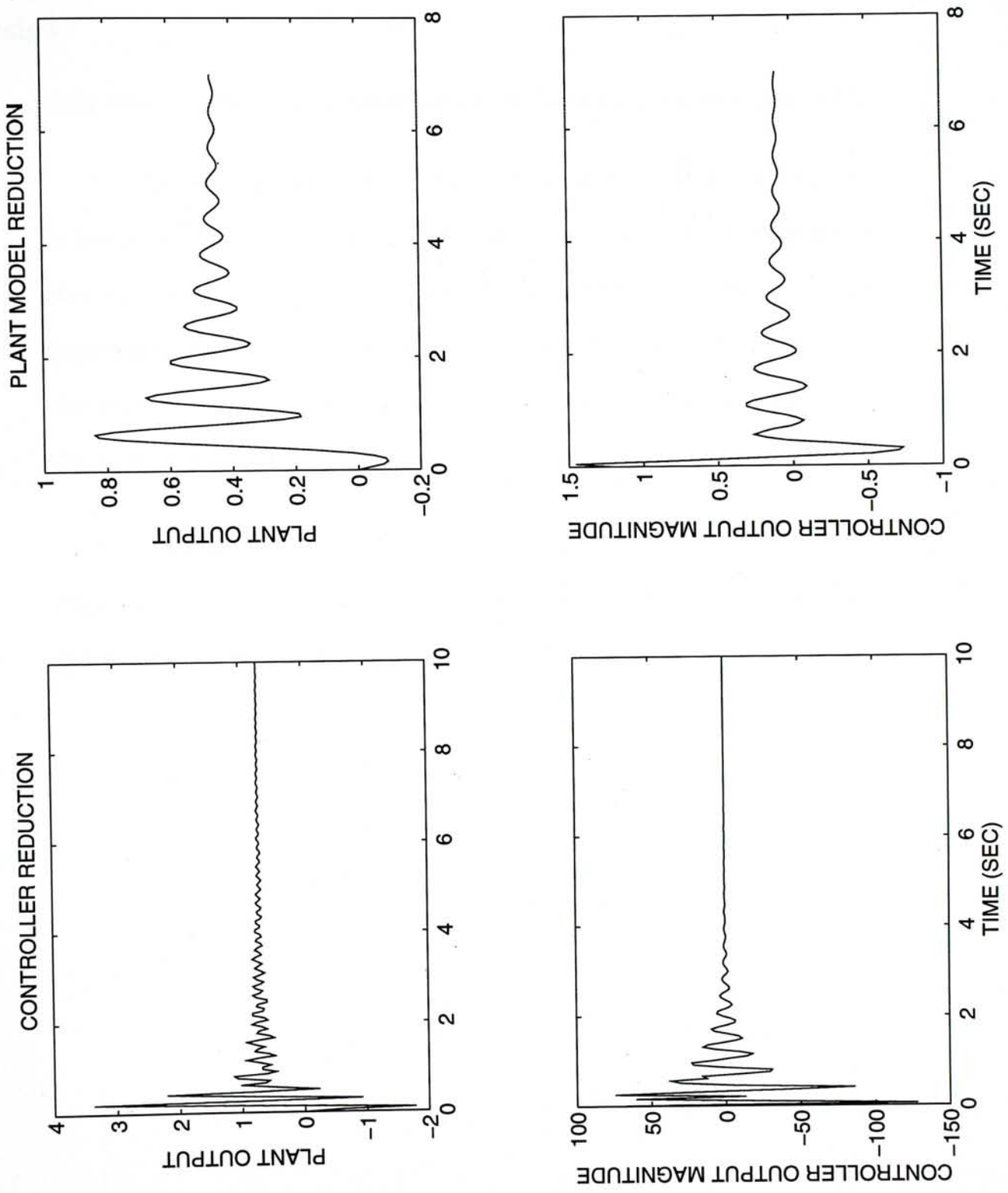

Figure 7.8: Comparison of controller effort between IFWCR [Left] and plant reduction approach [Right]

Other criticisms of plant reduction approach for low order controller design

Regarding other criticisms on plant model reduction, we quote from [41]:

> " ... the approximation (of plant) is carried out at an earlier step in the process than if the controller is approximated; each subsequent step in a design after an approximation propagates the effects of that approximation, and the ultimate effect at the end can be unclear, the more so the greater the number of design steps subsequent to the approximation."

> " ... satisfactory approximation of the plant requires some knowledgy in advance of the controller. So the designer is caught in an awkward logical loop."

Chapter 8

A Comparative Example on a Benchmark problem

In this chapter, we apply the ISI/CD scheme outlined in chapter 5 to a benchmark plant. This example will illustrate the strength of our scheme for an unknown time-varying system.

Using this benchmark for evaluating our approach has the following advantages :

- Nine other groups of researchers [45–53] have implemented their control designs for this benchmark and we could evaluate our design comparatively.
- Due to the design of the benchmark plant, we do not have any prior information about the model structure, noise covariances, parameter variations, ... etc. It resembles the control problems commonly faced in industrial environment.

- The benchmark plant is noisy and is time-varying, these characteristics could be an effective way to test out the robust H_∞ controller, which is designed with the purpose of robust performance in mind.

The benchmark plant and the design specifications will be described in section 8.1. Section 8.2 will discuss the considerations in choosing suitable design weightings. Then the system identification results and the robust control design results will be presented.

8.1 The Benchmark plant [54]

8.1.1 Benchmark Format and Design Information

The benchmark were standard C source code that simulates a plant* [54]. Given a user generated control signal at any sampling instant, the code simulates the resulting plant output response at the next sampling instant. Other than the user interface, the code is scrambled and virtually unintelligible to human readers, thus concealing the true nature of the system.

The information supplied about the plant is as follows :

- A single-input single-output and time-varying at three user-selectable "stress levels", with higher stress level inducing larger time variations.

- The setpoint to the loop is a square wave varying between $+1$ and -1 with a period of 20 seconds.

*This benchmark plant was developed by a group led by Professor S. F. Graebe of Centre for Industrial Control Science, University of Newcastle.

- A representative picture of the variations is achieved if the plant is simulated over at least 300 s.
- Due to noise and parameter variations and a randomly initialized random number generator, the response will be different every time a simulation is run (larger variations at a higher stress levels).

In order for the reader to have some idea of the benchmark plant, we plot fifteen open loop step responses at stress level 1 in Figure 8.1.

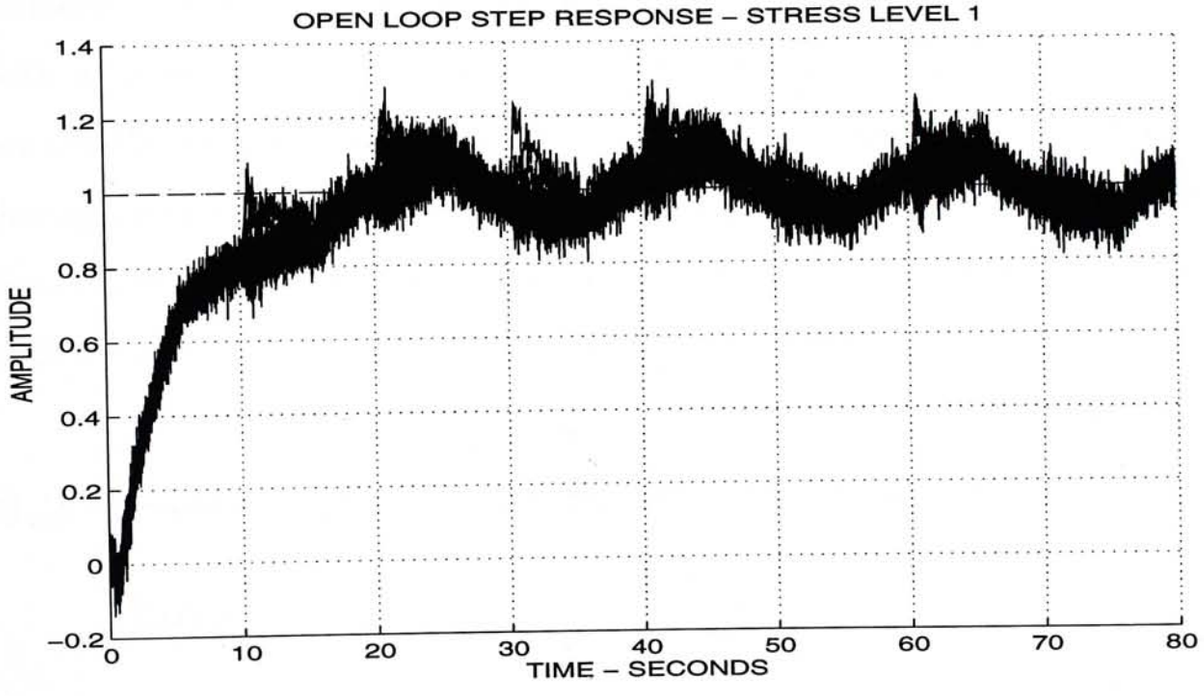

Figure 8.1: Open loop step response - Stress level 1

8.1.2 Control Design Specifications

For each of the three stress levels, it is require to design a controller to achieve rise times as fast as possible, subject to the following conditions:

- Plant output must be between -1.5 and $+1.5$ at all times.
- Zero steady state tracking error (modulo high frequency noise).
- The over/under-shoot should preferably be less than 0.2 "most of the time", though occasional larger over/under-shoots are acceptable if the ± 1.5 limits are observed.
- Fast settling is preferable

Remark. The design specifications were deliberately kept vague and in style with what is frequently encountered in industrial control applications: there are usually hard limits on certain variables that would otherwise cause physical damage, then there is a somewhat more vague specification on preferred overshoots, and finally it is desired to get set point tracking simply as fast as possible with the achievable limits not really being known in advance.

8.2 Selection of Performance Weighting function

To impose the close-loop specifications under the framework of H_∞ controller design, the bridge between the theory and practice is the selection of the frequency domain weighting functions, W_1, W_2 and W_3 mentioned in section 2.4 and 2.6. For example, in Figure 2.5,

- W_1 corresponds to the requirements of the specifications on error signal, in our case zero steady state error.

- W_2 is related to the control effort and the level of additive uncertainty in the plant.
- W_3 is related to the output level of the plant and the multiplicative uncertainty.

8.2.1 Reciprocal Principle

This principle illustrates the interaction between the sensitivity function and the weighting function W_1. Let's consider the case of *sensitivity minimization problem* in section 2.4.4, i.e. minimizing e in Figure 2.1.

Theorem 8.2.1 *Assumes a controller $C_o(s)$ minimize the sensitivity function $S_o = (1 + PC_o)$, i.e.*

$$\min_{C(s)} \|W_1(s)(1 + P(s)C(s))^{-1}\|_\infty = \|W_1(s)(1 + P(s)C_o(s))^{-1}\|_\infty = \rho$$

then

$$S_o(j\omega) = A(j\omega)\frac{\rho}{W_1(j\omega)}, \qquad \forall\, \omega \in \mathcal{R} \tag{8.1}$$

and $A(s)$ is a all-pass function, i.e. $|A(j\omega)| = 1 \quad \forall\, \omega$.

Proof : See section 6.1 in [55] or chapter 10 in [14]

So, the designer only has to specify the shape of the sensitivity function, $S_o(s)$ in frequency domain, then its *reciprocal* will be $W_1(s)$. Using this in the H_∞ controller design, the H_∞ optimal controller will make the shape of the sensitivity function equal to $S_o(s)$.

8.2.2 Selection of W_1

If we shape the transfer function from input to output, $T(s)$, so that it approximates a standard second order system, the ideal $T(s)$ and $S(s)$ will then respectively be

$$T_o(s) := \frac{\omega_n^2}{s^2 + 2\zeta\omega_n s + \omega_n^2} \tag{8.2}$$

$$S_o(s) := 1 - T_o(s) = \frac{s(s + 2\zeta\omega_n s)}{s^2 + 2\zeta\omega_n s + \omega_n^2} \tag{8.3}$$

If we take $W_1(s)$ to be $S_o(s)^{-1}$, according to (8.1), $W_1 S \approx \sigma A(s)$, that is

$$S \approx AS_o$$

Now A(s) behaves approximately like a time delay (this is a property of all-pass functions). So we arrive at the rough approximation

$$S \approx (timedelay) \times S_o$$

and our design should produce

$$\text{Actual step response} \approx \text{Delayed ideal step response}$$

The above idea is taken from [14].

8.2.3 Selection of W_2

The selection of W_2 with respect to additive uncertainty has been discussed in detail in chapter 3. Two other considerations which will affect the selection are the *available actuator output* and the *plant input saturation level.*

In this benchmark, the controller output is the same as the actuator output. Since the controller effort is produced by the control program of the user, it

could be as large as possible. Thus, no limitation is made for control effort level. However, in practical implementation, this consideration could be an important factor in the control design step.

As for the plant input saturation level, due to the limited information provided, it is decided not to take this factor into account during the early stage of the control design. Although the level of plant input saturation is known to be within ± 5 from [54], this is not a *a prior* information supplied to the designer. This information would not be used during the initial design stage. The control design without input saturation consideration is then implemented, and checked to see if there is any severe degradation in performance. A comparison of a group of step responses of the actual plant are made with that of the step response of the simulation using the identified plant.

It is concluded that no severe degradation in performance due to plant input saturation is observed. Thus, this consideration is neglected in this study.

If we want to limit the control effort to avoid plant input saturation, the magnitude of $W_2(s)$ could be increased at suitable frequency region. Since in H_∞ controller design, the condition,

$$\|W_2(s)R(s)\|_\infty \leq 1$$

must be satisfied[†]. And $R(s)$ is directly related to the level of control effort (section 2.4.2), increasing $W_2(s)$ results in decreasing $R(s)$.

[†]See section 2.5

8.3 System Identification by ERA

System identification was done using two different methods and the 2-norm minimization curve fitting (section 4.2) results were better, especially in the low frequency region which is instrumental for controller designed for step response. Thus the plants identified by 2-norm minimization curve fitting were chosen for control design.

However, the results of the ERA method could be used as a reference for the curve fitting methods. The curve fitting method required a prior specification of the plant order for the minimization process. And the plot of the Hankel Singular Values from the ERA method indicated that the plant order was around 5 (Figure 8.2). The results of the ERA method is given for stress level 1 in this section.

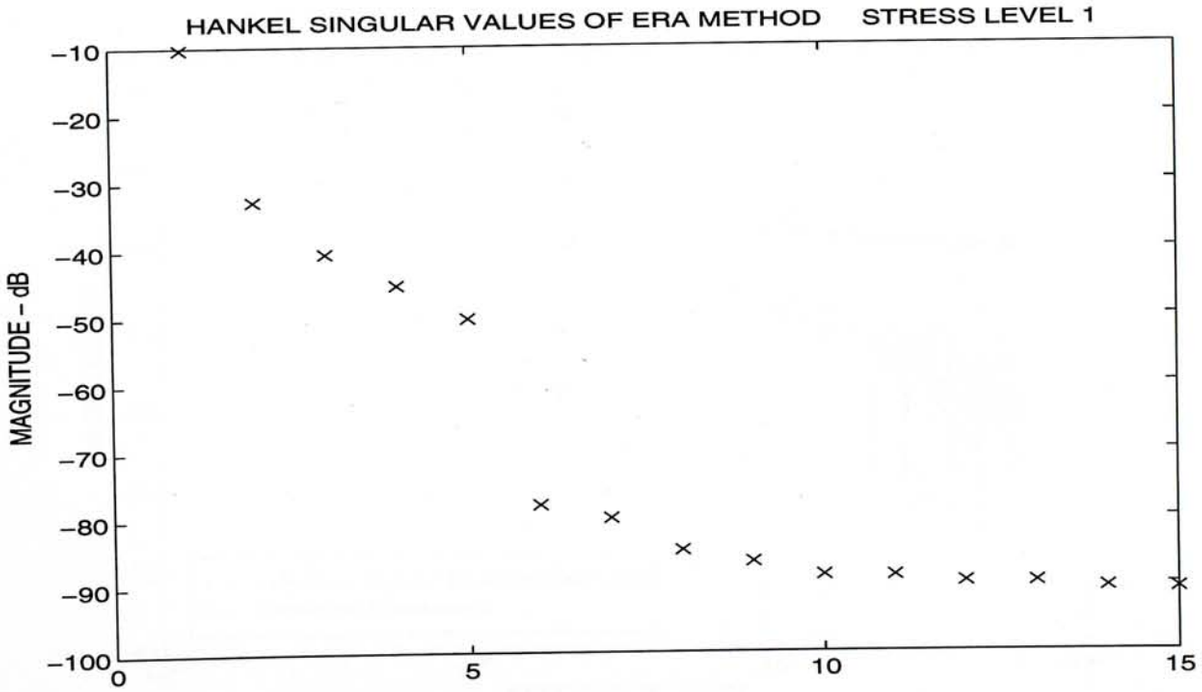

Figure 8.2: Stress level 1 Hankel Singular Values

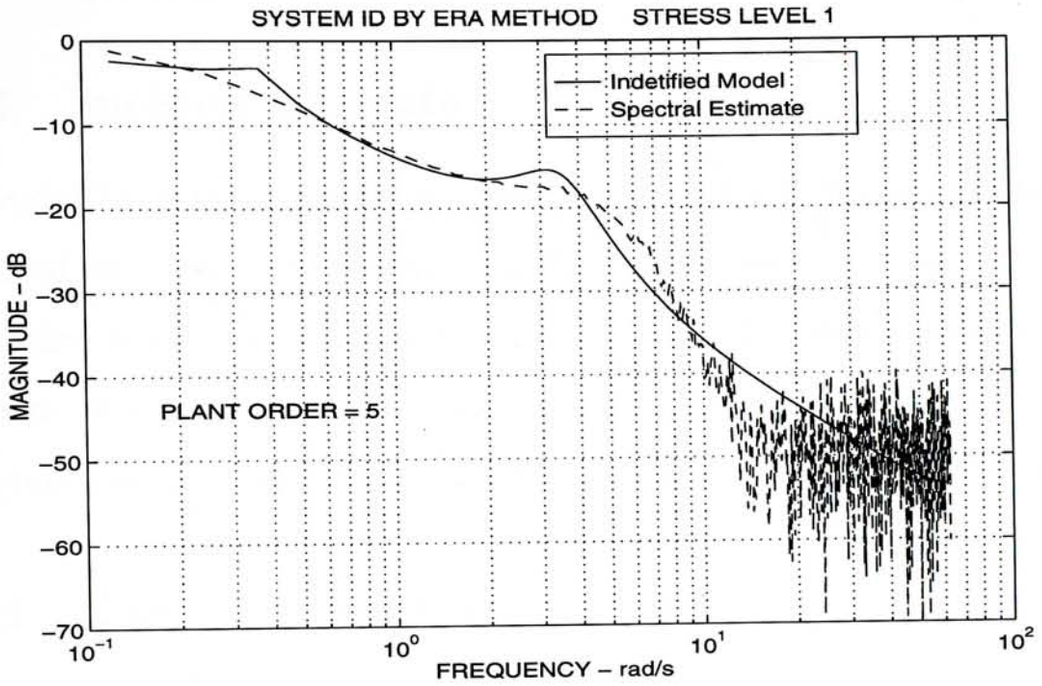

Figure 8.3: Stress level 1 ERA identification results

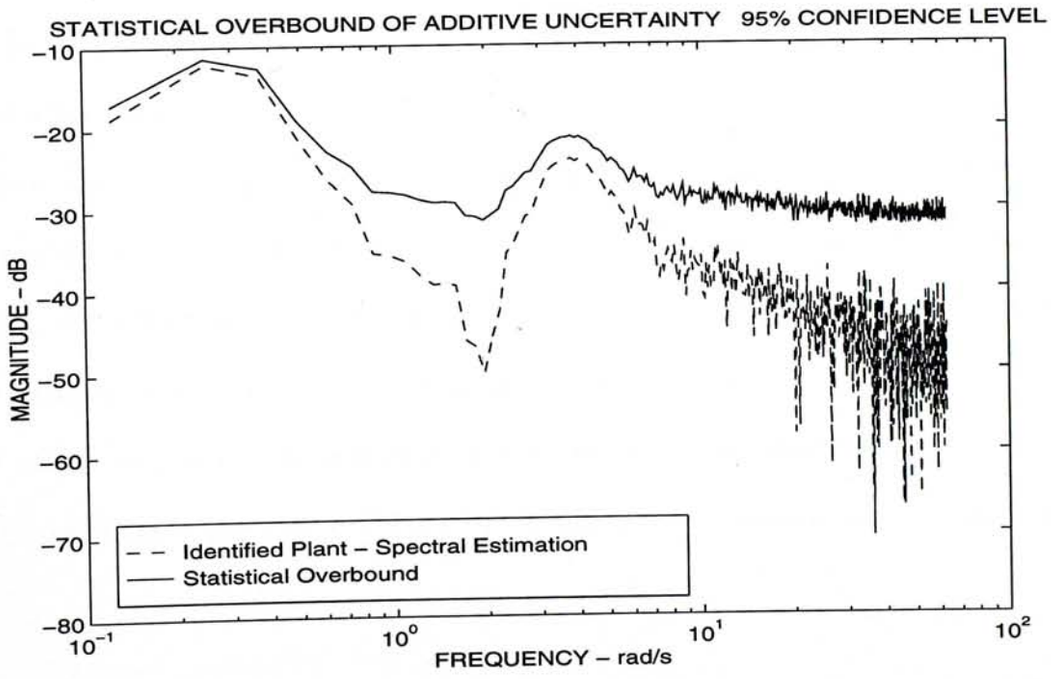

Figure 8.4: Statistical overbound of ERA method

8.4 System Identification by Curve Fitting

8.4.1 Spectral Estimate

To obtain the statistical additive uncertainty bound mentioned in section 3.3, a spectral estimate of 64 windows using the input/output data from the benchmark plant was generated. The input was a Schroeder-phased signal (section 3.2) with 1024 points per period with sampling frequency set to 20 Hz. This procedure was also done with the benchmark plant for stress levels 2 and 3.

8.4.2 Curve Fitting Results

The curve fitting procedures (section 4.2) were then used to obtain a transfer function in z-domain. The program required the user to specify the order of the plant. To determine the system order, the information obtained in the ERA procedures was called as a reference. The Hankel Singular Values reveal that the system order to be around 5.

Then several trials of curve fitting the spectral estimate with different orders were performed and the minimum error of the 2-norm minimization was noted. And the system order was then determined. A low order of the plant is preferred if the minimum error is not much greater than the higher order result, since the order of the controller increases with the order of the plant.

The results of the curve fitting procedures were tabulated in table 8.1

Stress Level	Curve fit order				Estimated Variance σ^*	System Order selected
	4	5	6	7		
1	0.1108	0.0939	0.0938	0.0936	$3.91e-3$	5
2	0.1571	0.1008	0.1006	0.1004	$4.39e-3$	5
3	0.1885	0.1172	0.1174	0.1181	$5.40e-3$	5

Table 8.1: Summary of 2-norm error in Curve Fitting

8.5 Robust Control Design

8.5.1 The selection of W_1 weighting function

According to the discussion in section 8.2.2, we set the settling time to be 8 s and 10 % overshoot. Thus $\zeta = 0.5912$ and $\omega_n = 0.9583$. Rounding $\zeta = 0.6$ and $\omega_n = 1$, we obtained the ideal $T_o(s)$ and $S_o(s)$,

$$T_o(s) = \frac{1}{s^2 + 1.2s + 1} \qquad S_o(s) = \frac{s(s+1.2)}{s^2 + 1.2s + 1}$$

and

$$W_1(s) = \frac{s^2 + 1.2s + 1}{s(s+1.2)}$$

Note that due to the zero steady state requirement, $W_1(s)$ must possess the factor $\frac{1}{s}$ such that $\|S(0)\|_\infty = 0$. Because $e = \|S(j\omega)\|_\infty r$.

Such a design weighting will be used throughout the design for stress levels 1, 2 and 3, so that the design results could have the same basis for comparison at different stress levels. However, it should be pointed out that tailoring different W_1 for each stress level could enable the design to achieve better performance (less over/under-shoot, faster settling, etc.)

A way to select suitable design weightings using experimental planning method that has been used in quality control is suggested in [56].

8.5.2 Summary of Design Results

Before going into the detail analysis of the robust design results, we would like to summarize the design results for the reader to have an overview.

Table 8.2 summarizes the major design parameters. It should be noted that controller model reduction has been carried out whenever possible using the scheme discussed in chapter 6.

Stress level	Controller Order	Optimal γ_o achieved	Maximum $T_{y_1u_1}$	Reduced controller order	γ_o of reduced controller	Order of W_2
1	9	0.5898	0.8190	8	0.5898	2
2	9	0.7148	0.9364	not reducible	NA	2
3	9	0.6211	0.8698	6	0.6211	2

Table 8.2: Summary of design results

In the reduced controller case, the order of the reduced controller was the minimum order which are still stabilizing when they are reduced by balanced truncation with uniform weighting (section 4.3. And the reduced controller achieved the same γ_o as the full order ones. No frequency weighted model reduction iteration was require. In the stress level 2 case, the balanced reduced controller was unstable and thus no further weighted reduction iteration was performed.

Since the control design considerations and results do not differ much for different stress levels, we will only discuss the robust control design issues in detail for stress level 1. The control design results of stress levels 2 and 3 could be found in the appendix A. For stress levels 2 and 3, we will only discuss the system identification and step response results.

The step responses of the reduced order controller case for stress levels 1 and 3 is listed in appendix B.

8.6 Stress Level 1

8.6.1 System Identification Results

The plots of the system identification results and the corresponding statistical overbound of additive uncertainty with 95 % confidence level are plotted, respectively, in Figure 8.5 and Figure 8.6. The $W_2(s)$ function in Figure 8.7 was obtained using the LPSOF Algorithm in section 3.4.

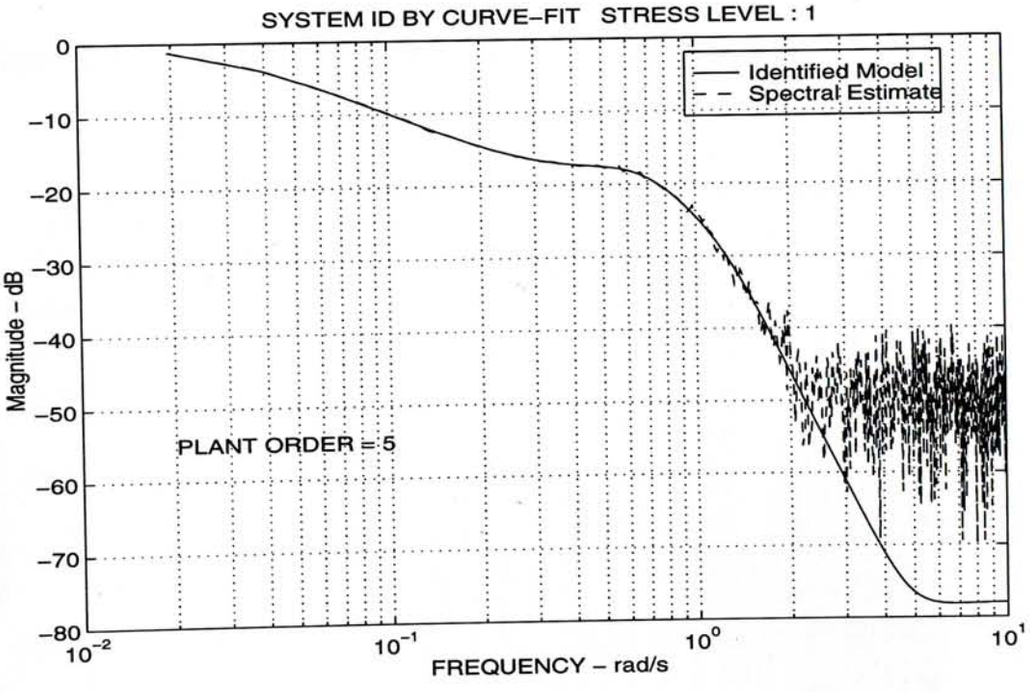

Figure 8.5: Stress level 1 curve fitting results

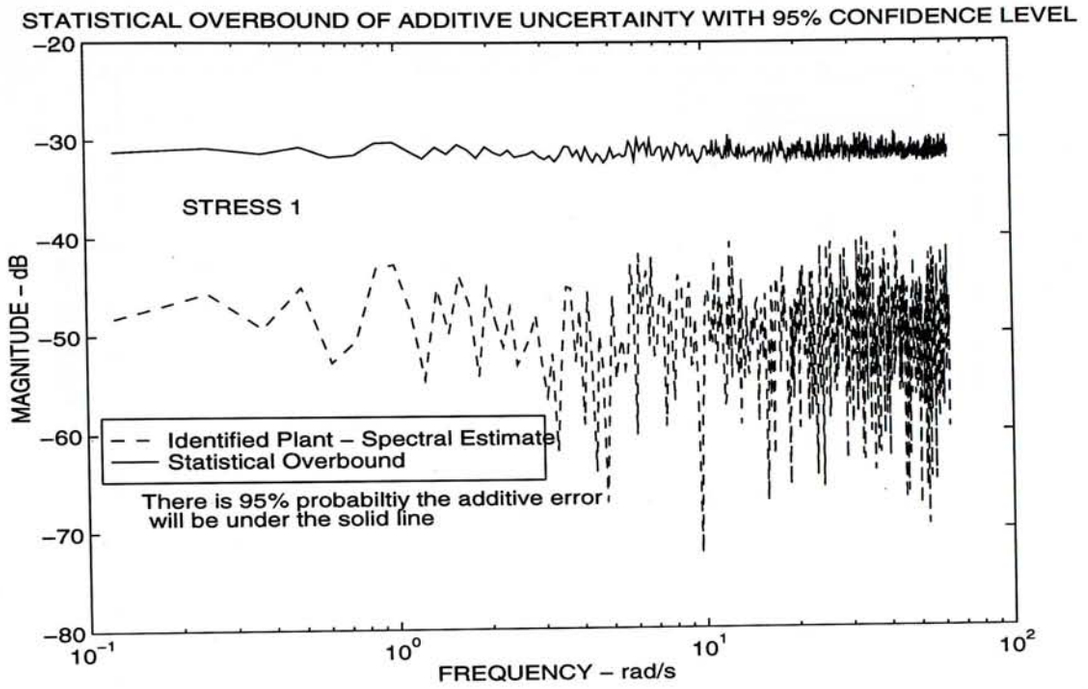

Figure 8.6: Additive error and the corresponding statistical overbound

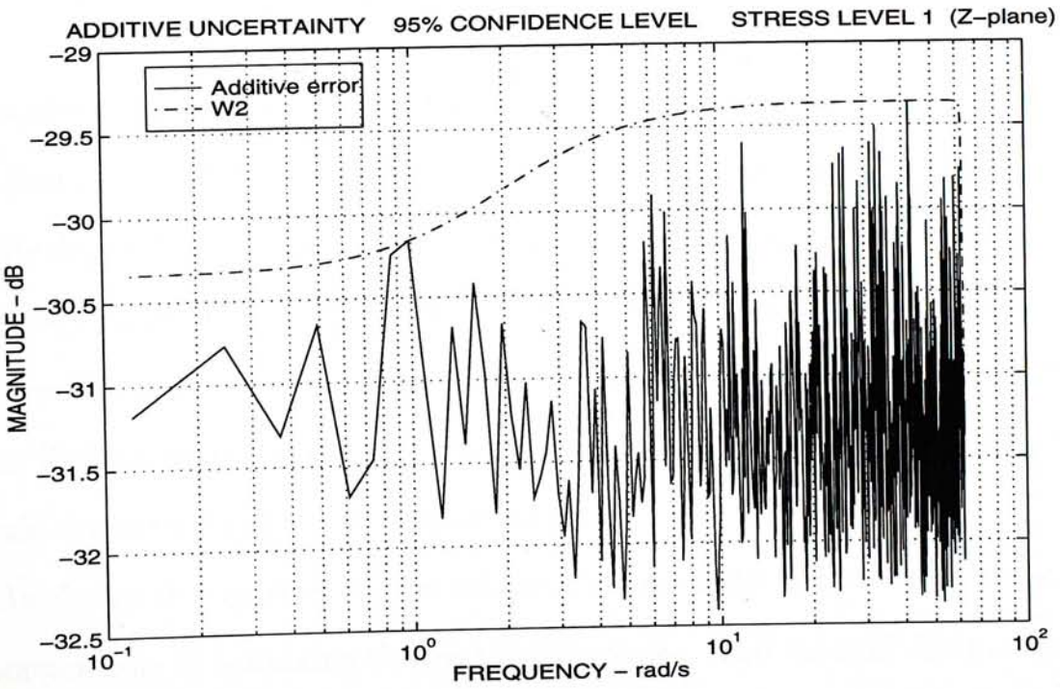

Figure 8.7: $W_2(s)$: a tight overbound of the non-parametric statistical bound

8.6.2 Design Results

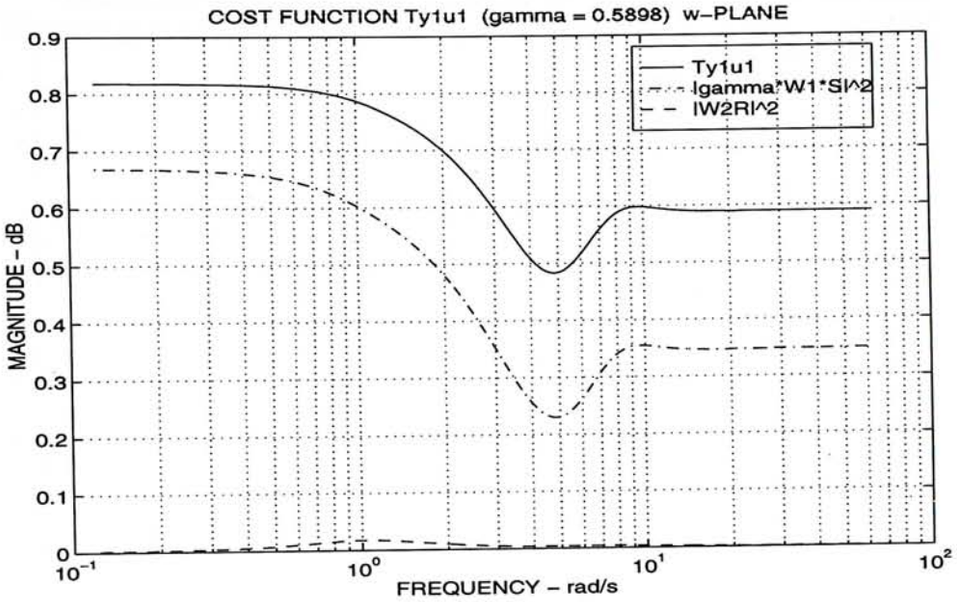

Figure 8.8: The cost function $T_{y_1u_1}$ and its components

For the cost function, in SISO case

$$T_{y_1u_1} = \sup_{\omega} \sqrt{(\gamma W_1 S)^2 + (W_2 R)^2} < 1 \tag{8.4}$$

the optimal γ, γ_o obtained through the γ-iteration is $\gamma_o = 0.5898$. Putting equation (8.4) and Figure 8.8 together, we could observe that the cost function is mainly dependent on the value of the term $\gamma W_1 S$ throughout the whole relevant frequency range. The term $W_2 R$ is much less than the first term and has little effect on the achievable performance. From Figure 8.9, we could observe that the major limitation for achieving better performance comes from the low frequency region, the zero steady state requirement.

As shown in Figure 8.10, the additive uncertainty in this case do not play a important role in achieving the best performance. The value of $R(s)$ is much less than the parametric additive uncertainty overbound W_2. W_2^{-1} could have been lowered if the consideration of plant input saturation were taken into account.

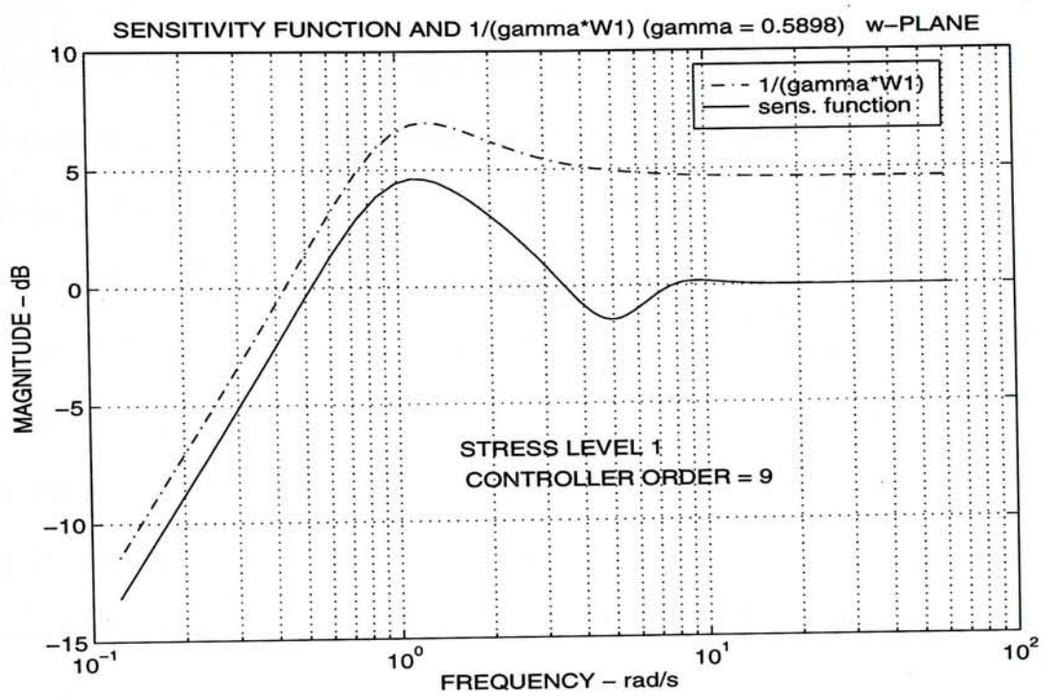

Figure 8.9: The $S(s)$ and $(\gamma_o W_1)^{-1}$

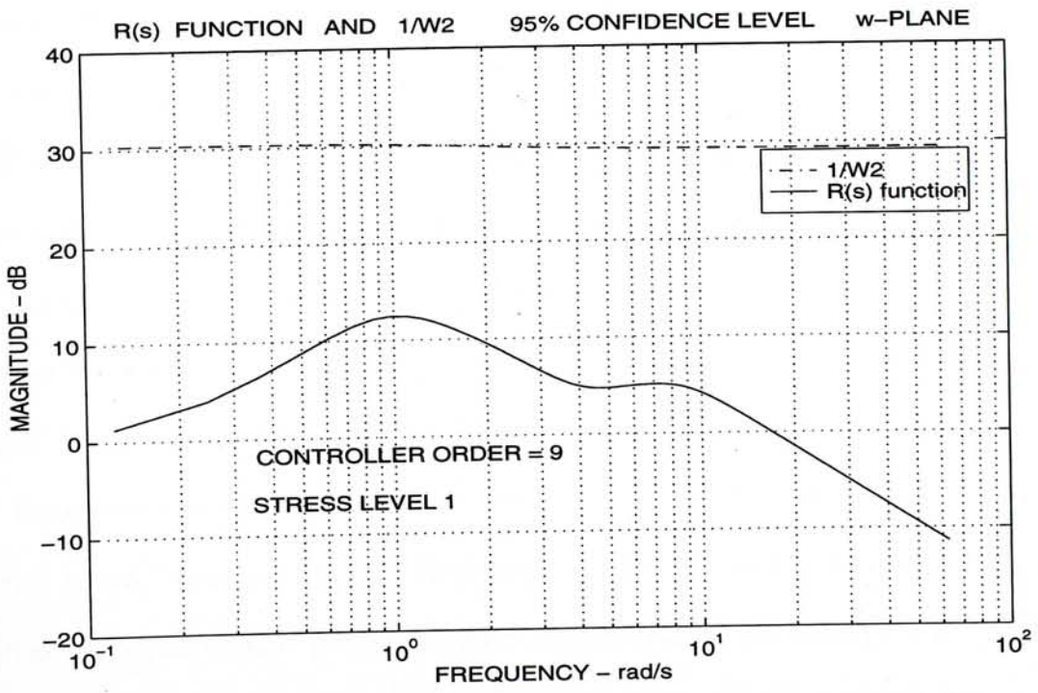

Figure 8.10: The $R(s)$ and W_2^{-1}

8.6.3 Step Response

Figure 8.11 is the simulated step response of the identified plant. It should be noted that a satisfactory simulated step response do not necessarily produce satisfactory results for the benchmark plant when the controller is implemented. Plant saturation has not been taken into account for the identified linear plant. The identified plant could take unrealistic input to give a superior step response; while the true plant input may be saturated, which is a non-linear effect.

In order to compare with other groups, it is required to implement the controller for the plant and run 15 times over a period of 20 s. Figure 8.12 and 8.13 shows the results of the compensated benchmark plant. For stress levels 1 and 2, the specifications requested for the control system have been completely satisfied by the designed controller in the initial "up" pulse of the first ten seconds.

The simulated step response using the identified plant is in close resemblance to that of the compensated benchmark plant. The maximum control effort in both case is around 3. Thus we could conclude that the controller output has not caused plant input saturation. Otherwise, the close-loop step responses would be much different. The decision of neglecting the plant input saturation in the selection of W_2 in section 8.2.3 is valid for this case.

However, for the "down" pulse response from 10s to 20s, the peak overshoot is slight higher than that of the "up" pulse. This is most likely due to the plant input saturation as the controller input level doubles when the system is required to go from $+1$ to -1. Redesign of the controller in the future may be required to enhance the performance. The redesign process probably involve a repeated iterations in design incorporation a lower W_2^{-1} to limit the controller effort until overshoot level is satisfactory.

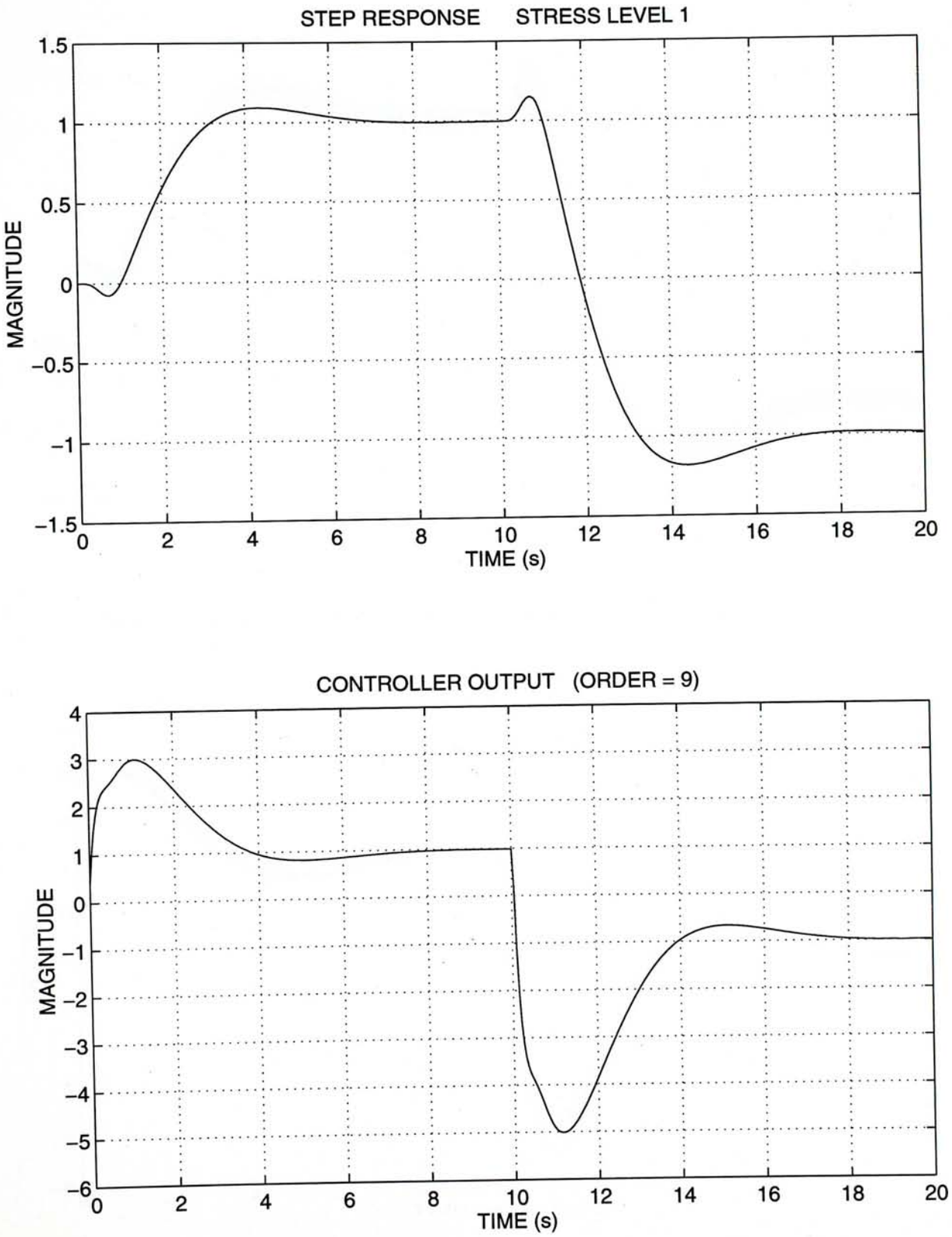

Figure 8.11: Step response based on the compensated identified plant

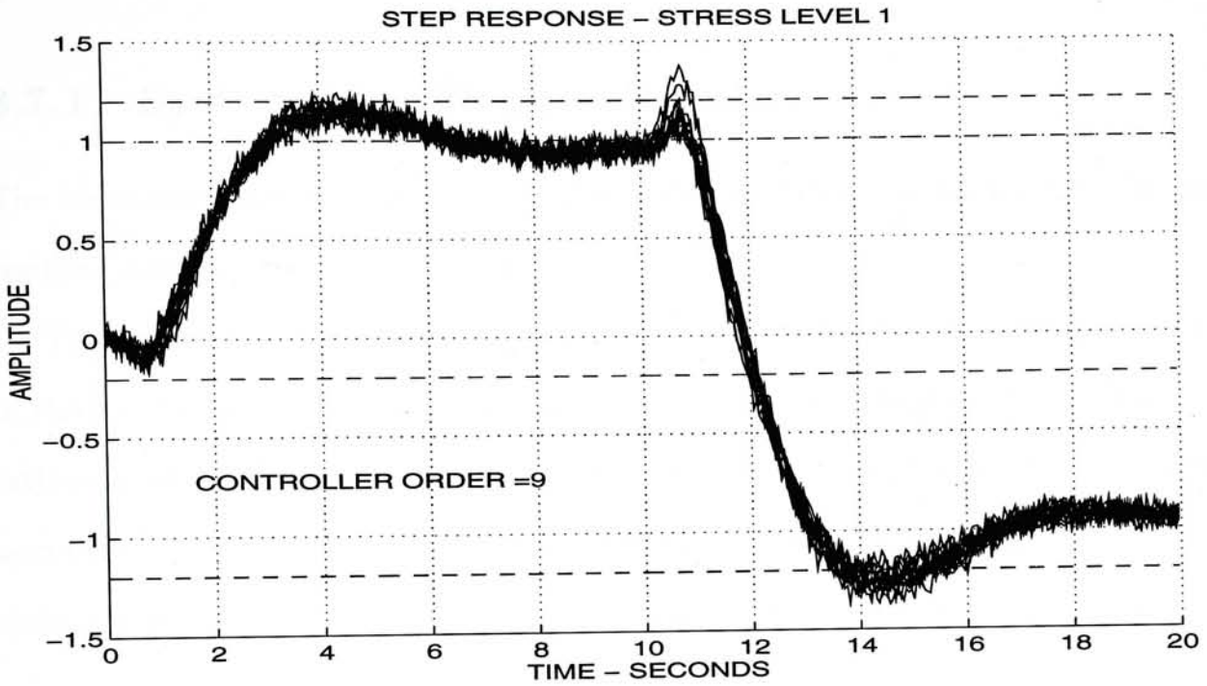

Figure 8.12: Step response of the compensated benchmark plant

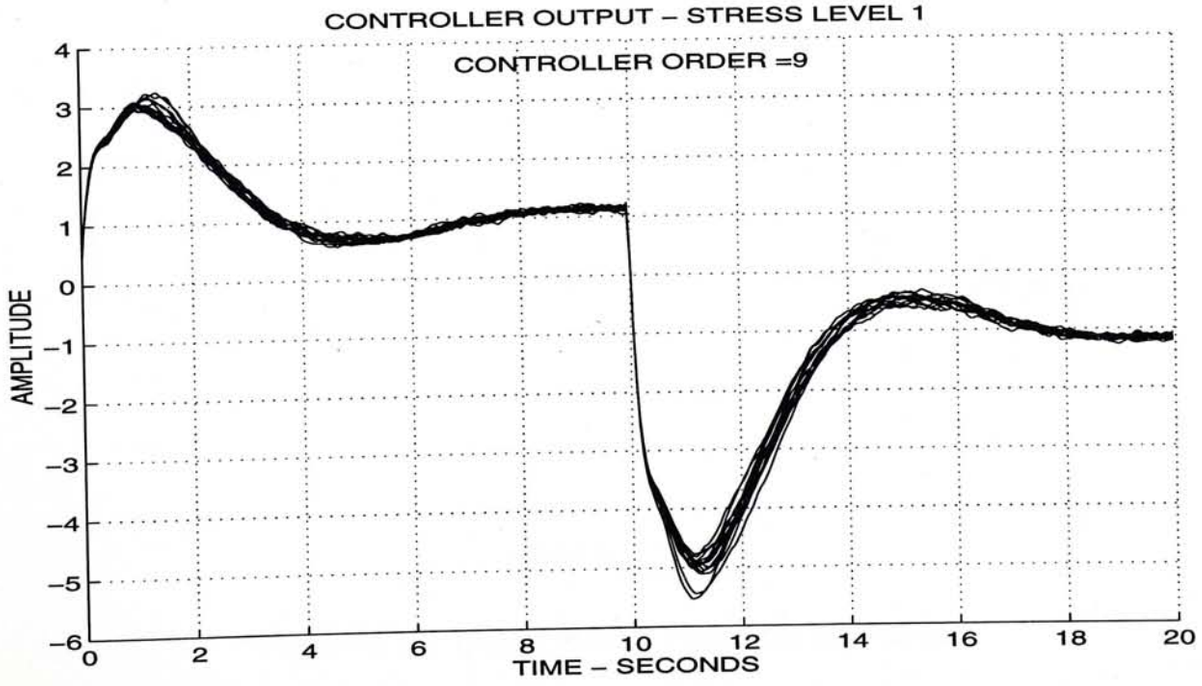

Figure 8.13: Controller output of the compensated benchmark plant

8.7 Stress Level 2

8.7.1 System Identification Results

The identified plant is of order 5. Higher order identification did not give better results (smaller total 2-norm error).

The additive uncertainty is a little higher than that of stress level 1, mainly in the low frequency region. This may due to the larger variation of the spectral estimate with a higher stress level. As can be seen in Table 8.1, both the total 2-norm error and the estimated variance is higher that those in stress level 1. The main component may come from low frequency modes variation of the plant.

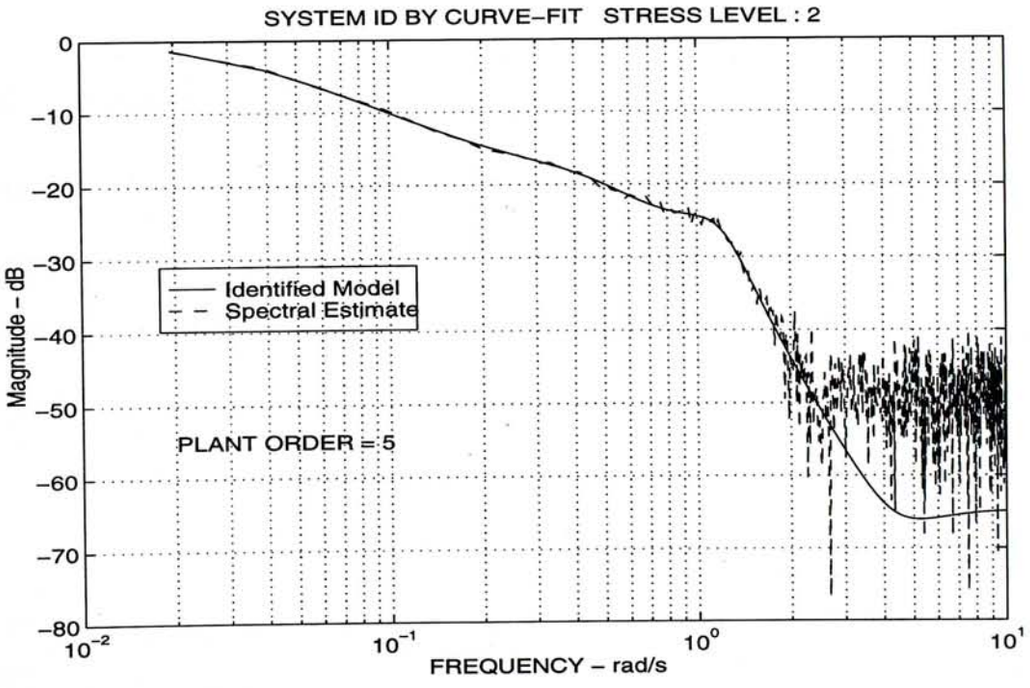

Figure 8.14: Stress level 2 curve fitting results

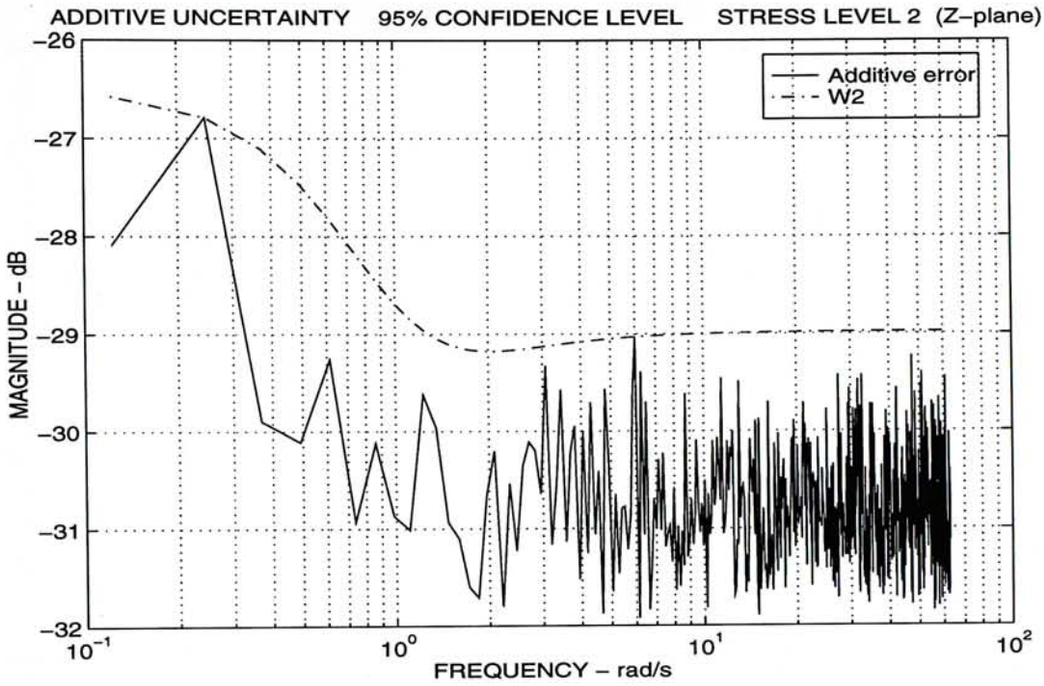

Figure 8.15: $W_2(s)$: a tight overbound of the non-parametric statistical bound

8.7.2 Step Response

Although the two simulated step responses of stress levels 1 and 2 do not differ much (Figures 8.11 and 8.16); the actual ones do have marked difference. Comparing Figure 8.12 and 8.17, the output deviate from the nominal one more frequently.

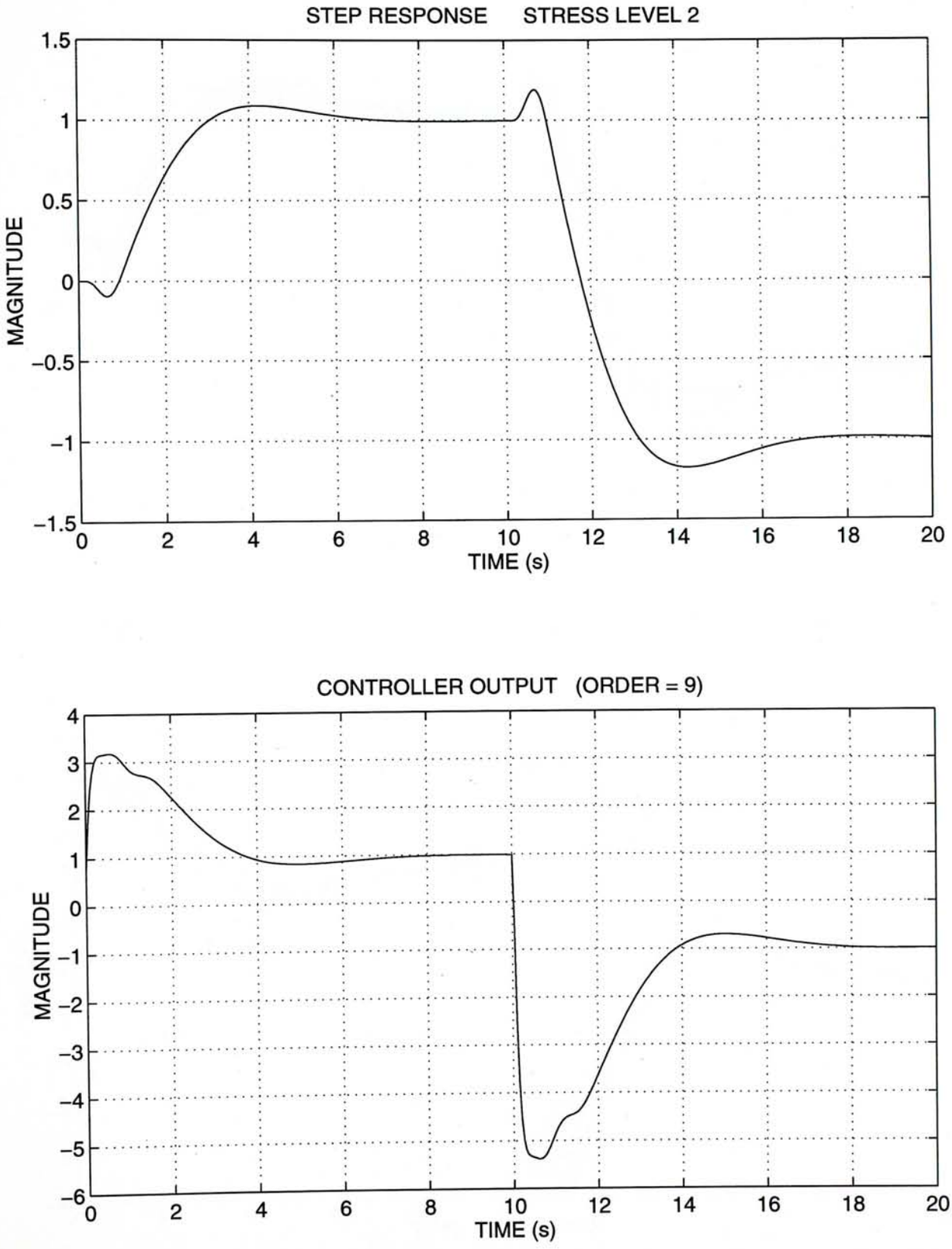

Figure 8.16: Step response based on the compensated identified plant

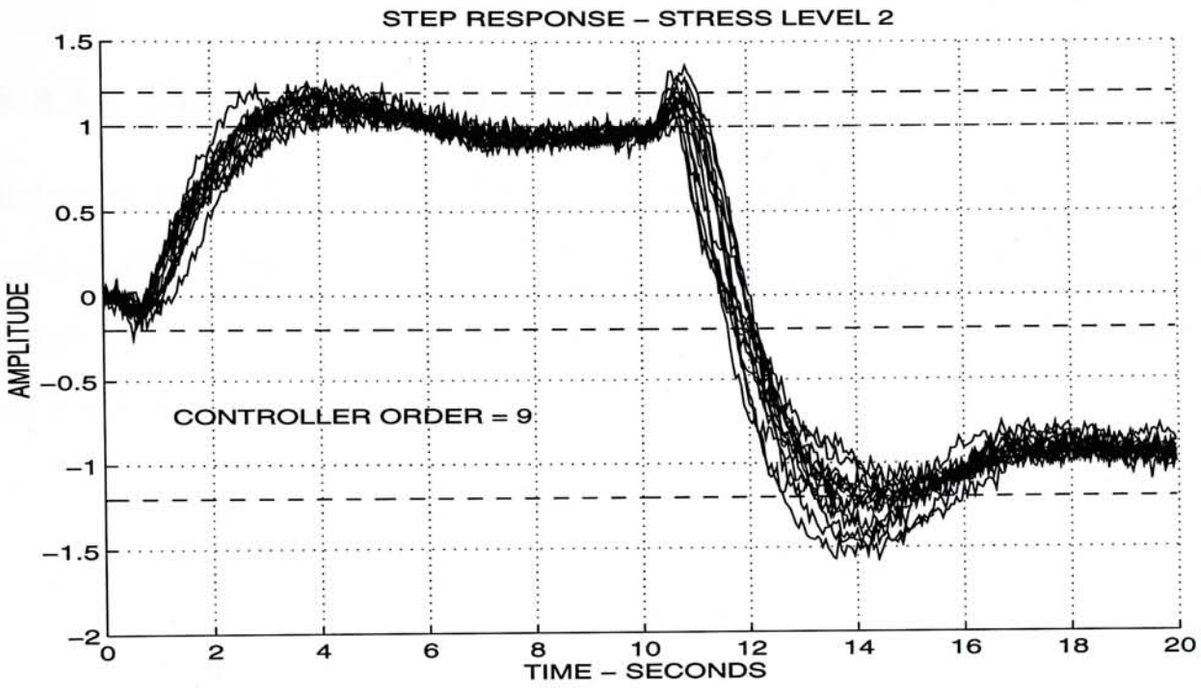

Figure 8.17: Step response of the compensated benchmark plant

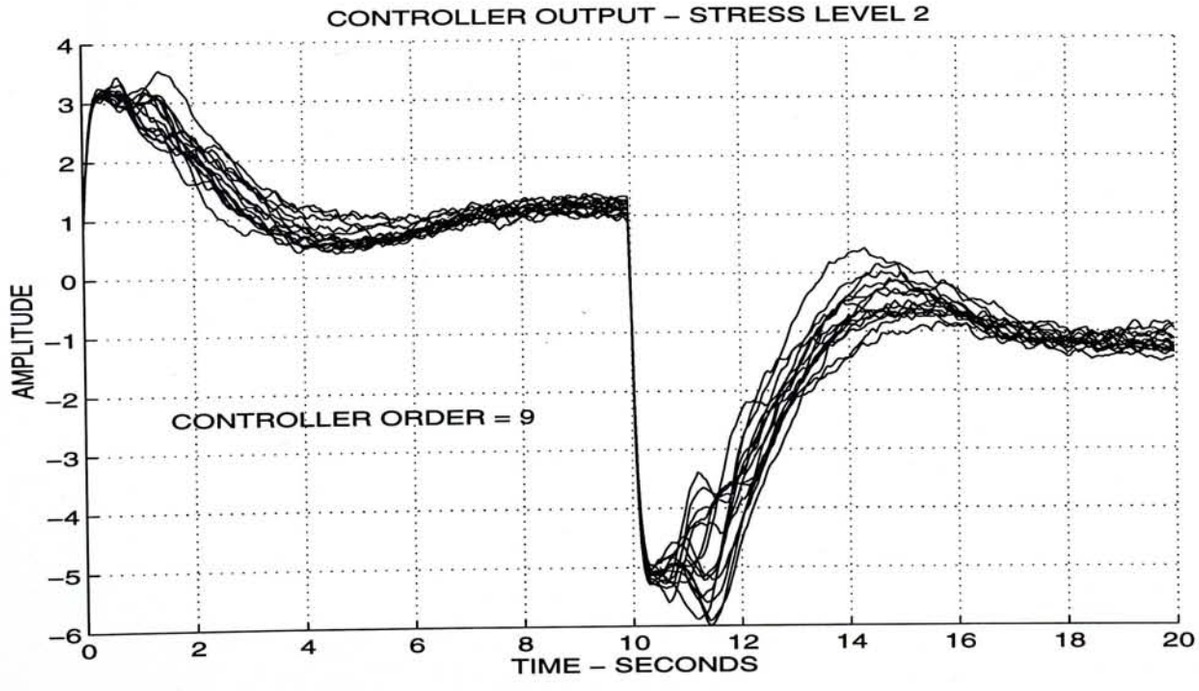

Figure 8.18: Controller output of the compensated benchmark plant

8.8 Stress Level 3

8.8.1 System Identification Results

Referring to Table 8.1, stress level 3 has the largest total 2-norm error and estimated variance. These coincide with the additive uncertainty results plotted in figure 8.20. The magnitude in the low frequency region is the highest among all stress levels.

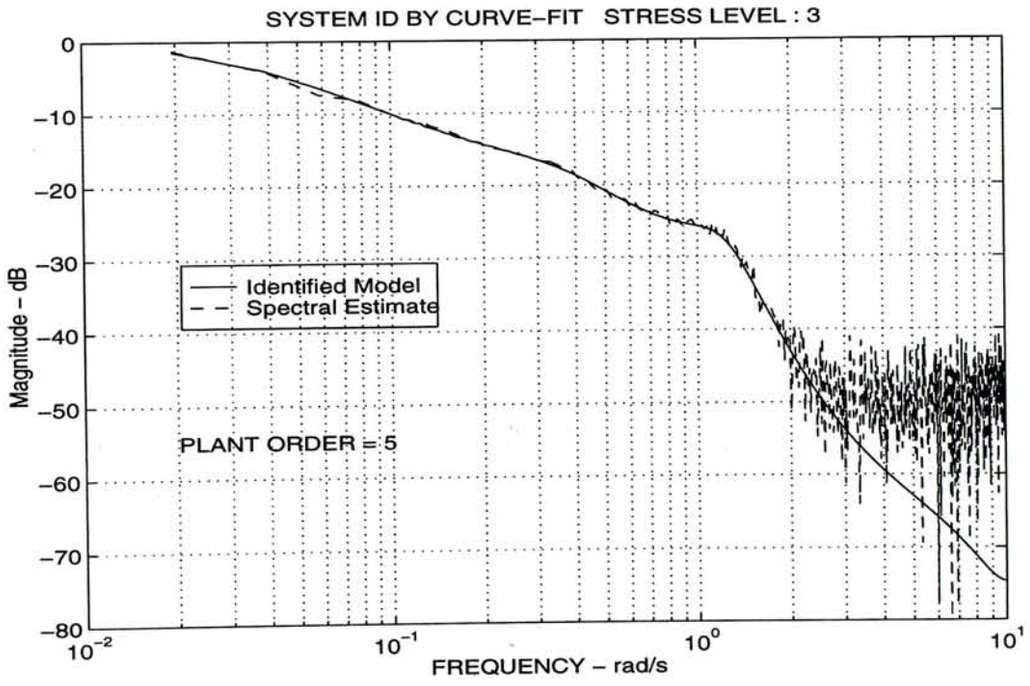

Figure 8.19: Stress level 3 curve fitting results

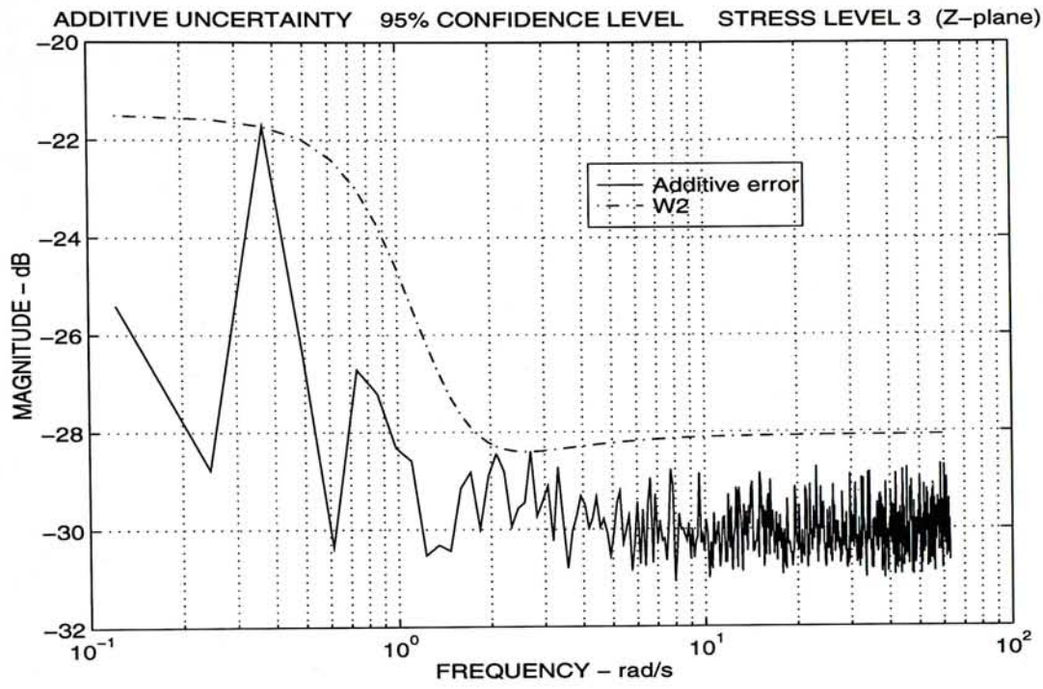

Figure 8.20: $W_2(s)$: a tight overbound of the non-parametric statistical bound

8.8.2 Step Response

The step responses of the stress level 3 has the highest variation. Sometime the compensated system become lightly damped, as seen in large overshoot; and sometimes over damped. Simulation results showed that a fixed controller can be designed to stabilize all of the possible transfer functions belonging to this stress level, but the prescribed specification for transient response cannot be met well.

It may be explained that the plant parameter variation interval is too large for a single controller to achieve the desirable performance for all of the possible plant transfer function.

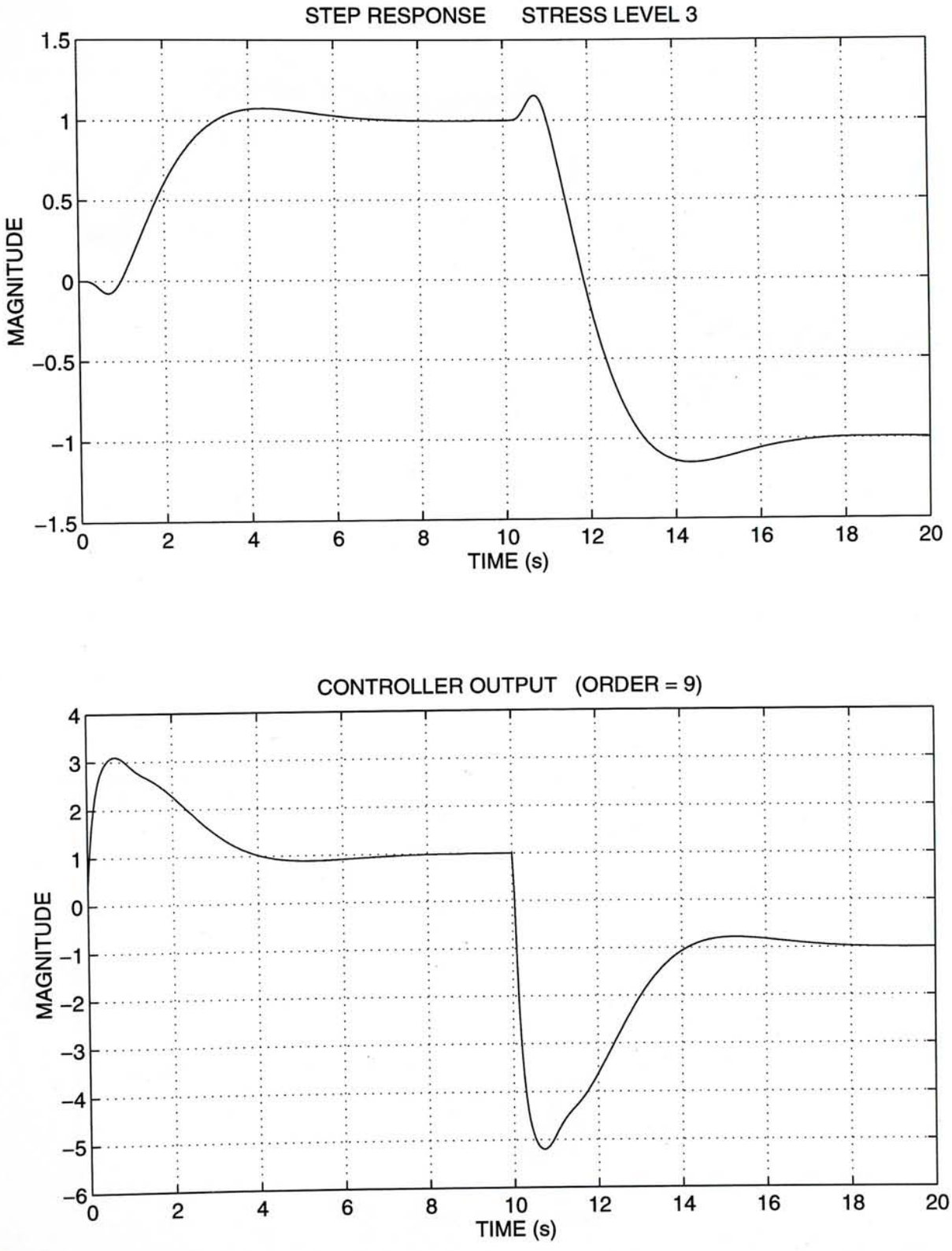

Figure 8.21: Step response based on the compensated identified plant

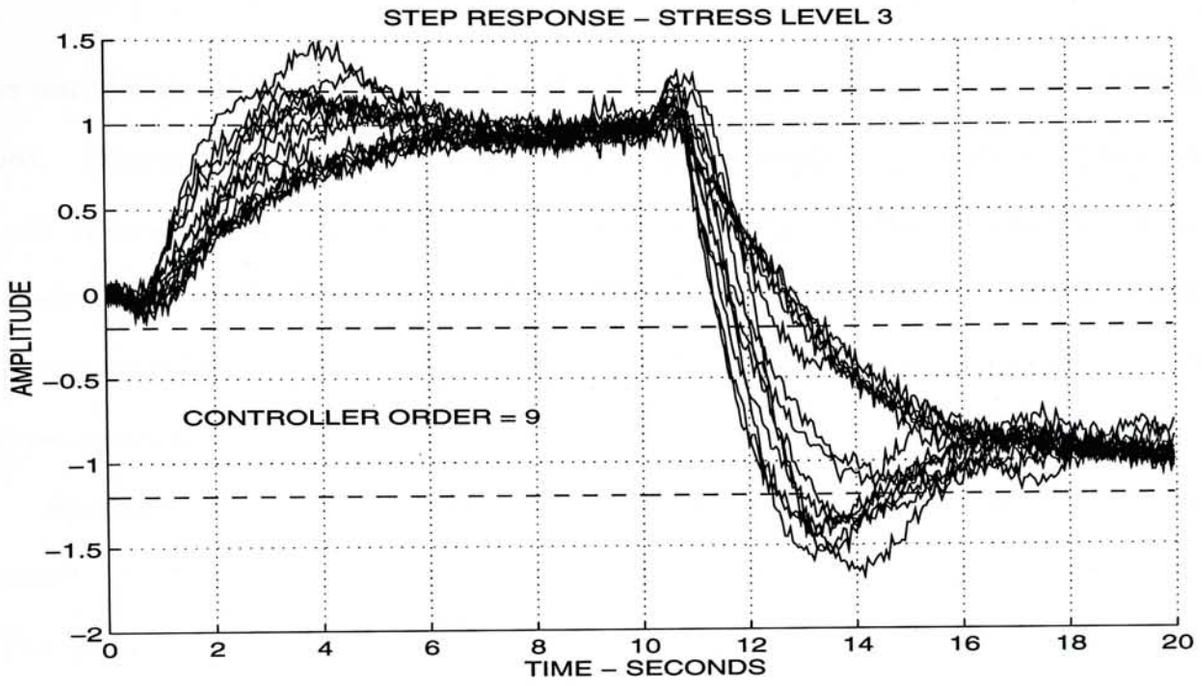

Figure 8.22: Step response of the compensated benchmark plant

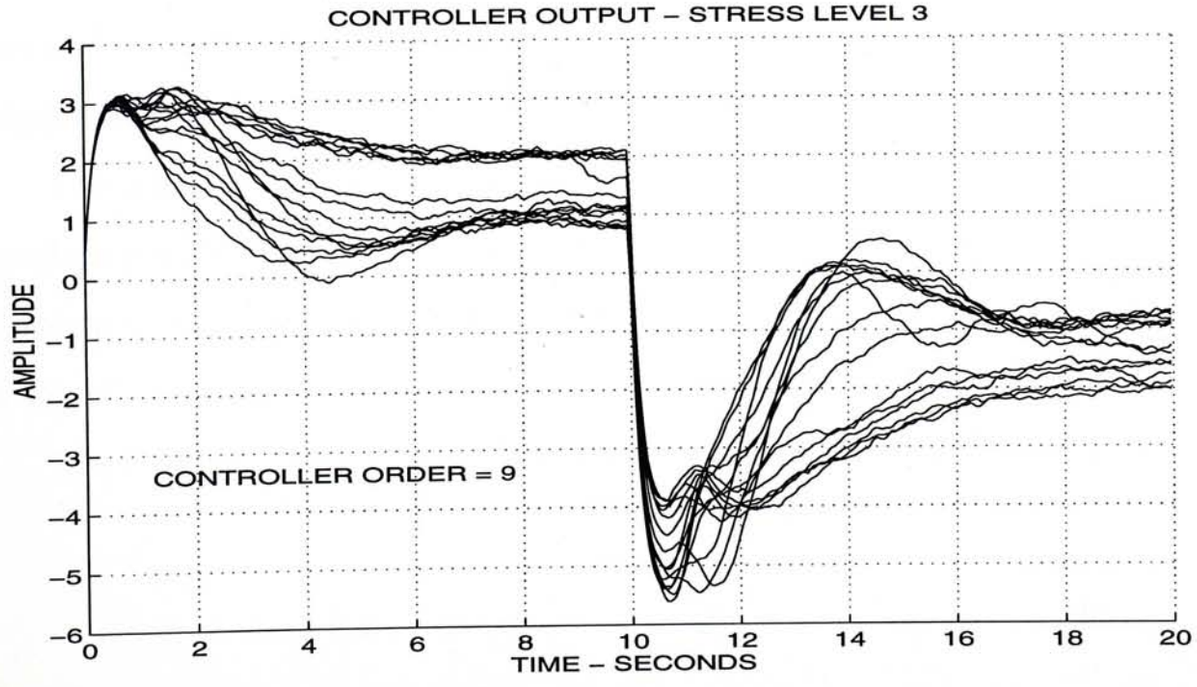

Figure 8.23: Controller output of the compensated benchmark plant

8.9 Comparisons with Other Designs

In our design approach, we treat the unknown time-varying system as a black box. Minimal prior information iss used in the modelling process. Then robust time-invariant H_∞-based controllers are design for three different stress levels. This appears to be successful to the extent that the achieved performance matches or exceeds the results of other groups of researchers which uses time-invariant controllers.

Specifically, [51] and [53] also used H_∞-criterion based technique. And our results is very similar to these two groups (Figures C.9, C.10, C.13 and C.14). The robust performance at stress 1 is good, but not better than the simpler PI designs [48,52] (Figures C.33 and C.21).

At stress level 3, the deterioration of performance indicates that some degree of adaptation is important for improvement. For example, the adaptive controllers in [52] (Figure C.38) and [53] (Figure C.16) improved performance significantly than the time-invariant counterparts.

The major advantage of robustness is achieved at stress level 2, which has moderate variations, our H_∞-based controller exhibit less deterioration in performance than other kinds of time-invariant controllers (See for example, [48] Figure C.21)

The results of other groups of researcher was summarized in appendix C.

Chapter 9

Conclusions and Recommendations for Further Research

9.1 Conclusions

The H_∞ norm is a valid measure for designing practical robust control systems: control of a plant with uncertainty. Different control design problems could be group under a unified framework using H_∞ norm.

In order to be able to exercise satisfactory control on a physical plant, a accurate nominal model must be obtained. But still, modelling error is bounded to occur in any process of modelling, a robust control design should incorporate the information about the bound of the uncertainty in the design.

One of the method to obtain a system model is to perform system identification on the physical plant. Based on the input/output data, we obtain two

models. One is a non-parametric model in frequency domain, i.e. the spectral estimate. The other is a parametric model which could be a transfer function obtained by 2-norm minimization or Eigensystem Realization Algorithm.

Using Schroeder-phased input signal for non-parametric system identification, a non-parametric "soft" statistical bound of plant uncertainty could be obtained. A additive parametric overbound function, W_2, could then be generated by a linear programming algorithm automatically. With the closed-loop requirement represented by the W_1 function, and the additive uncertainty bound W_2, an H_∞ controller could then be designed.

A integrated system identification/control design scheme with iterative reweighting has been proposed which will perform the identification step and the control design in turn iteratively. The objective is to obtain a nominal plant with accompanying uncertainty description, which will enhance the closed-loop performance in the next design step. The frequency weighted system identification uses information from the previous design step to initiate the weighting.

An approximate fraction frequency weighting scheme has also been proposed which could achieve better performance than a non-fractional one. The idea to to perform optimization of performance index, γ, at a reduced step. Both the full and fractional weighting scheme could also applied in a special case of system identification without noise, i.e. integrated plant model reduction/control design with iterative reweighting.

A iterative controller reduction scheme with iterative reweighting has also be proposed. The idea is to approximate the full order controller with an reduced order one closer in critical frequency region. An example showing that the controller reduction approach could achieve better closed-loop performance than

the plant model reduction scheme has been given.

Finally, the integrated system identification/control design scheme has been applied on a benchmark plant which has three user selectable stress levels with increasing level of plant uncertainty. The results have been compared to nine group of researchers and it has been shown that the performance of this scheme is comparable with other time-invariant designs. The best performance has been achieved at stress level 2.

9.2 Recommendations for Further Research

Some of the directions for further research are:

1. A time-domain frequency weighted system identification method based on Eigensystem Realization Algorithm could be further pursued. It will enable all the system identification/control design procedures to be carried out in time-domain.

2. In this thesis, the discrete H_∞ controller design is carried out with the help of Tustin transform to transform the w-plane H_∞ controller to a discrete one. Method to perform direct design of discrete-time controller based on discrete-time plant could simplify the whole design process; enabling the designer to gain more physical insight in the design procedures. The method based on minimax principle using *game theory* is a promising approach [35].

3. System identification methods that could also identify the plant input saturation level will be a great help in the control design step.

4. A frequency weighted spectral estimate to be developed may be helpful in reducing the additive uncertainty bound at regions where the plant has a low level of gain.

5. A better method to generate frequency weighting for parametric system identification, which could guarantee convergence of the performance index has yet to be developed.

Appendix A

Design Results of Stress Levels 2 and 3

A.1 Stress Level 2

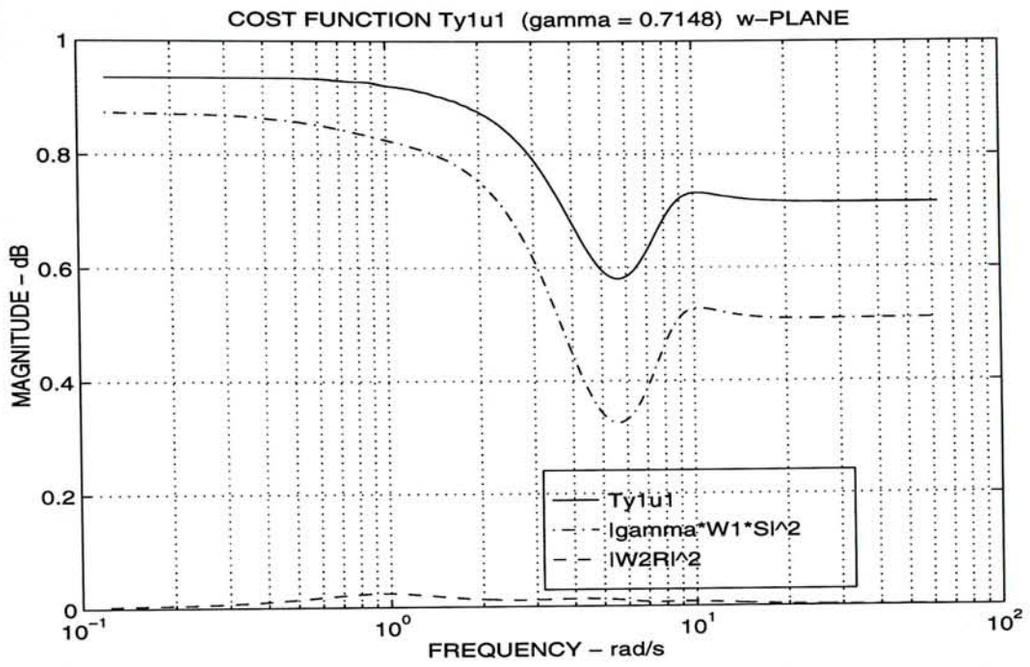

Figure A.1: The cost function $T_{y_1u_1}$ and its componenets

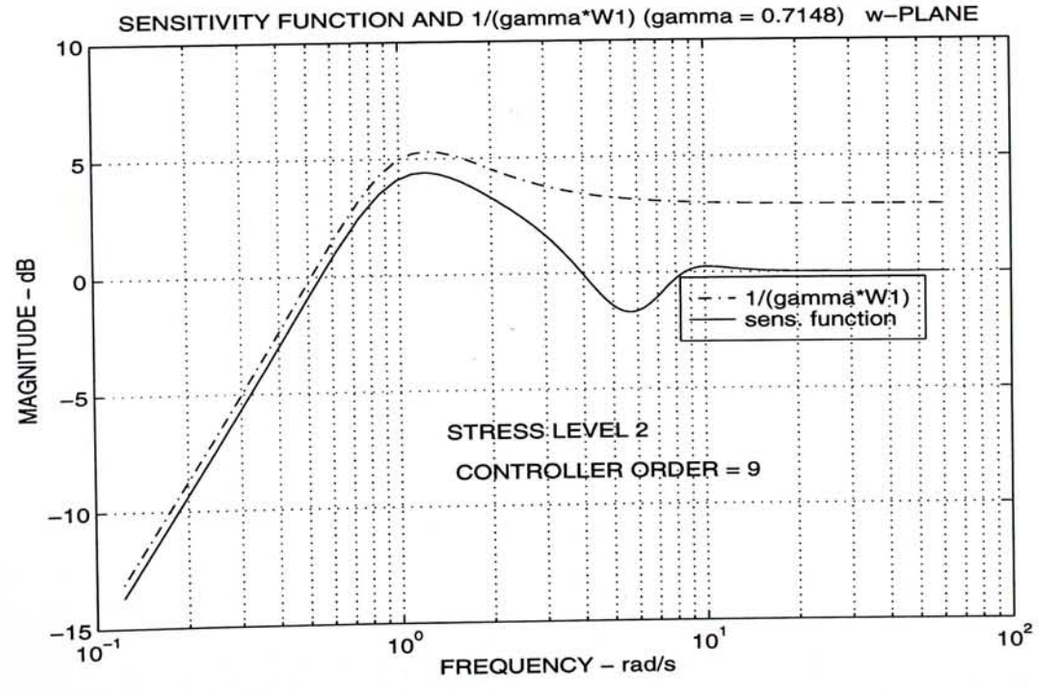

Figure A.2: The $S(s)$ and $(\gamma_o W_1)^{-1}$

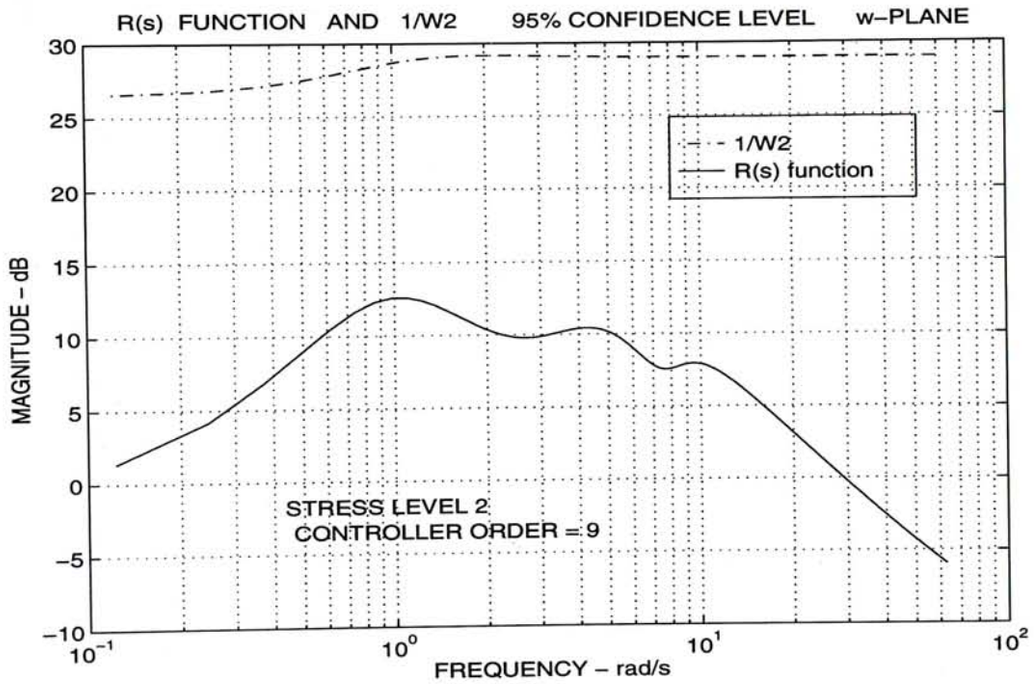

Figure A.3: The $R(s)$ and W_2^{-1}

A.2 Stress Level 3

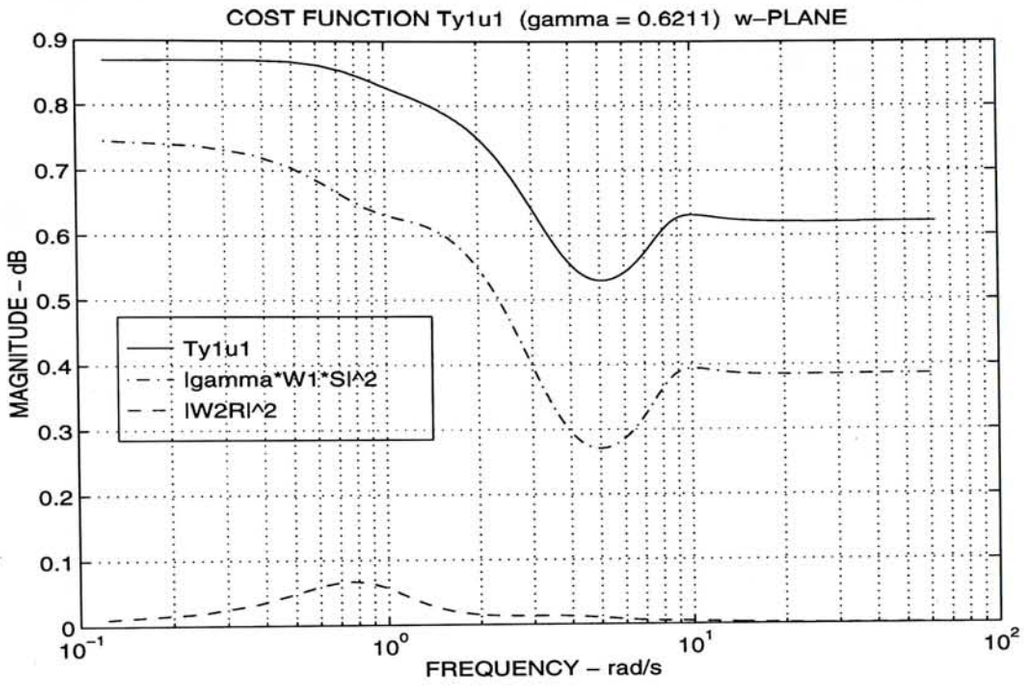

Figure A.4: The cost function $T_{y_1 u_1}$ and its componenets

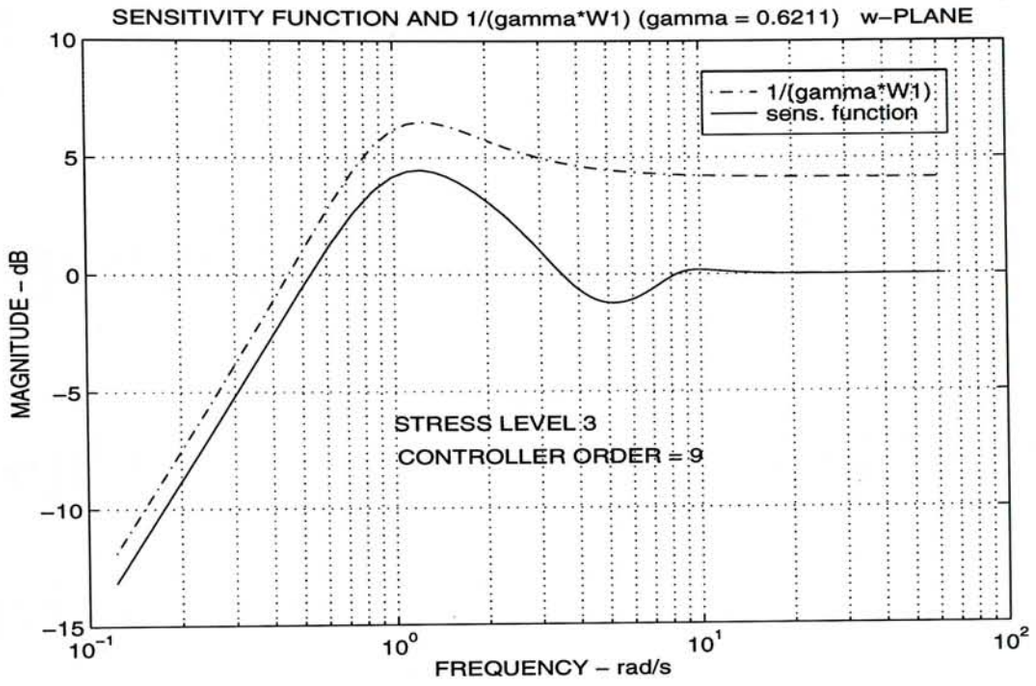

Figure A.5: The $S(s)$ and $(\gamma_o W_1)^{-1}$

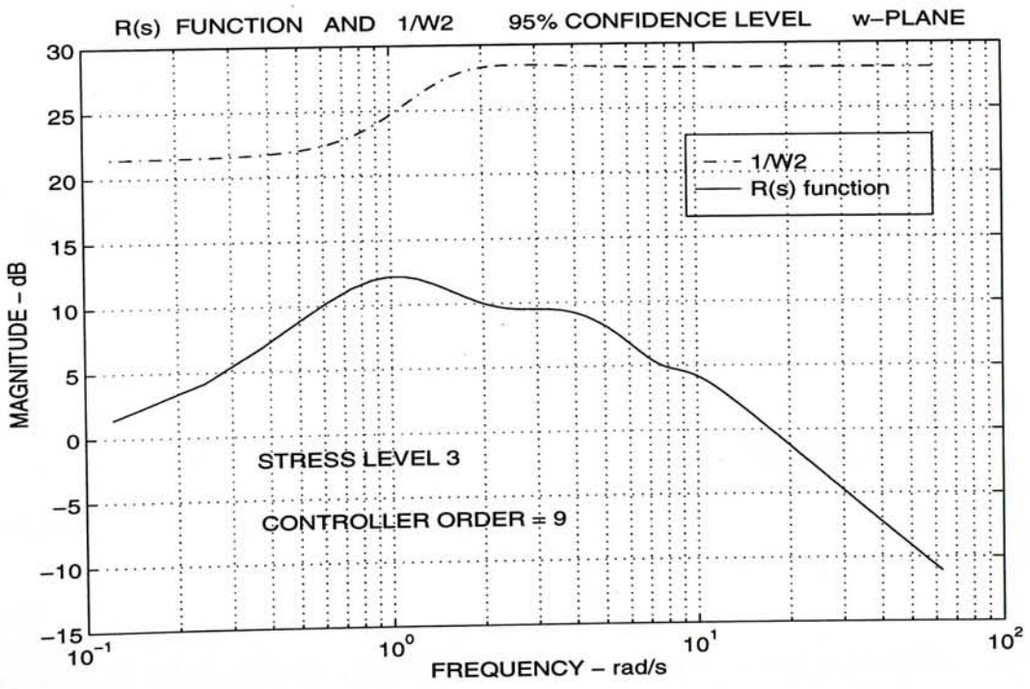

Figure A.6: The $R(s)$ and W_2^{-1}

Appendix B

Step Responses with Reduced Order Controller

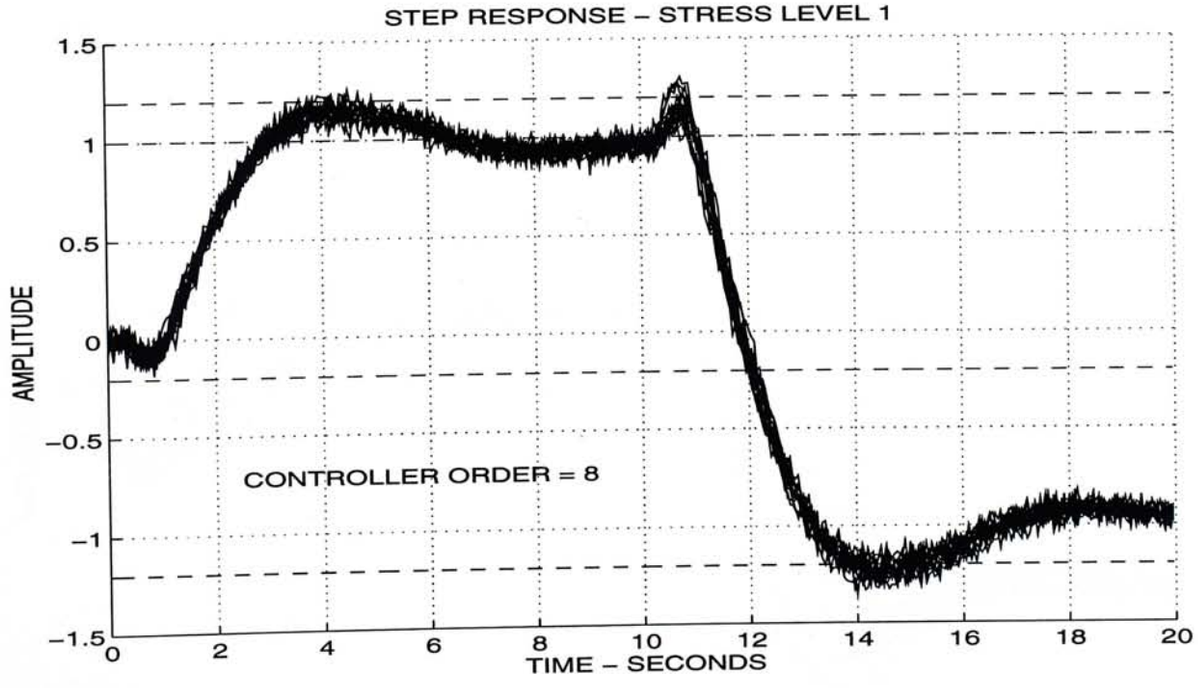

Figure B.1: Closed-loop step response of reduced order controller: Stress 1

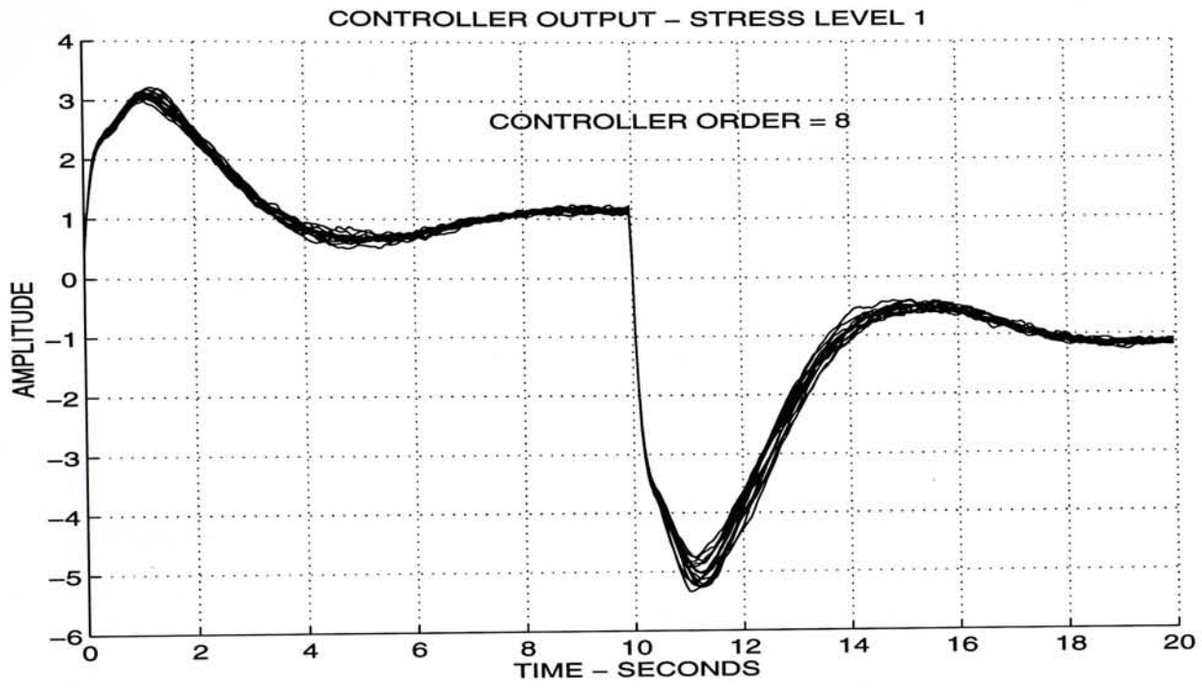

Figure B.2: Controller output of the reduced order controller: Stress 1

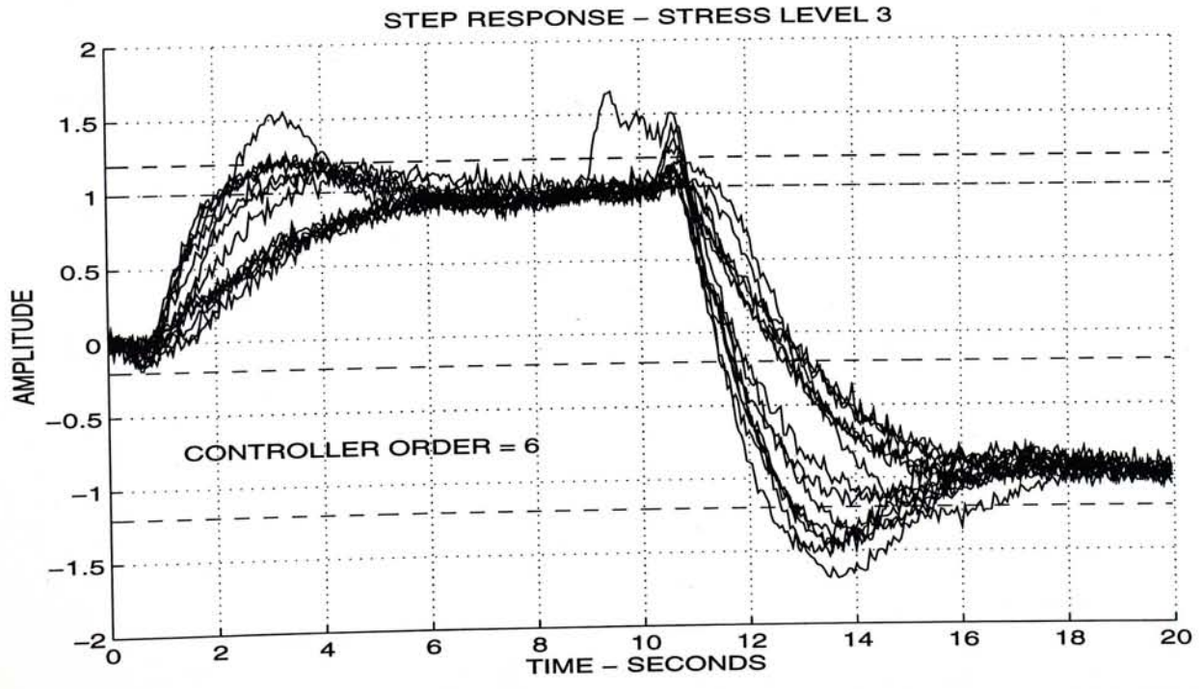

Figure B.3: Closed-loop step response of reduced order controller: Stress 3

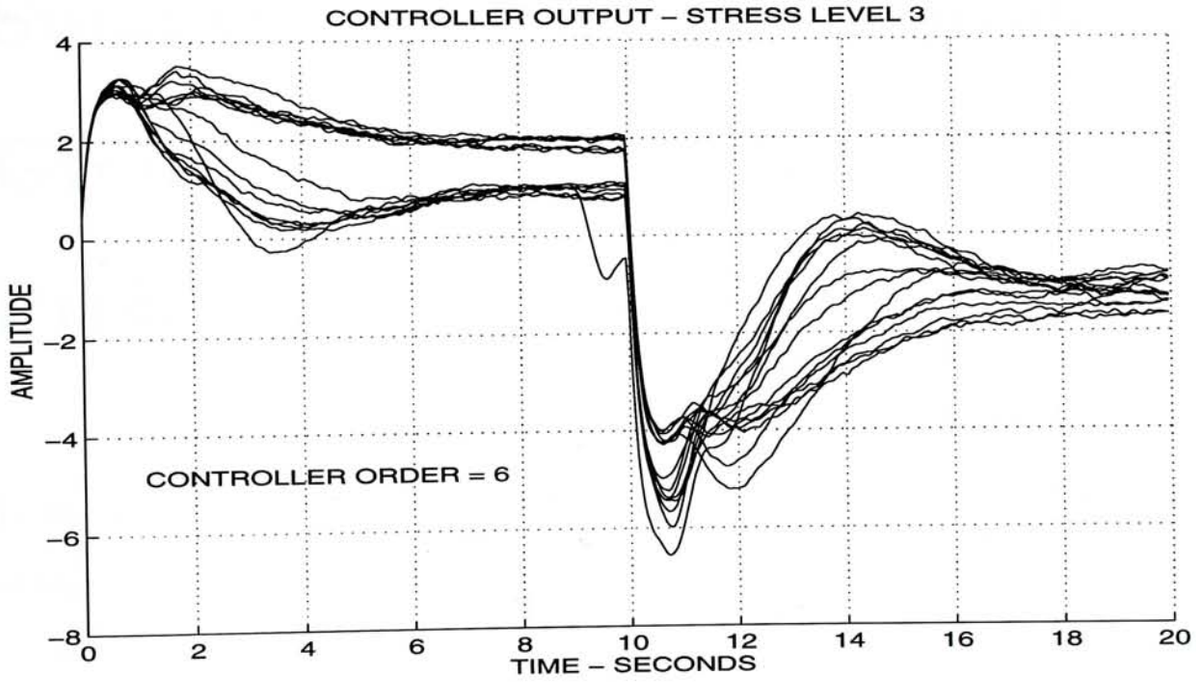

Figure B.4: Controller output of the reduced order controller: Stress 3

Appendix C

Summary of Results of Other Groups on the Benchmark Problem

In this appendix, the plottings of the closed-loop step response of other groups of researcher are scanned and printed.

For a detail summary of approaches and comparisons of results, refer to [54]. The following only act as a summary for easy visual comparison with the results in chapter 8.

C.1 Indirect and implicit adaptive predictive control [45]

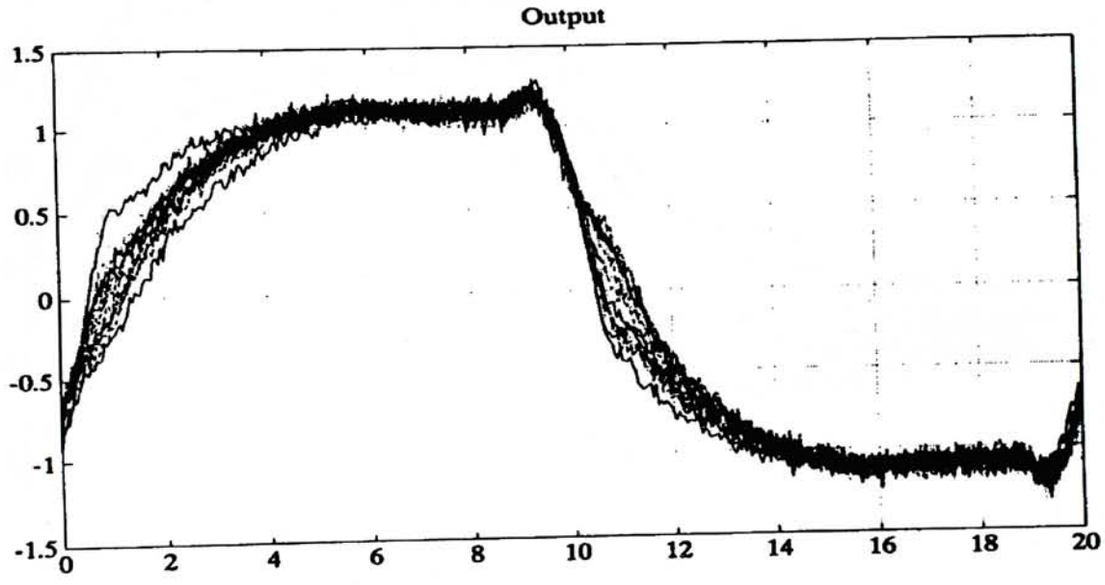

Figure C.1: Indirect adaptive predictive control: stress level 1

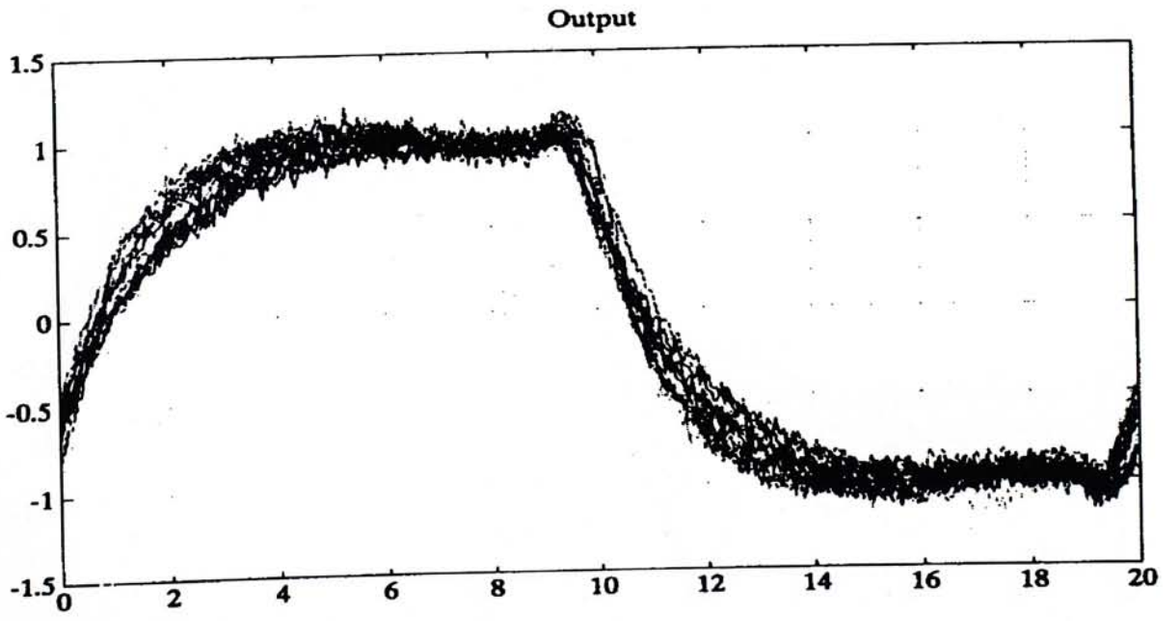

Figure C.2: Indirect adaptive predictive control: stress level 2

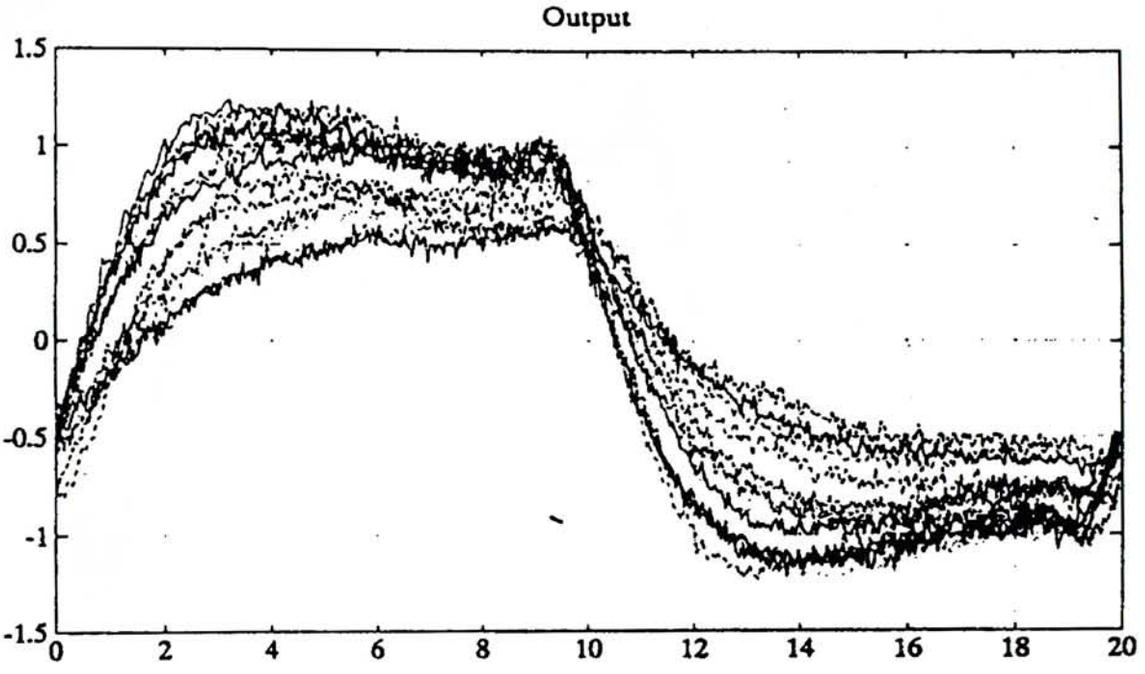

Figure C.3: Indirect adaptive predictive control: stress level 3

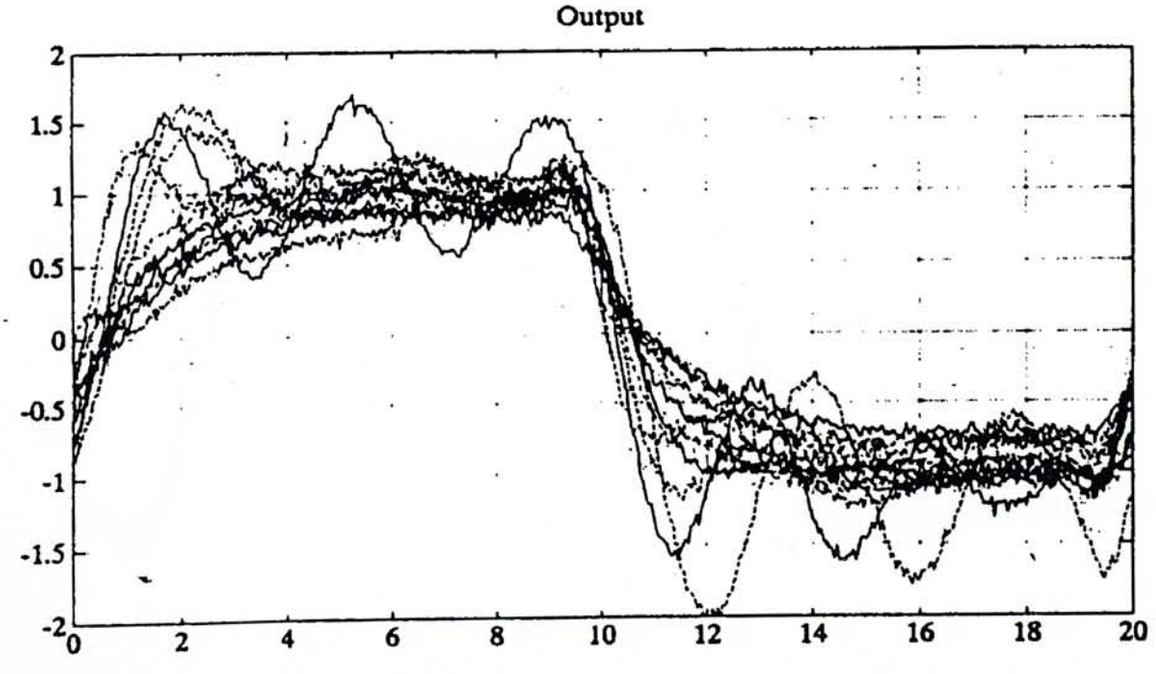

Figure C.4: Autotuned indirect adaptive predictive control: stress level 3

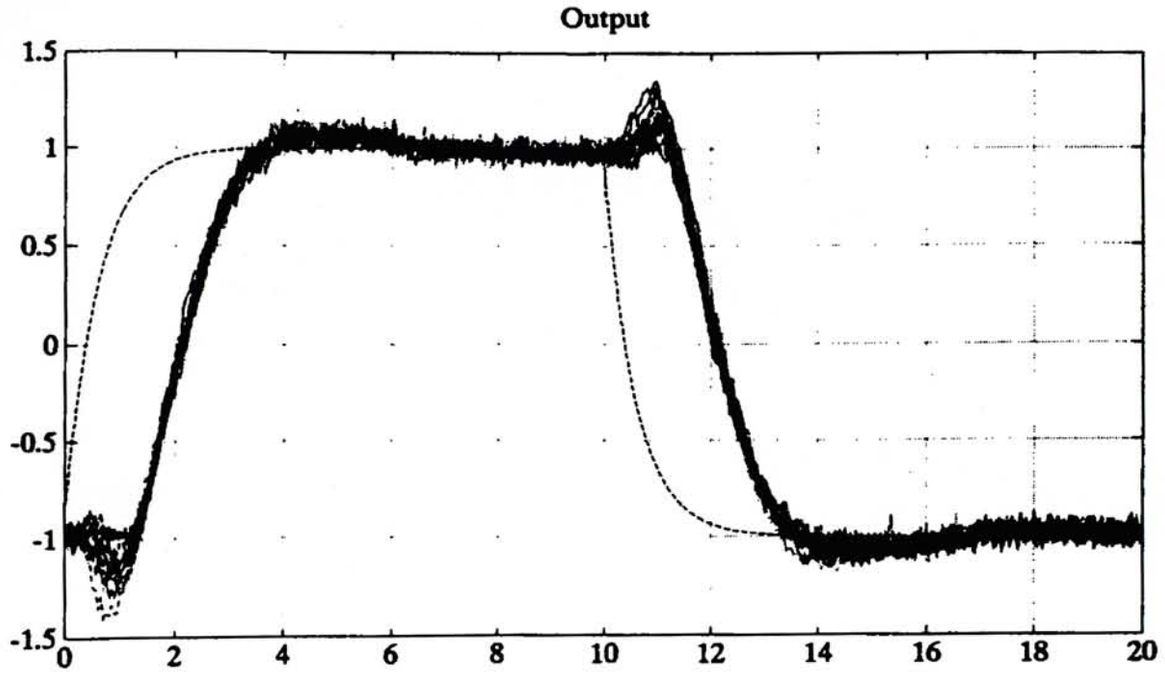

Figure C.5: Implicit adaptive predictive control: stress level 1

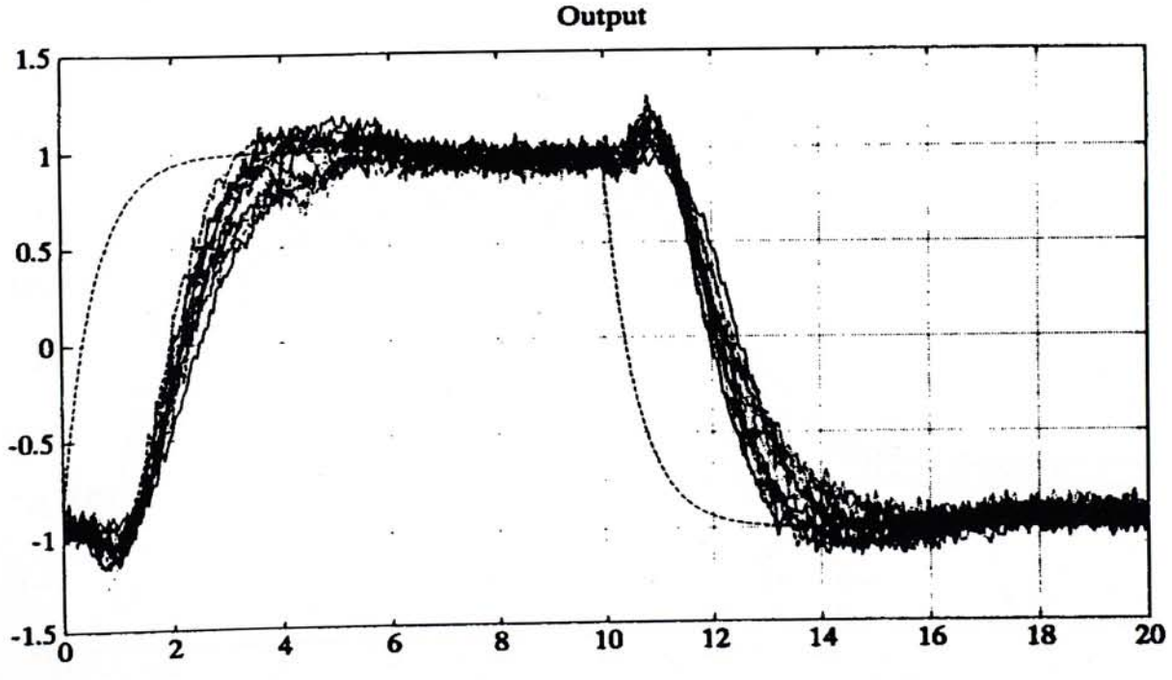

Figure C.6: Implicit adaptive predictive control: stress level 2

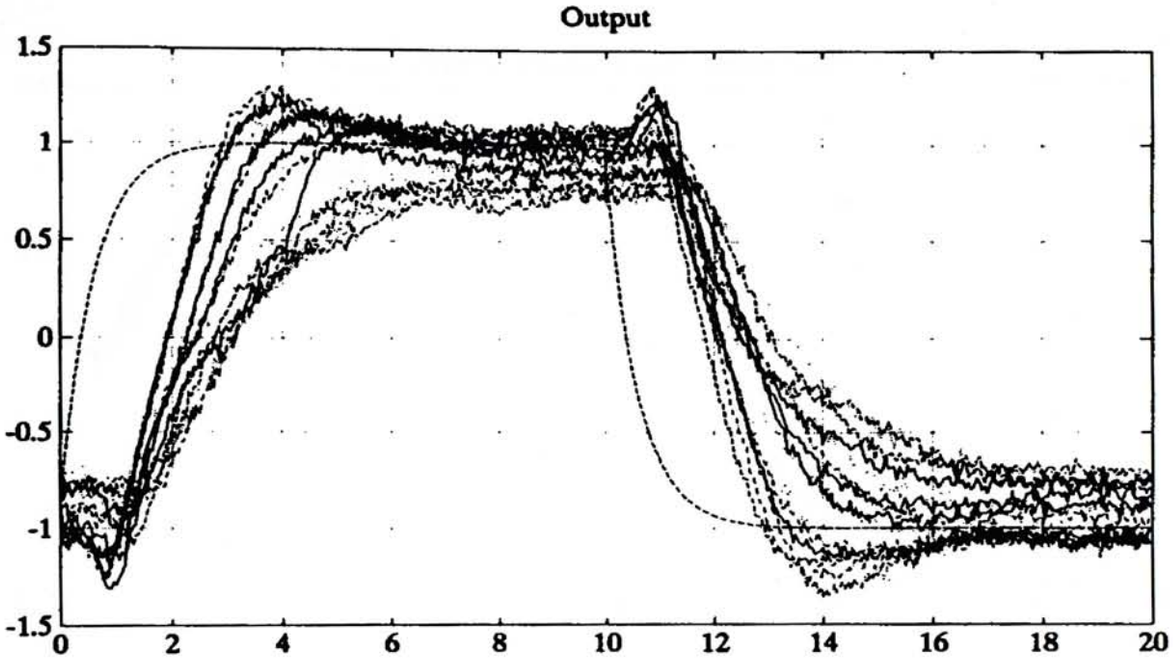

Figure C.7: Implicit adaptive predictive control: stress level 3

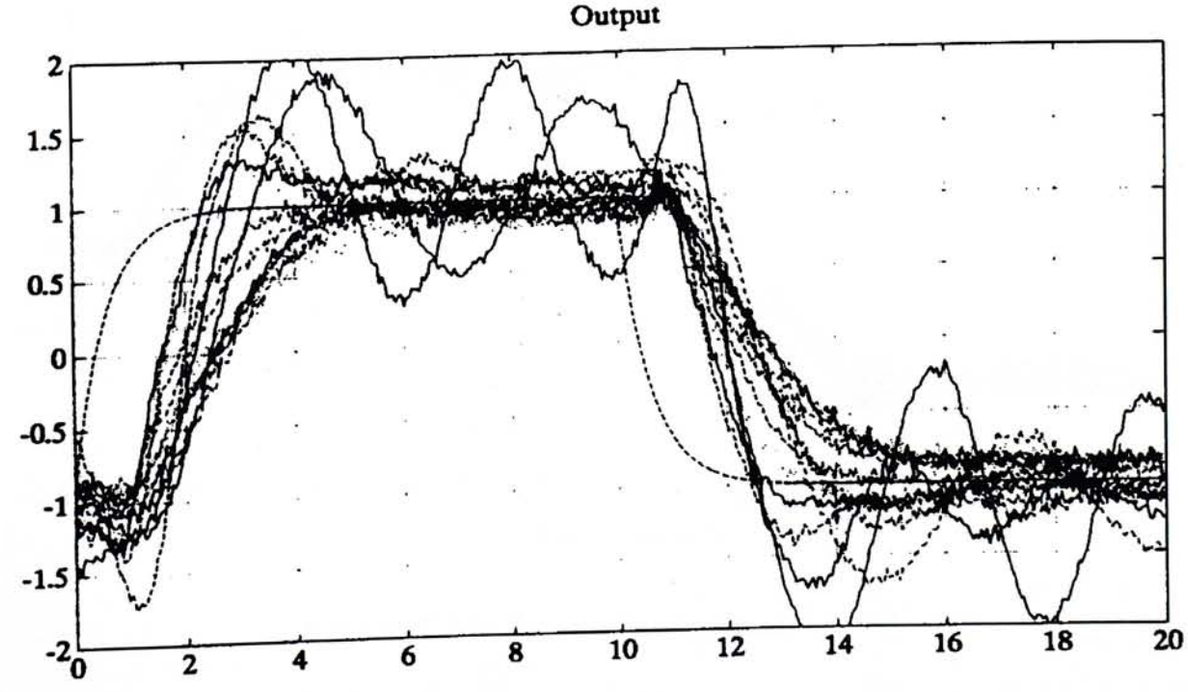

Figure C.8: Autotuned Implicit adaptive predictive control: stress level 3

C.2 H_∞ Robust Control [51]

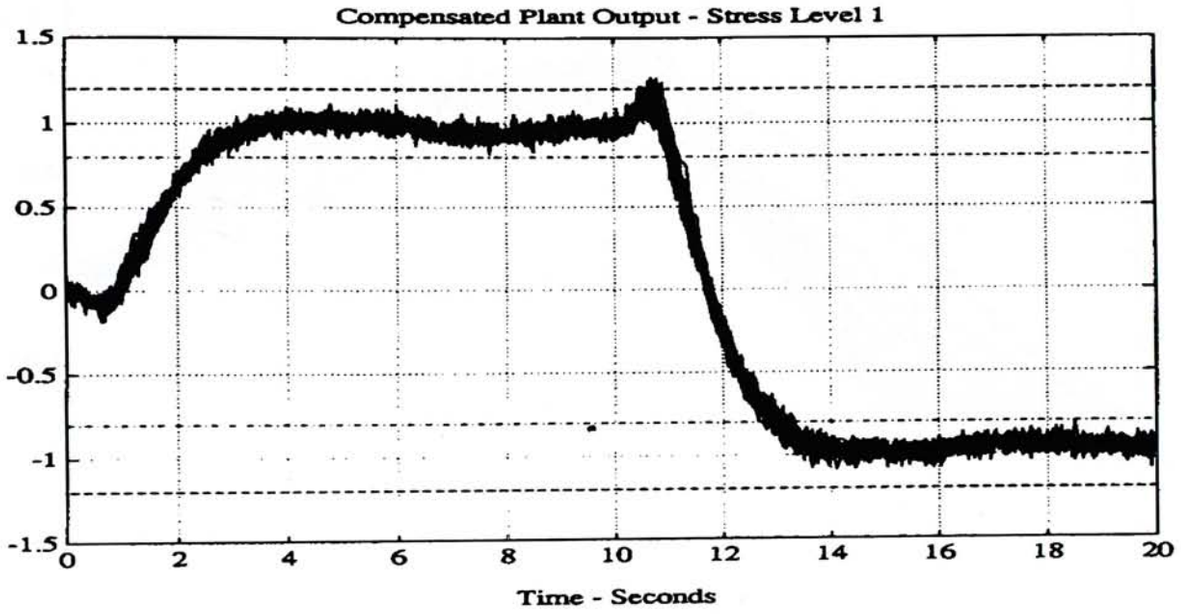

Figure C.9: H_∞ control: stress level 1

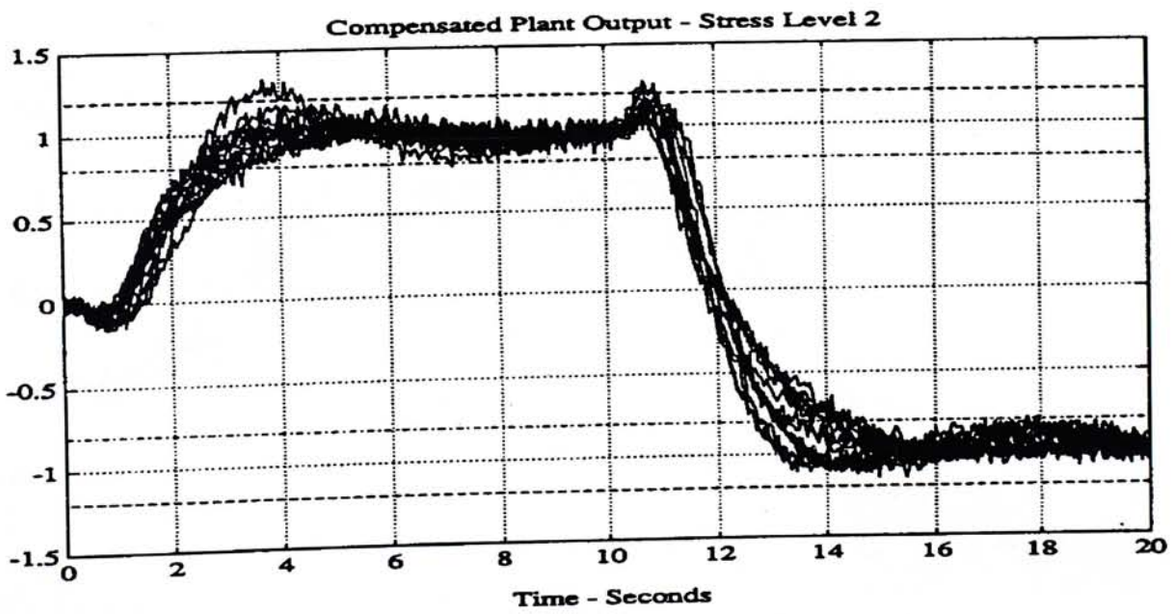

Figure C.10: H_∞ control: stress level 2

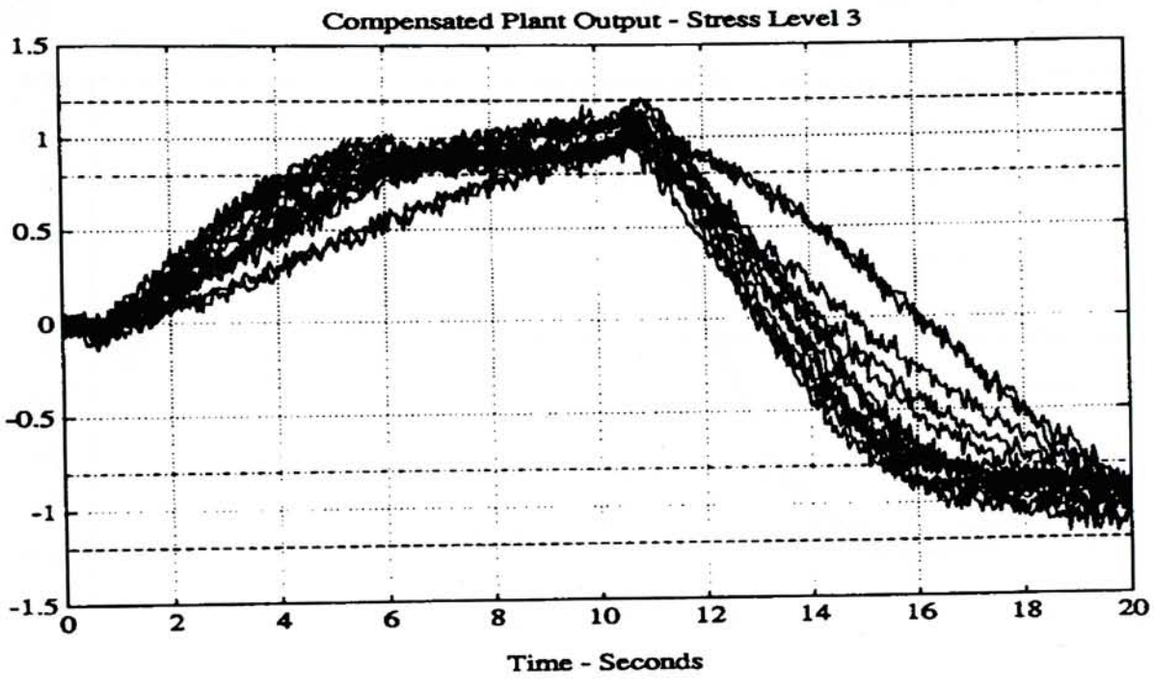

Figure C.11: H_∞ control: stress level 3

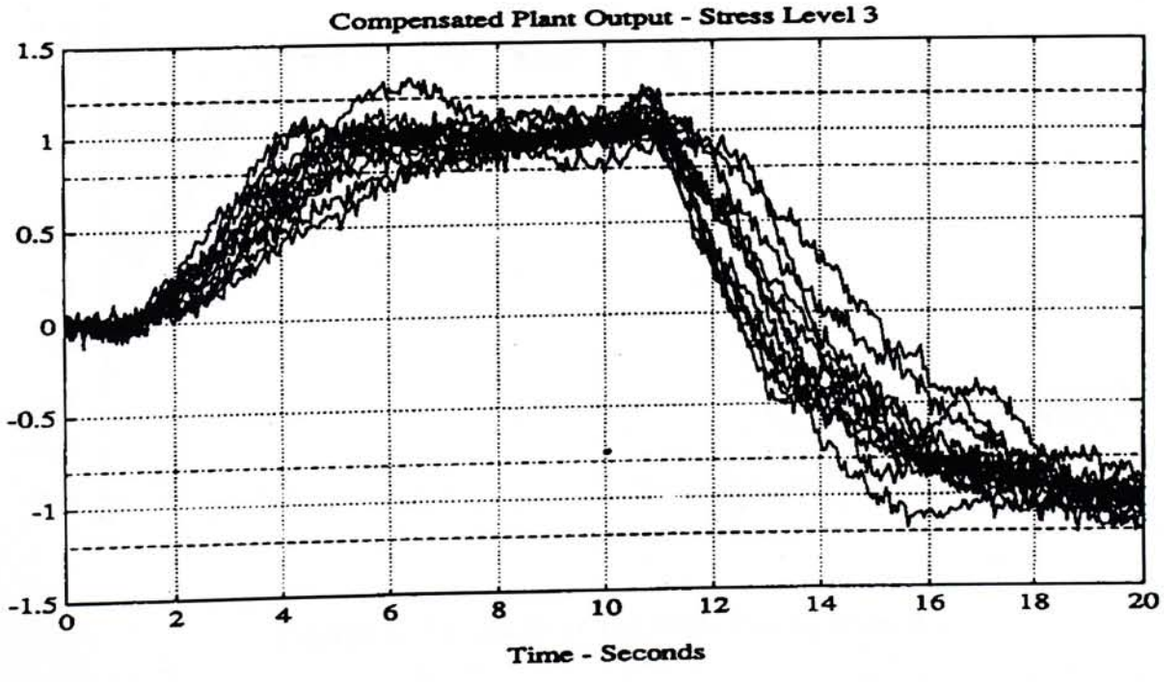

Figure C.12: H_∞ control with adaptive gain: stress level 3

C.3 Robust Stability Degree Assignment [53]

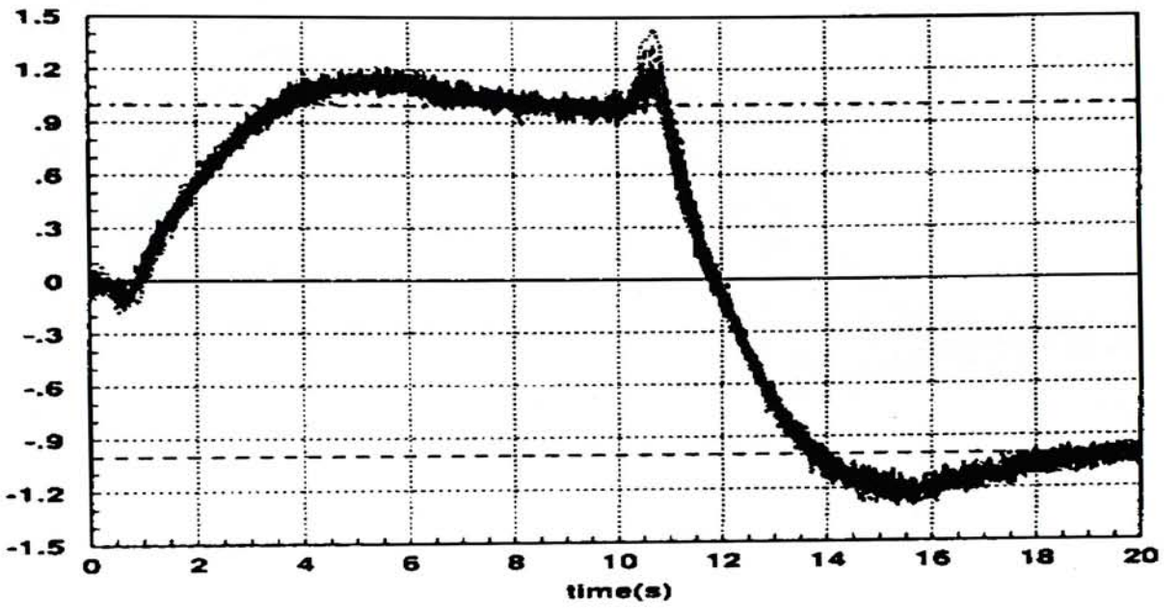

Figure C.13: Robust control: stress level 1

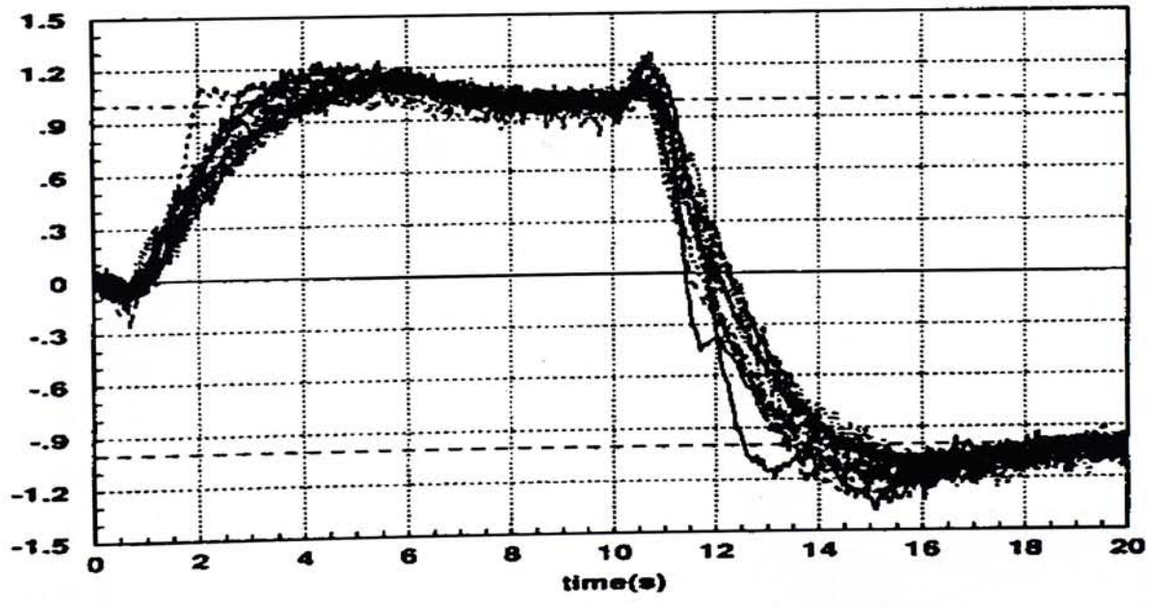

Figure C.14: Robust control: stress level 2

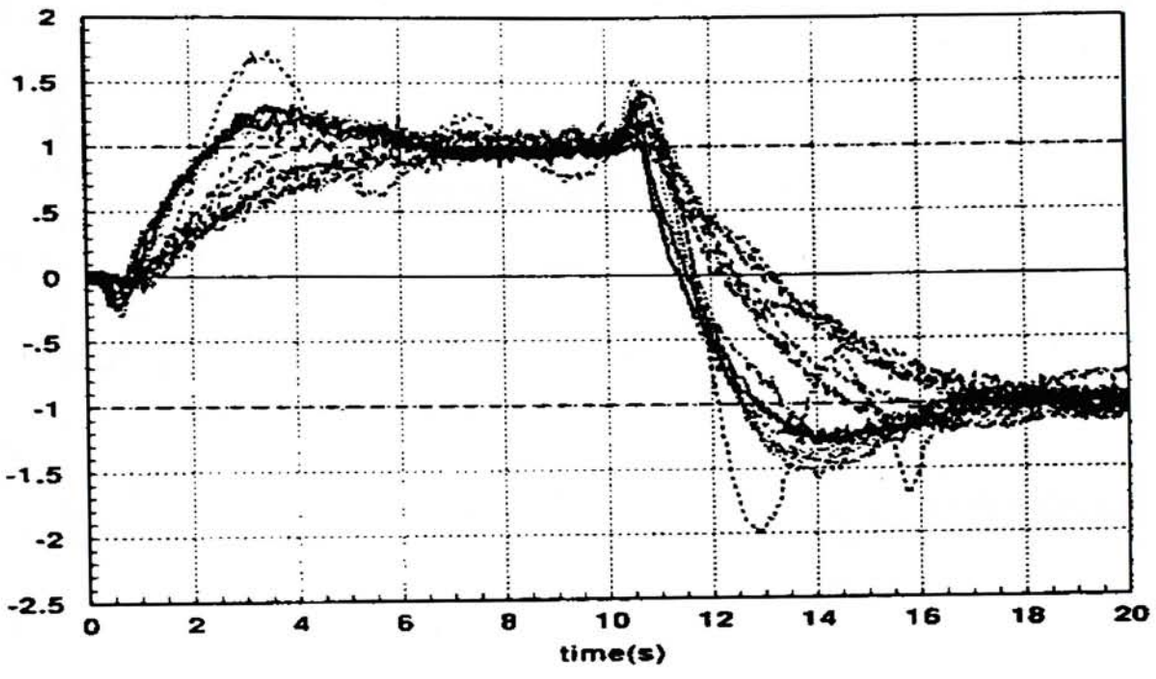

Figure C.15: Robust control: stress level 3

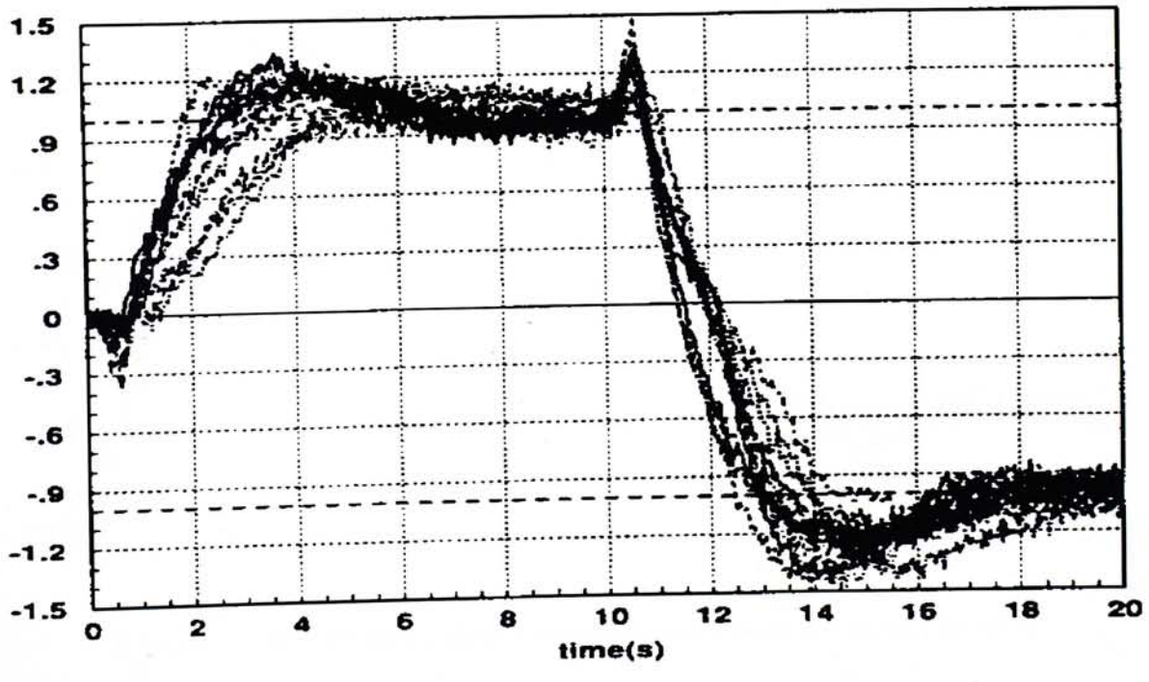

Figure C.16: Adaptive robust control: stress level 3

C.4 Model Reference Adaptive Control [46]

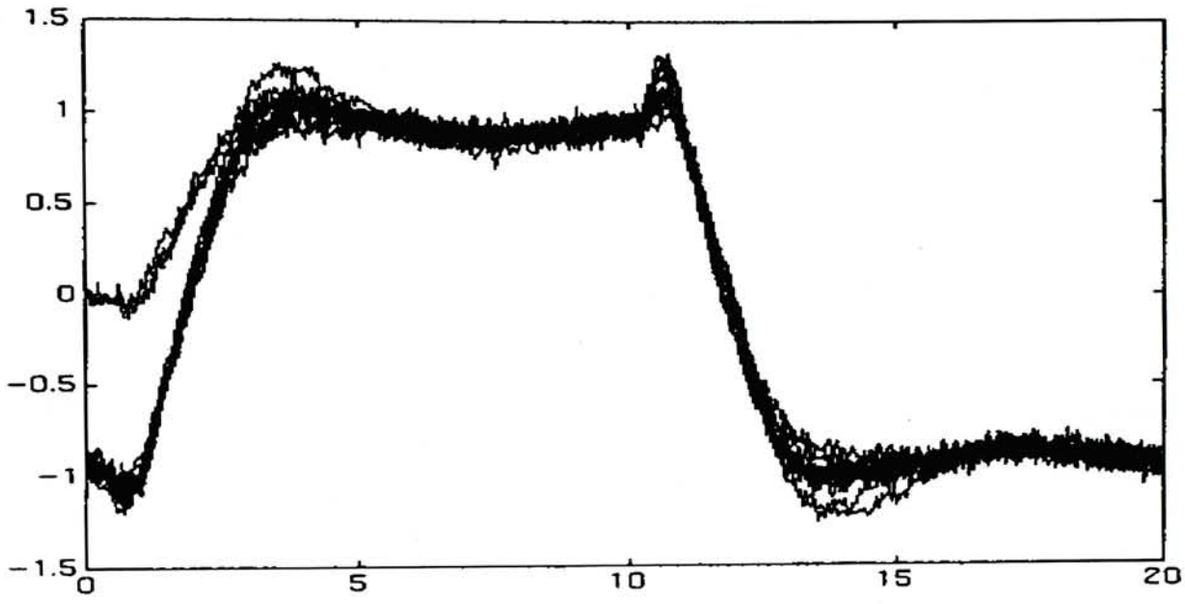

Figure C.17: Model reference adaptive control: stress level 1

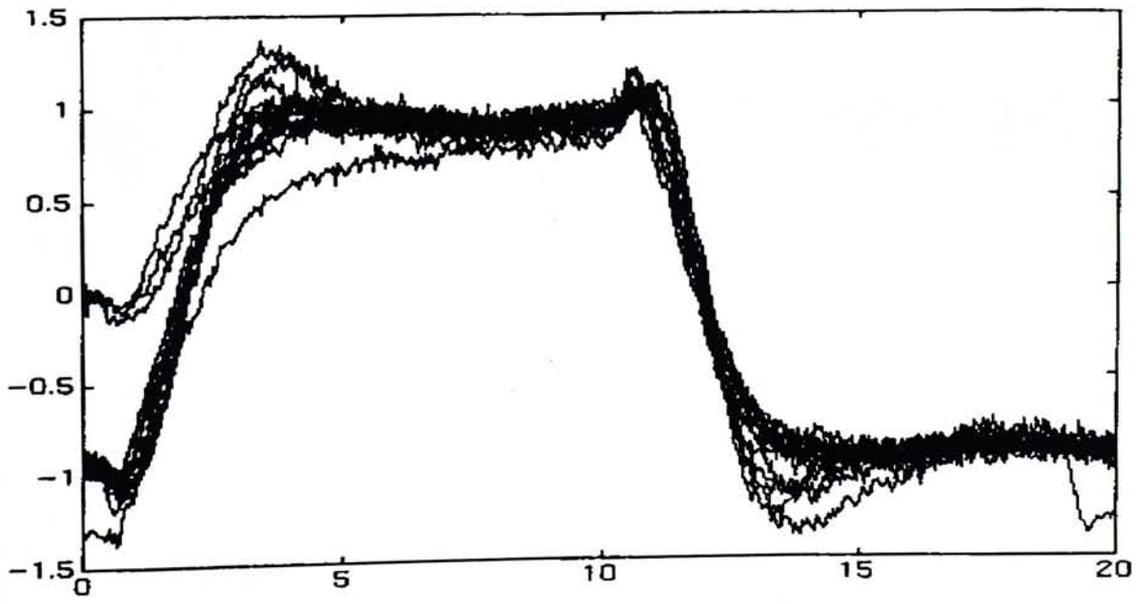

Figure C.18: Model reference adaptive control: stress level 2

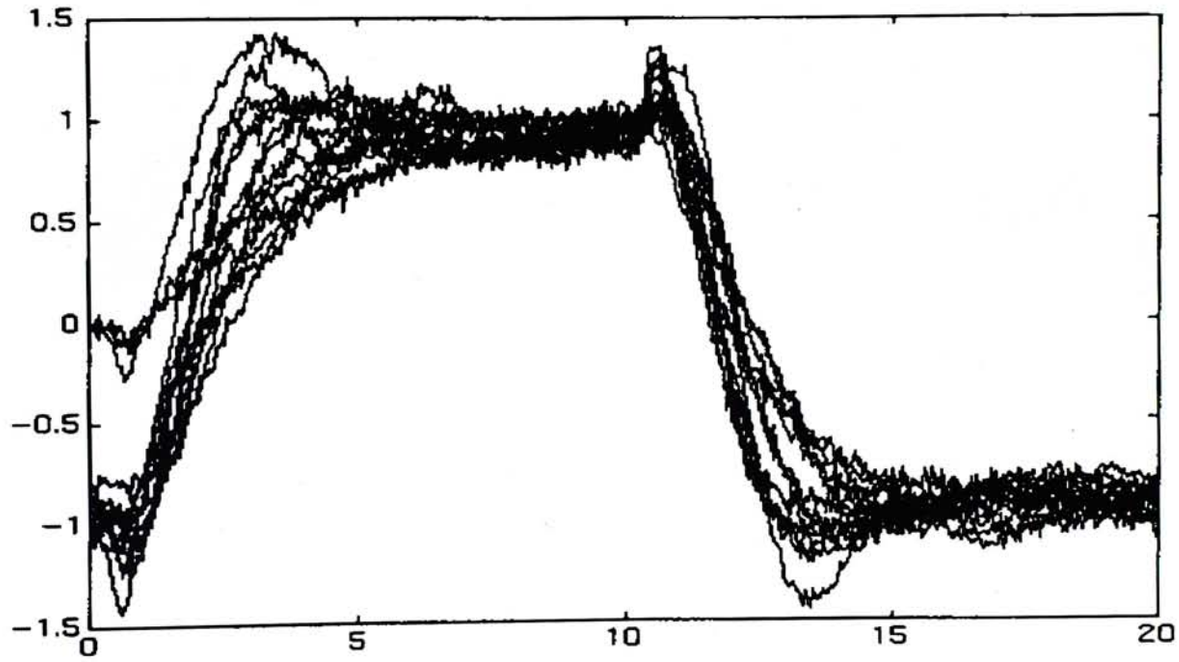

Figure C.19: Model reference adaptive control: stress level 3

C.5 Robust Pole Placement using ACSYDE (Automatic Control System Design) [47]

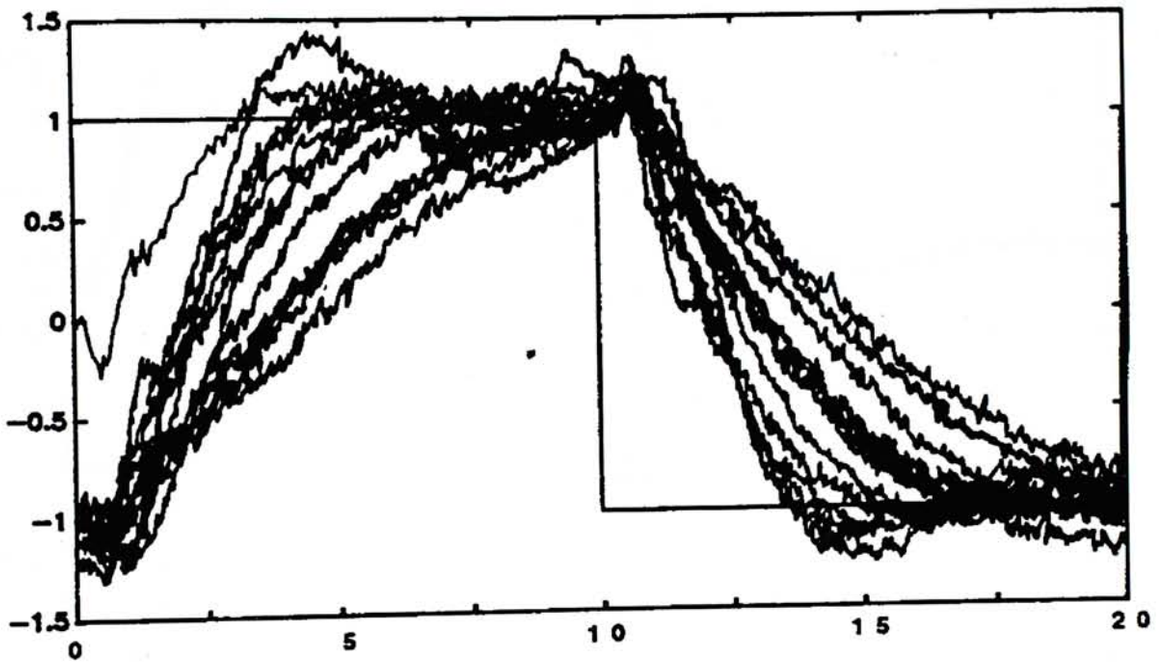

Figure C.20: Robust pole placement using ACSYDE: stress level 3

C.6 Adaptive PI Control [48]

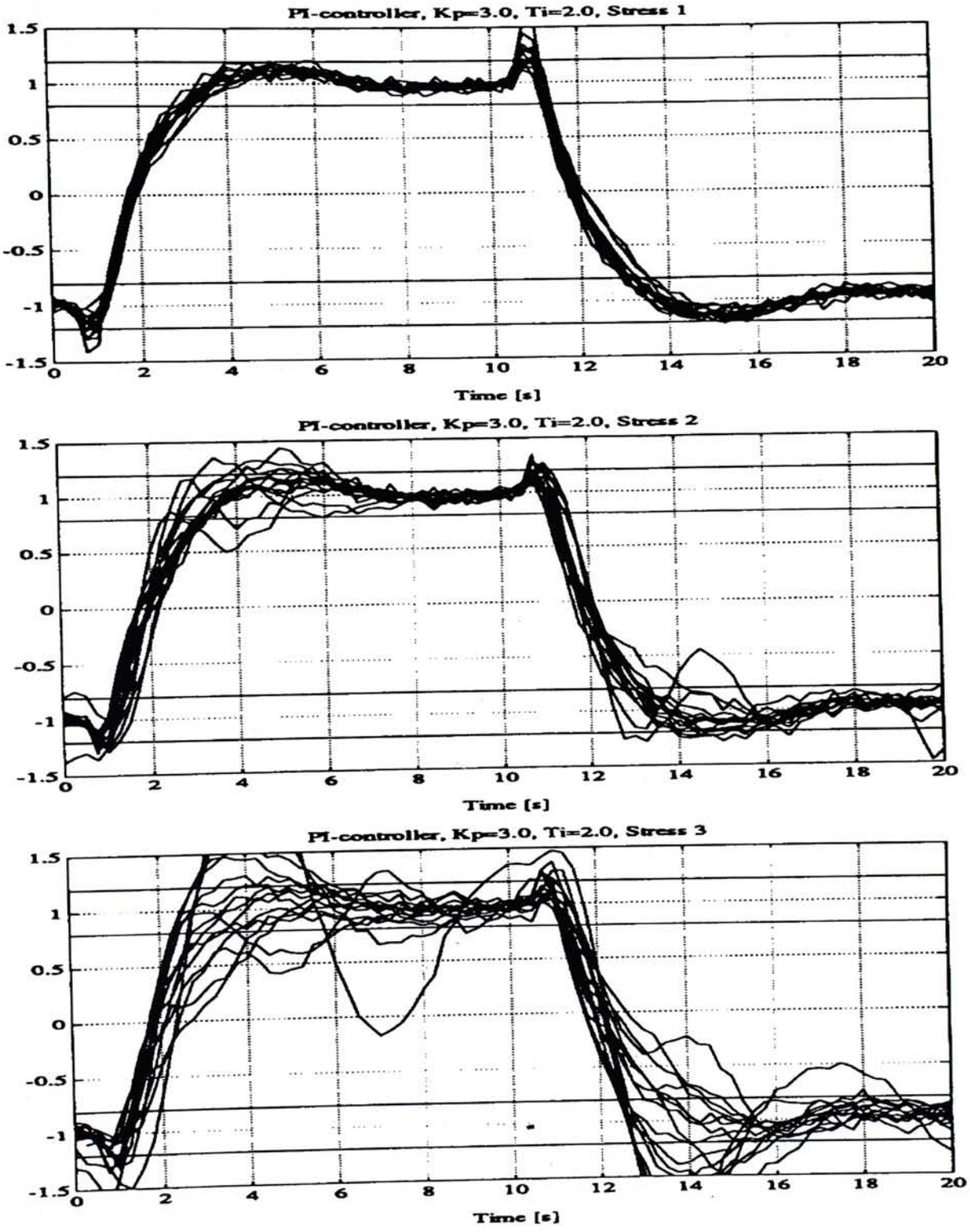

Figure C.21: Fixed proportional + integral (PI) control

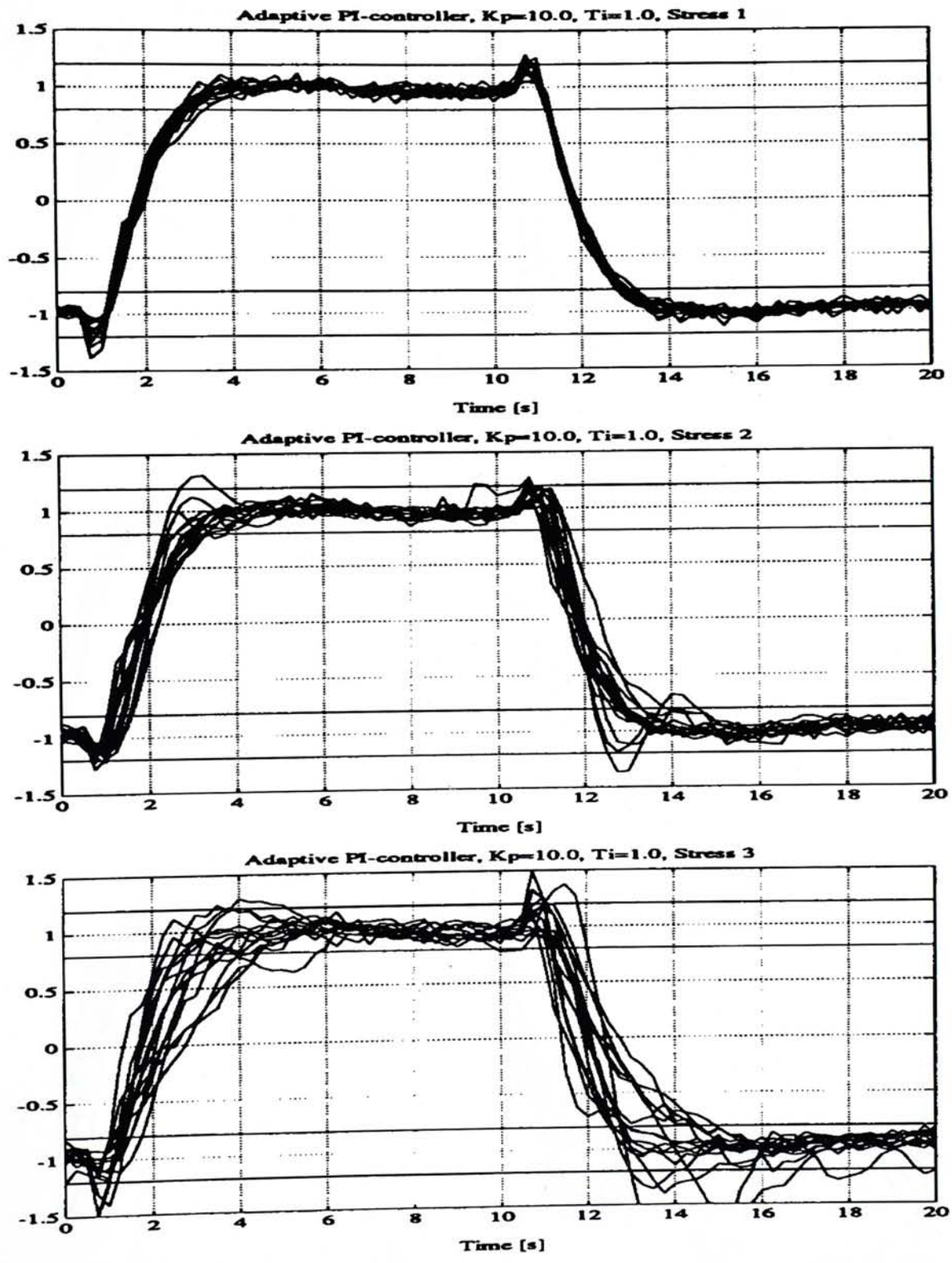

Figure C.22: Adaptive PI control

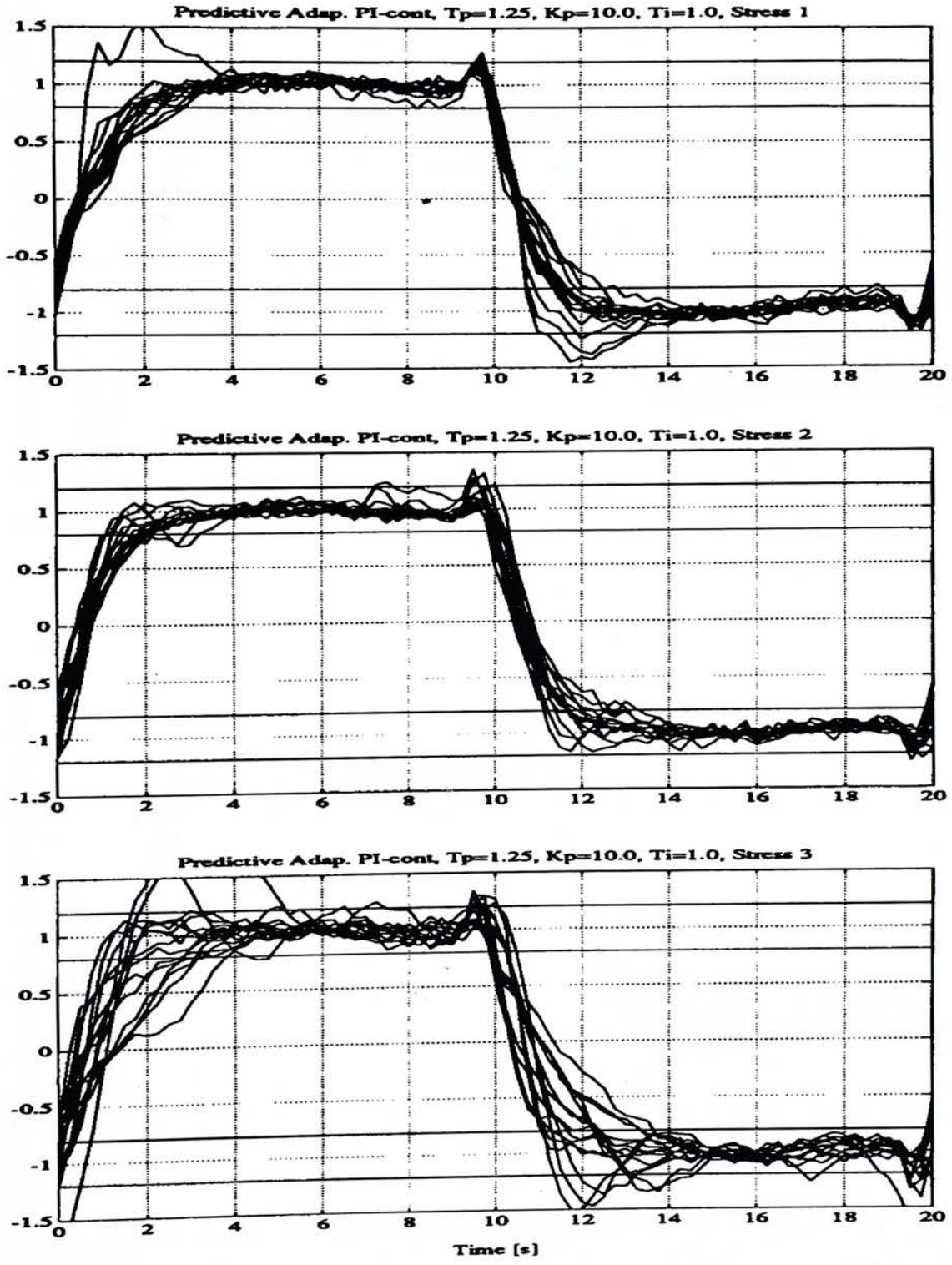

Figure C.23: Adaptive PI control with predictive setpoint

C.7 Adaptive Control with supervision [49]

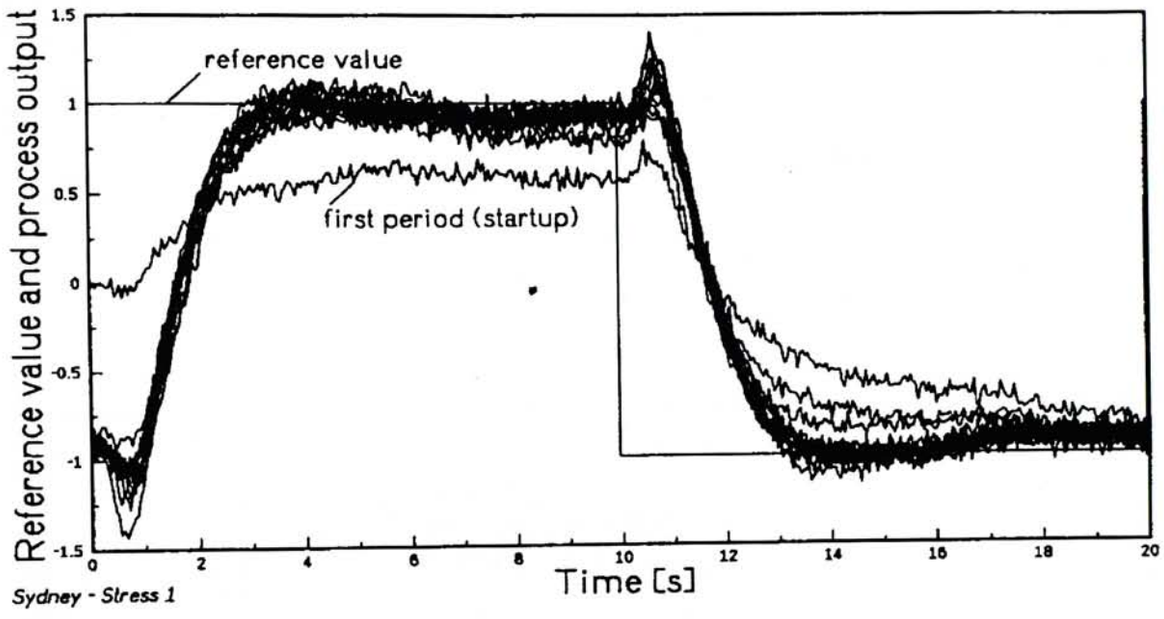

Figure C.24: Adaptive control with supervision: stress level 1

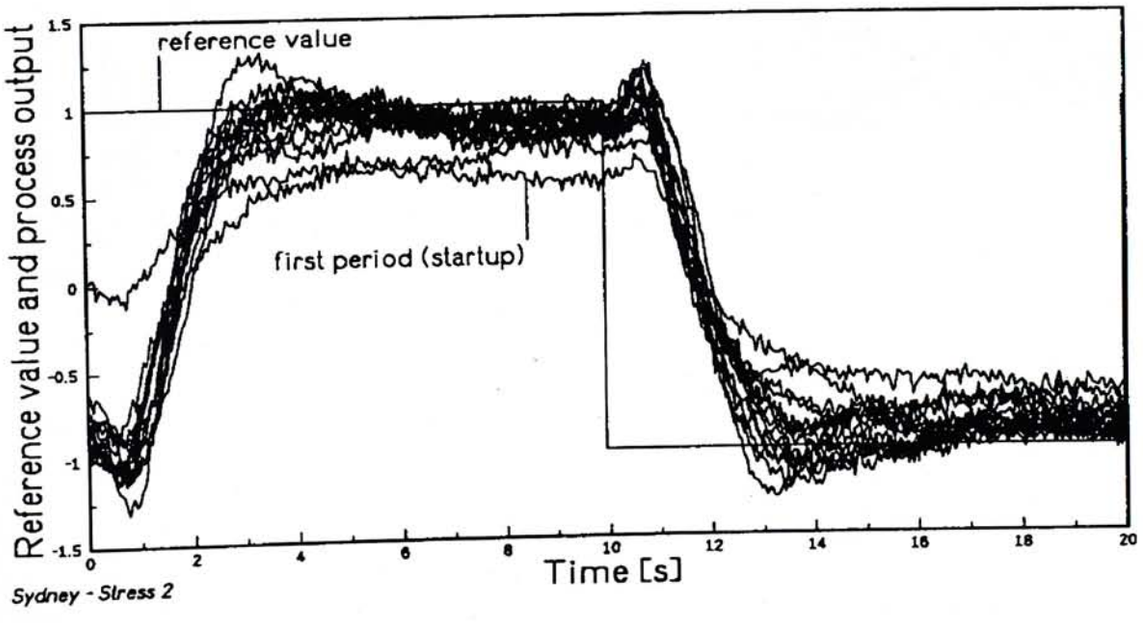

Figure C.25: Adaptive control with supervision: stress level 2

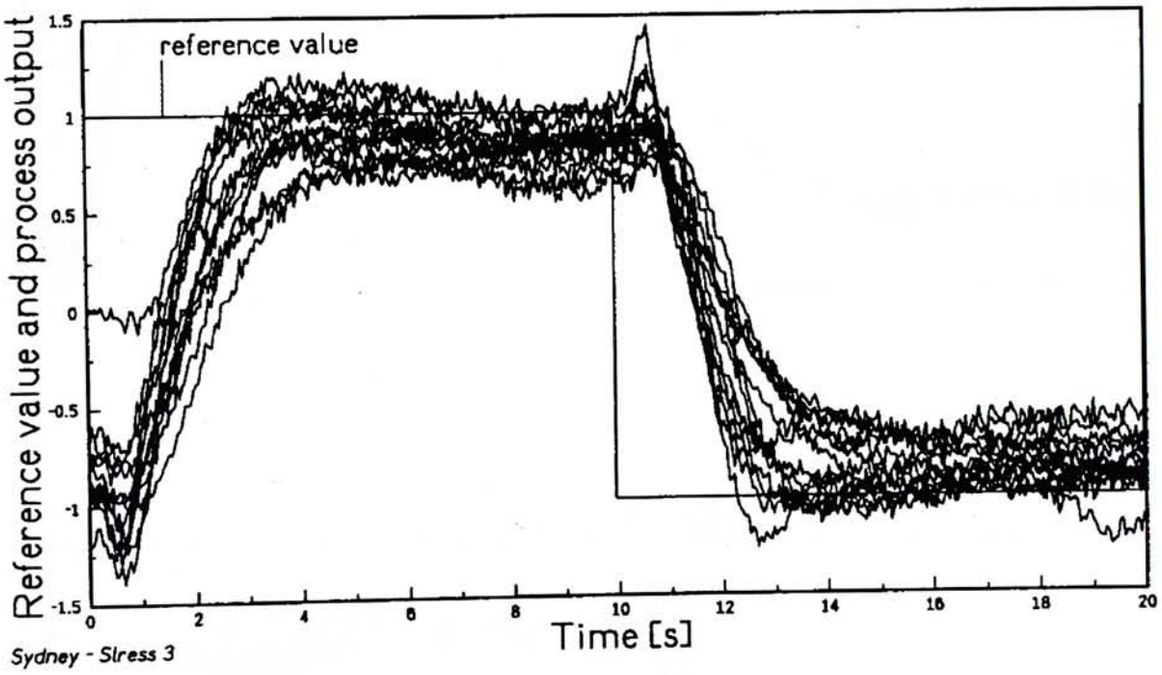

Figure C.26: Adaptive control with supervision: stress level 3

C.8 Partial State Model Reference (PSRM) Control [50]

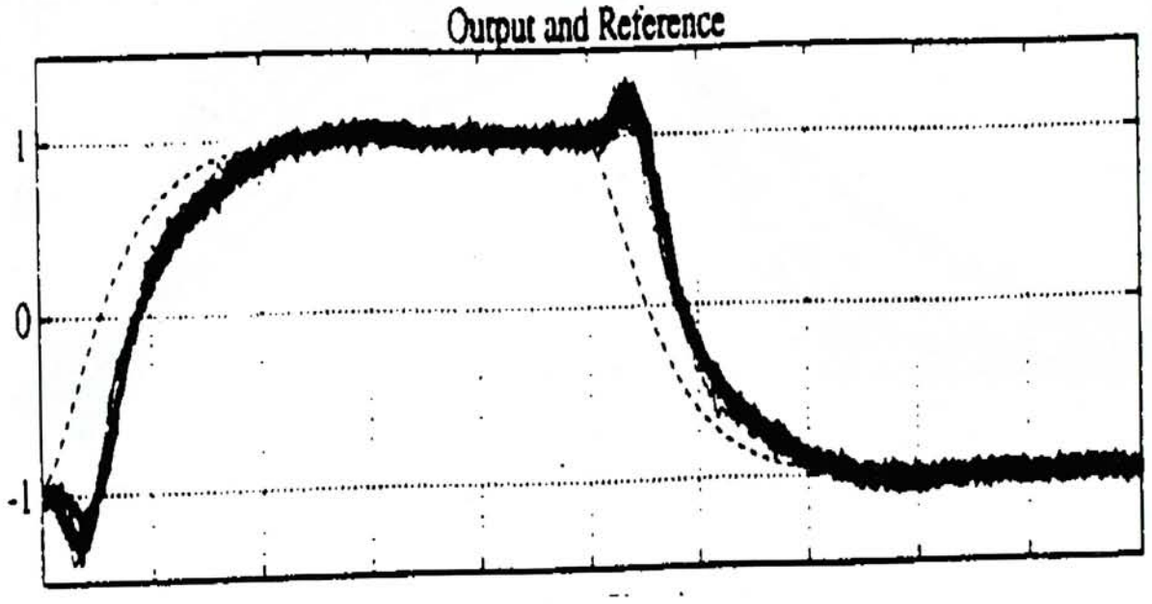

Figure C.27: Fixed robust PSRM control: stress level 1

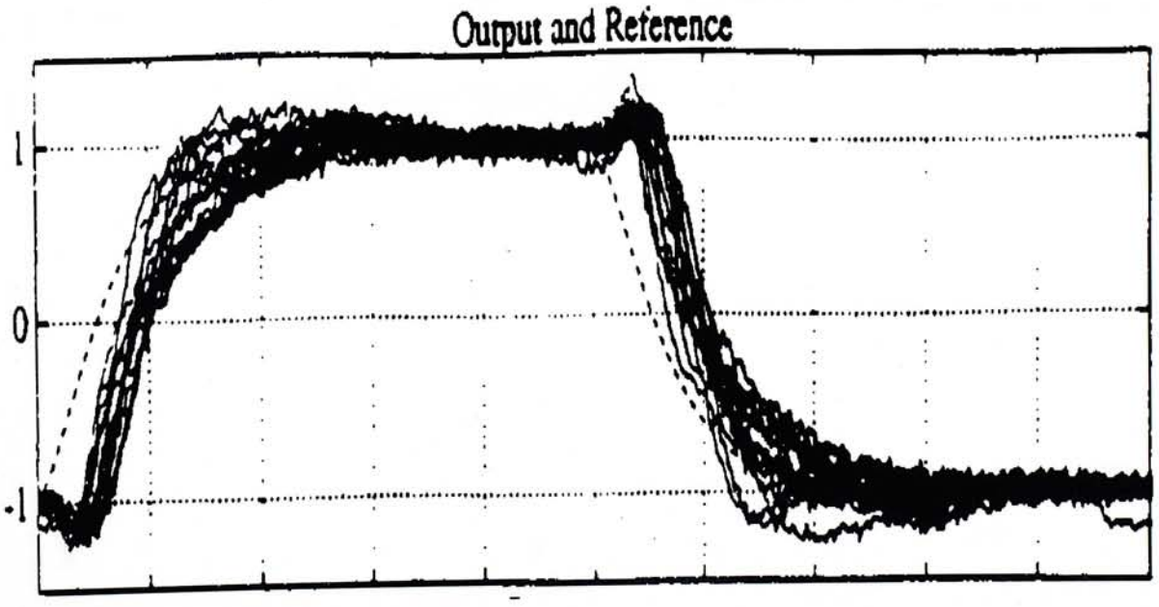

Figure C.28: Fixed robust PSRM control: stress level 2

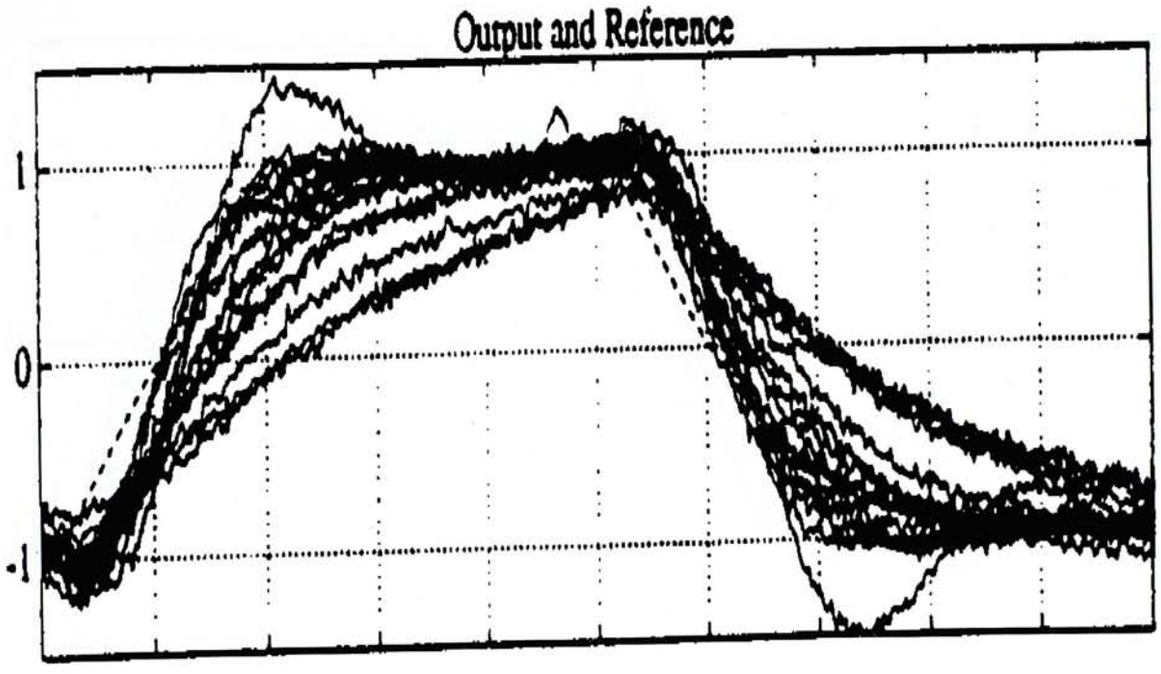

Figure C.29: Fixed robust PSRM control: stress level 3

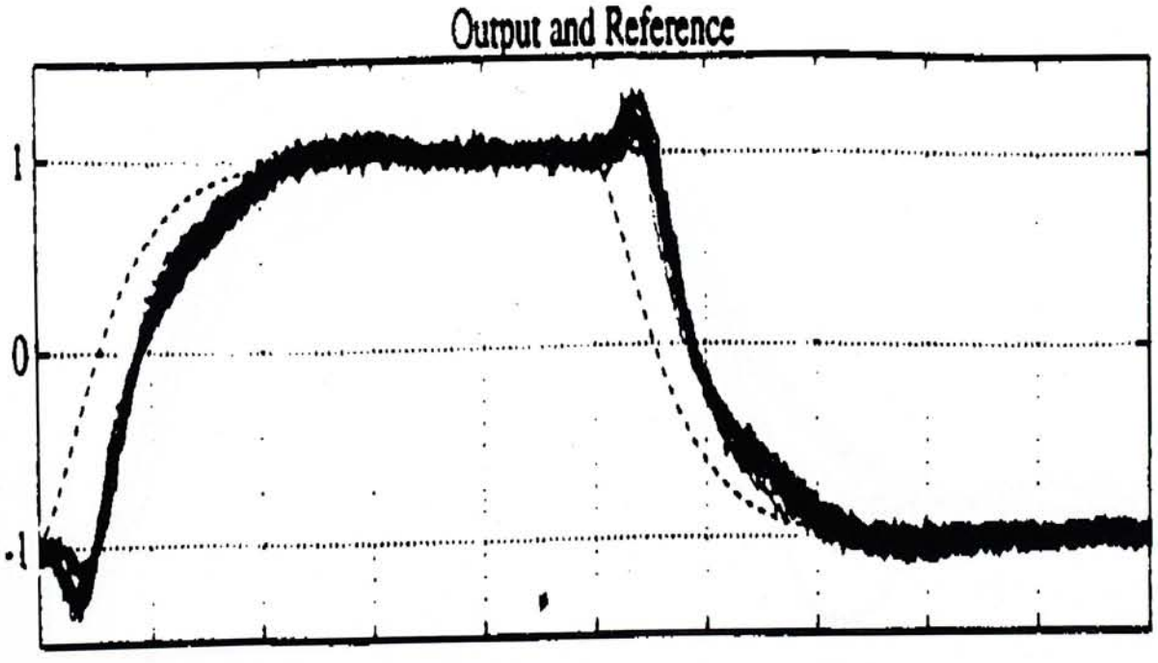

Figure C.30: Adaptive PSRM control: stress level 1

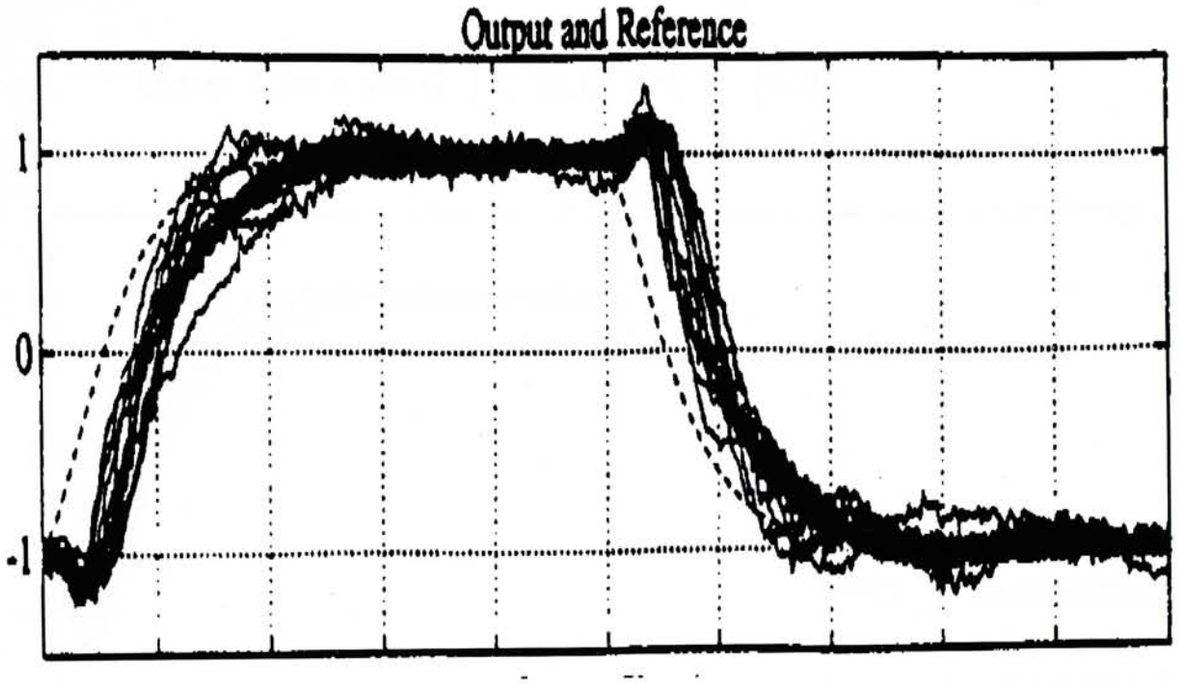

Figure C.31: Adaptive PSRM control: stress level 2

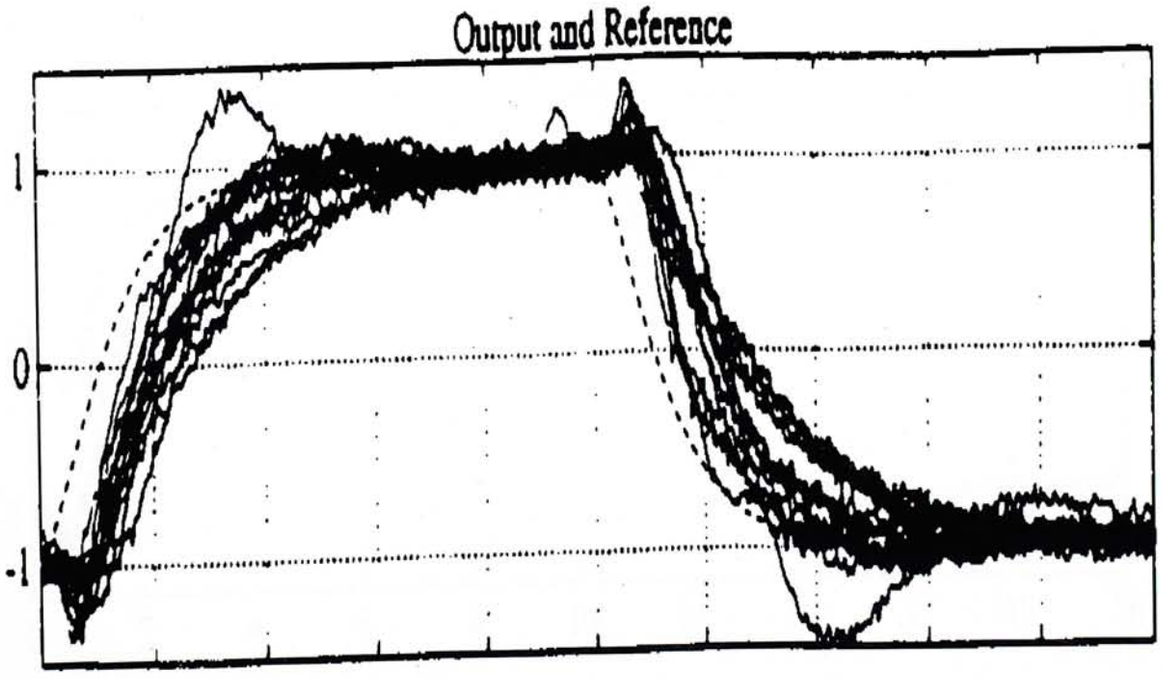

Figure C.32: Adaptive PSRM control: stress level 3

C.9 Contstrainted Receding Horizon Predictive Control (CRHPC) [52]

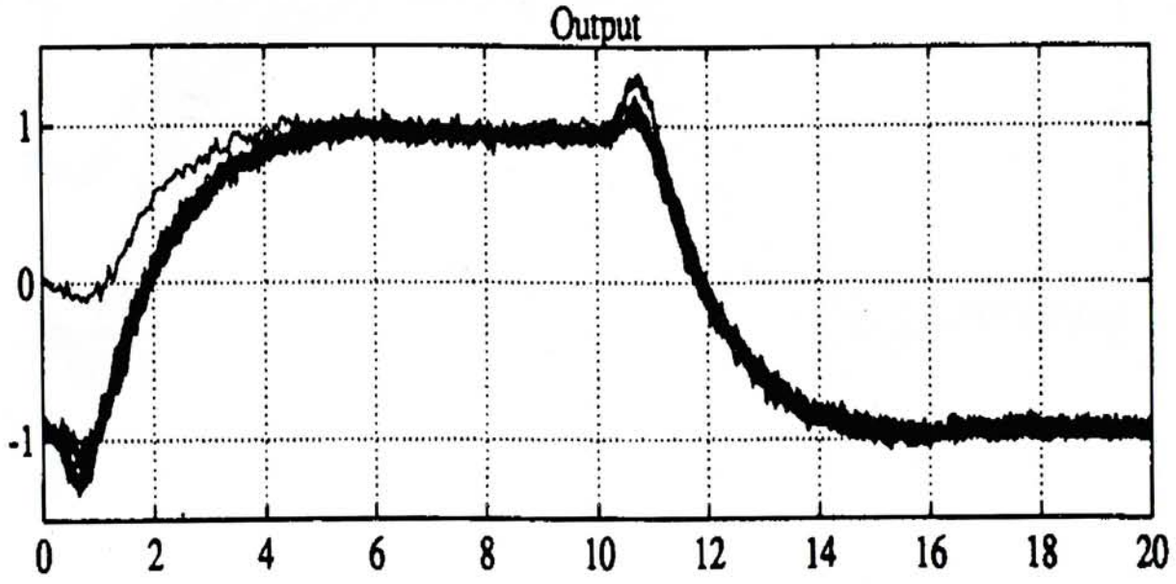

Figure C.33: Fixed two term control: stress level 1

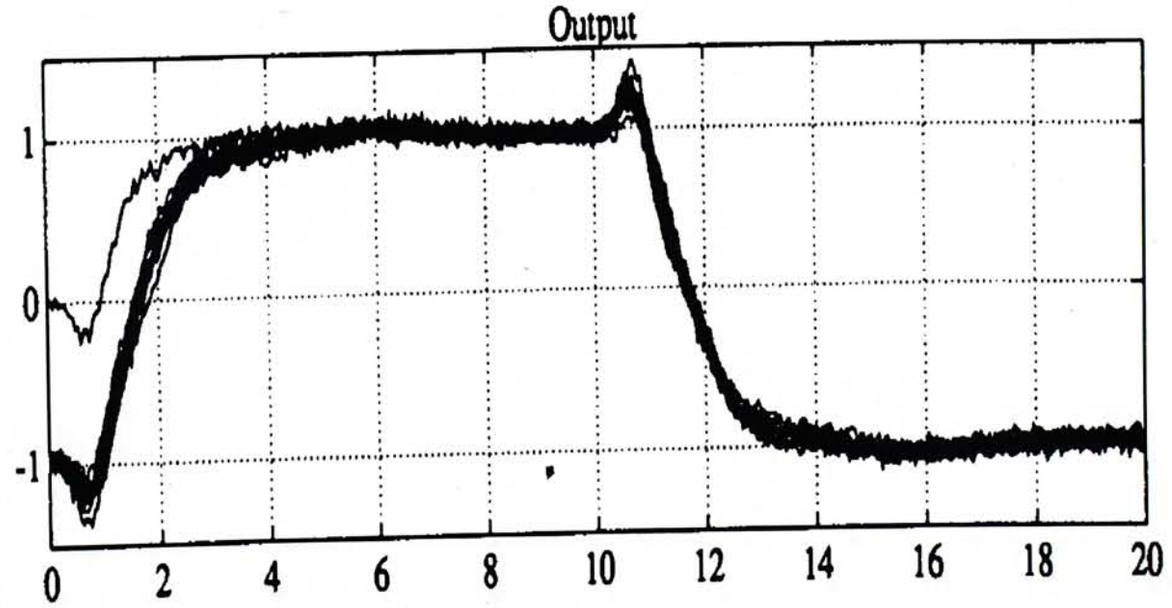

Figure C.34: Fixed CRHPC control: stress level 1

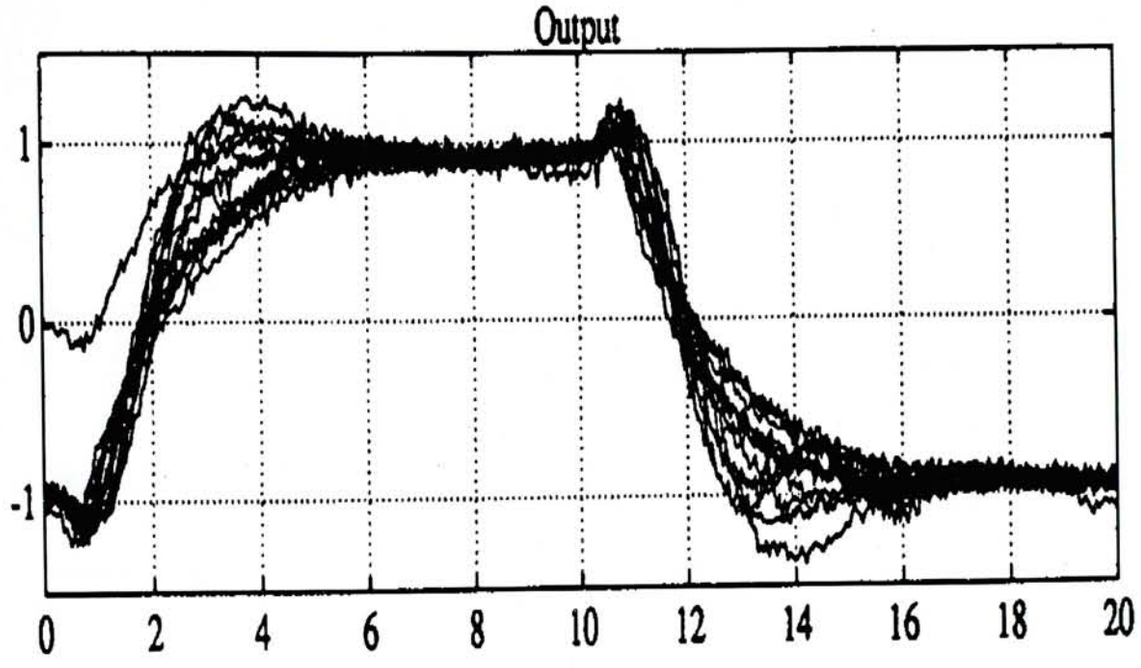

Figure C.35: Fixed two term control: stress level 2

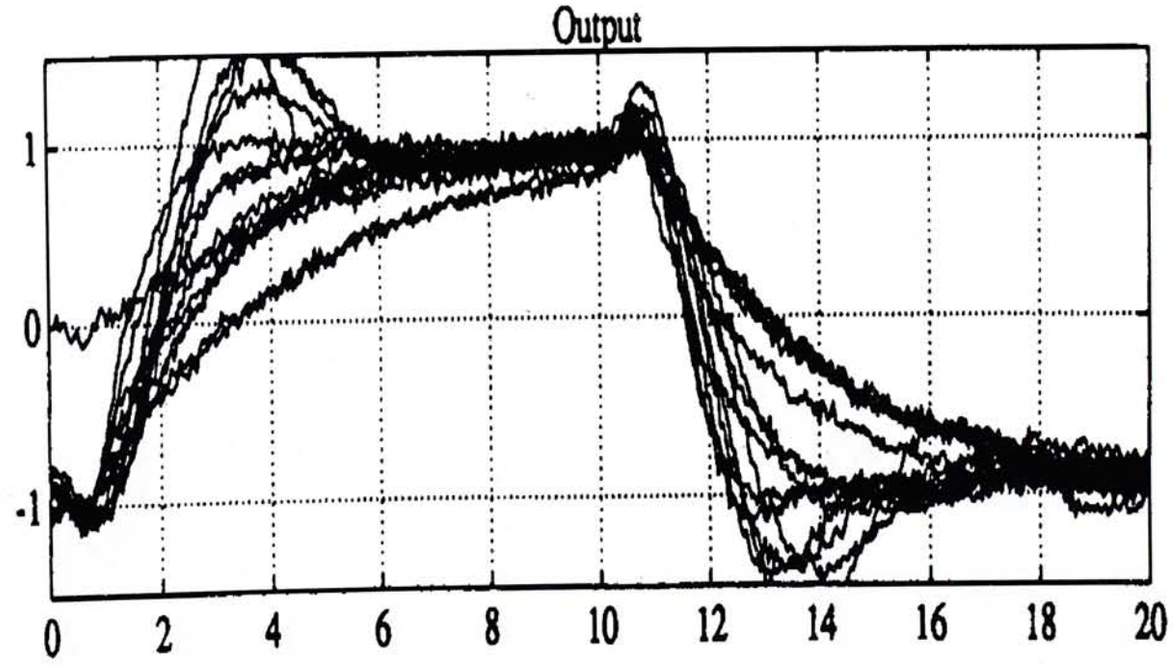

Figure C.36: Fixed two term control: stress level 3

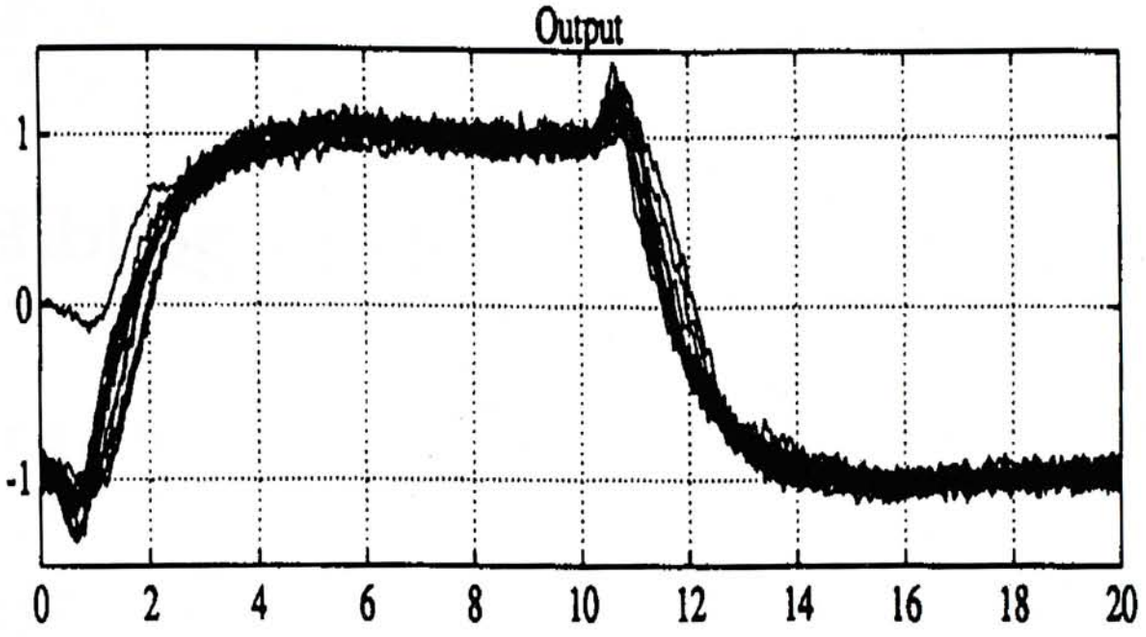

Figure C.37: Adaptive CRHPC control: stress level 2

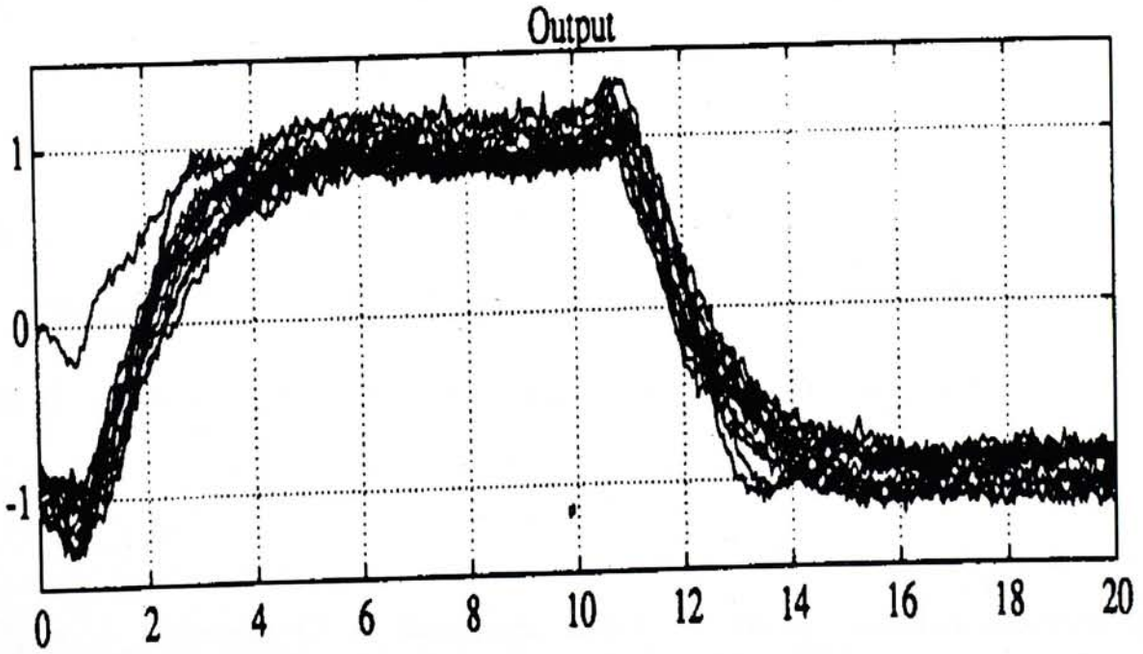

Figure C.38: Adaptive CRHPC control: stress level 3

Bibliography

[1] S. L. DeVilbiss, *System Identification for H_∞ Robust Control Design*, PhD thesis, Ohio State University, 1995.

[2] H. S. Black, "Inventing the negative feedback amplifier", *IEEE Spectrum*, pp. 55–60, Dec. 1977.

[3] K. J. Astrom and B. Wittenmark, *Adaptive Control*, Addison-Wesley, 1989.

[4] R. L. Kosut, M. K. Lau, and S. P. Boyd, "Set-membership identification of systems with parametric and nonparametric uncertainty", *IEEE Transactions on Automatic Control*, vol. 37, no. 7, pp. 929–941, 1992.

[5] K. J. Astrom, "Toward intelligent control", *IEEE Control Systems Magazine*, Apr. 1989, Keynote Speech to the 1988 American Control Conference.

[6] R. L. Kosut, "Adaptive uncertainty modeling: On-lin robust control design", in *Proceedings of the American Control Conference*, Minneapolis, MN, 1987.

[7] A. J. Helmicki, C. A. Jacobson, and C. N. Nett, "Control-oriented system identification: A worst-case/deterministic approach in H_∞", *IEEE Transactions on Automatic Control*, vol. 36, pp. 1163–1176, 1991.

[8] A. J. Helmicki, C. A. Jacobson, and C. N. Nett, "Fundamentals of control oriented system identification and their application for identification in H_∞", in *Proceedings of the American Control Conference*, Boston, MA, 1991, pp. 88–89.

[9] D. S. Bayard, "Statistical plant set estimation using schroeder-phased multisinusoidal input design", *Journal of Applied Mathematics and Computation*, vol. 58, pp. 169–198, 1993.

[10] D. S. Bayard, Y. Yam, and E. Mettler, "A criterion for joint optimization of identification and robust control", *IEEE Transactions on Automatic Control*, vol. 37, no. 7, pp. 986–991, July 1992.

[11] Y. Yam, D. S. Bayard, and R. E. Scheid, "Frequency domain identification for robust large space sructure control desing", in *Proceedings of the American Control Conference*, Boston, MA, 1991, pp. 3021–3023.

[12] *IEEE Transactions on Automatic Control*, vol. 37, July 1992, Special Issue on System Identification for Robust Control Design.

[13] K. Godfrey, Ed., *PERTURBATION SIGNALS FOR SYSTEM IDENTIFICATION*, Prentice Hall International Series in Acoustics, Speech, and Signal Processing. Prentice hall International (UK) Ltd., 1993.

[14] J. C. Doyle, B. A. Francis, and A. R. Tannenbaum, *Feedback Control Theory*, Macmillan, 1992.

[15] R. Y. Chiang and M. G. Safonov, *Robust Control Toolbox : For Use with MATLAB*, The Math Works Inc., 2nd edition, Aug. 1992.

[16] R. Y. Chiang, *Modern Robust Control Theory*, PhD thesis, University of Southern California, 1988.

[17] Kondo, Ryou, S. Hara, and T. Itou, "Characterization of discrete time H_∞ controller via bilinear transform", in *Proceedings of IEEE Conference on Decision and Control*, 1990, pp. 1763–1768.

[18] P. A. Iglesias and K. Glover, "State-space approach to discrete time H_∞ control", *International Journal of Control*, vol. 54, no. 5, pp. 1031–1073, 1991.

[19] D. S. Bayard, "Statistical additive uncertainty bounds using schroeder-phased sinusoidual input design", Tech. Rep., Jet Propulsion Laboratory, California Institue of Technology, Jan. 1991, JPL Internal Document D-8146.

[20] R. E. Scheid and D. S. Bayard, "A linear programming algorithm for determining norm bounded uncertainty", Tech. Rep., Jet Propulsion Laboratory, 1992.

[21] R. E. Scheid and D. S. Bayard, "A globally optimal minimax solution for spectral overbounding and factorization", *IEEE Transactions on Automatic Control*, vol. 40, no. 4, pp. 712–716, 1995.

[22] M. R. Schroeder, "Synthesis of low-peak factor signals and binarysequences with low autocorrelation", *IEEE Trans. Inf. Theory*, vol. 16, pp. 85–89, 1970.

[23] D. S. Bayard, "Frequency domain identification for robust control design", Tech. Rep., Jet Propulsion Laboratory, California Institue of Technology, 1992, Engineering Memorandum: 343-1285.

[24] J. N. Juang and R. S. Papa, "An eigensystem realization algorithm for modal parameter identification and model reduction", *Journal of Guidance, Control, and Dyanmics*, vol. 33, no. 5, pp. 620–627, Sept. 1985.

[25] S. Y. Kung, "A new identification and model reduction algorithm via singular value decomposition", in *Proc. 12th Asilomar Conference on Circuits, Systems and Computers.*, Pacific Grove, CA, Nov. 1978, pp. 705–714.

[26] J. N. Juang, *Applied System Identification*, Prentice Hall, 1994.

[27] J. N. Juang, M. Phan, L. G. Horta, and R. W. Longman, "Identification of observer/Kalman filter markov parameters: Theory and experiments", in *AIAA Guidance, Navigation and Control Conference*, NEW Orleans, LA, Aug. 1991, AIAA, Paper AIAA-91-2735-CP.

[28] M. Phan, L. G. Horta, J. N. Juang, and R. W. Longman, "Linear system identification via an asymptotically stable observer", in *AIAA Guidance, Navigation and Control Conference*, NEW Orleans, LA, Aug. 1991, AIAA, Paper AIAA-91-2734.

[29] D. S. Bayard, "Multivariable frequency domain identification via 2-norm minimization", Tech. Rep., Jet Propulsion Laboratory, California Institue of Technology, 1991.

[30] D. S. Bayard, "Multivariable frequency-domain identification via two-norm minimization", in *Proceedings of the American Control Conference*, Chicago, IL, June 1992, pp. 1253–1257.

[31] R. H. Middleton and G. C. Goodwin, *Digital Control and Estimation: A Unified Approach*, Prentice Hall, 1990.

[32] C. T. Chen, *Linear System Theory and Design*, Saunders College Publishing, 1984.

[33] T. Kailath, *Linear Systems*, Prentice Hall, 1980.

[34] R. Johansson, *System Modelling and Identification*, Prentice Hall, 1993.

[35] M. Green and D. Limebeer, *Linear Robust Control*, Prentice Hall, 1995.

[36] L. Pernebo and L. M. Silverman, "Model reduction via balanced state space representation", *IEEE Transactions on Automatic Control*, vol. 21, pp. 382–387, 1982.

[37] D. Enns, "Model reduction with balanced realization: An error bound and frequency-weighted generalization", in *Proceedings of IEEE Conference on Decision and Control*, Las Vegas, NV, Dec. 1984.

[38] Y. Yam, D. S. Bayard, and R. E. Scheid, "Integrated identification and robust control tuning for large space structures", in *Proceedings of the American Control Conference*, San Diego, CA, May 1990.

[39] Y. Yam and K. L. Tung, "Integrated identification/control synthesis with frequency weighted balanced realization", in *Intelligent Automation and*

Soft Computing : Trends in Research, Development and Applications, M. Jamshidi et al., Ed. 1994, vol. 1, TSI Press.

[40] K. L. Tung and Y. Yam, "Integrated identification/control synthesis with approximate fractional frequency weighting", in *Proceedings of the American Control Conference*, Seattle, WA, June 1995, pp. 1835–1836.

[41] B. D. O. Anderson and Y. Liu, "Controller reduction: Concepts and approaches", *IEEE Transactions on Automatic Control*, vol. 34, no. 8, pp. 802–812, Aug. 1989.

[42] D. Gangsaas, K. R. Bruce, J. D. Blight, and U.-L. Ly, "Application of modern synthesis to aircraft control: Three case studies", *IEEE Transactions on Automatic Control*, vol. 31, pp. 995–1104, Nov. 1986.

[43] D. S. Bernstein and D. C. Hyland, "The optimal projection equations for fixed-order dynamic compensation", *IEEE Transactions on Automatic Control*, vol. 29, pp. 1034–1037, Nov. 1985.

[44] B. D. O. Anderson, "Controller design: Moving from theory to practice", *IEEE Control Systems Magazine*, pp. 16–25, Aug. 1993, 1992 Bode Prize Lecture.

[45] L. Chisci, L. Giarrè, and E. Mosca, "Indirect and implicit adaptive predictive control of the benchmark", *Automatica*, vol. 30, no. 4, pp. 577–584, 1994.

[46] P. A. Cook, "Application of model reference adaptive control to a benchmark problem", *Automatica*, vol. 30, no. 4, pp. 585–588, 1994.

[47] de Larminat and P. Houisot, "Application of ACSYDE (Automatic Control System Design) to the IFAC-93 benchmark", *Automatica*, vol. 30, no. 4, pp. 589–591, 1994.

[48] B. A. Foss and S. O. Wasbo, "Benchmark IFAC93: Adaptive predictive PI-control of an unknown plant", *Automatica*, vol. 30, no. 4, pp. 593–598, 1994.

[49] O. Hecker, T. Knapp, and R. Isermann, "Robust adaptive control of a time-varying process using parallel recursive estimator", *Automatica*, vol. 30, no. 4, pp. 599–604, 1994.

[50] M. M'Saad and I. Heijda, "Partial state reference model (adaptive) control of a benchmark problem", *Automatica*, vol. 30, no. 4, pp. 605–613, 1994.

[51] I. Postlethwaite, J. F. Whidborne, G. Murrad, and D.-W. Gu, "Robust control of the benchmark problem using H_∞ methods and numerical optimization techniques", *Automatica*, vol. 30, no. 4, pp. 615–619, 1994.

[52] T.-W. Yoon and D. W. Clarke, "Adaptive predictive contorl of the benchmark plant", *Automatica*, vol. 30, no. 4, pp. 621–628, 1994.

[53] T. Zhou and H. Kiruma, "Robust control of the sydney benchmark problem with intermittent adaptation", *Automatica*, vol. 30, no. 4, pp. 629–632, 1994.

[54] S. F. Graebe, "Robust and adaptive control of an unknown plant: A benchmark of new format", *Automatica*, vol. 30, no. 4, pp. 575, 1994.

[55] P.-F. Yeh and C.-D. Yang, *Post-modern Control Theory and Design*, EurAsia Book Co., second edition, 1992.

[56] C.-D Yang, H.-S. Ju, and S.-W Liu, "Experimental design of H_∞ weighting functions for flight control systems", *Journal of Guidance, Control, and Dyanmics*, vol. 17, no. 3, pp. 544–552, May-June 1994.

CUHK Libraries
000733960